FACTA UNIVERSITATIS

Abdominal surgery

Anatomy

Advanced implantology
Anesthesiology

General practice
Biomedical engineering
Physiology
Biochemistry
Cardiology
Citology

Otorhinolaryngology
Dental medicine
Pharmaceutical science
Orthopedics Ophtalmology

Hygiene
Biology

Nephrology
Immunology
Hematology
Nutrition
Pathology
Endocrinology
Neurology
Forensic medicine

Microbiology

Pediatric medicine
Genetics
Infective diseases
Oncology

Psychiatry
Radiology

SERIES **MEDICINE AND BIOLOGY**

FACTA UNIVERSITATIS

Series **MEDICINE AND BIOLOGY**
Vol. 16, No 1, 2014

AUTHOR GUIDELINES

Facta Universitatis, Series: Medicine and Biology (FU Med Biol) is the official publication of the University of Niš, Serbia. It publishes original scientific papers relating to medicine, biology and pharmacy (editorials, original experimental or clinical works, review articles, case reports, technical innovations, letters to the editor, book reviews, reports and presentations from (inter)national congresses and symposiums which have not been previously submitted for publication elsewhere). All manuscripts are assumed to be submitted exclusively unless otherwise stated, and must not have been published previously except in the form of an abstract or as parts of a published lecture and/or academic thesis.

Original papers may not exceed 10 printed pages, including tables and/or figures.

Reviews may not exceed 16 printed pages, including tables and/or figures.

Case reports/technical innovations/book reviews/presentations from congresses may not exceed four printed pages, including tables and/or figures. The figures should not occupy more than two-thirds of one printed page. The editor or co-editor reserves the right to make the decision if a manuscript qualifies to be corresponding type of the article.

Manuscripts are normally subject to the assessments of reviewers and the editor. Manuscripts that have been extensively modified in the editorial process will be returned to the author for retyping. All submitted articles will be reviewed by at least 2 reviewers, and when appropriate, by a statistical reviewer. Authors will be notified of acceptance, rejection, or need for revision within 4–5 weeks of submission.

Paper submitted for publication may be written exclusively in English. Authors for whom English is a second language should have the manuscript professionally edited before its submission.

Each author that participated sufficiently in the work has public responsibility for the content. This participation must include: a) Conception of design, or analysis and interpretation of data, or both, and b) Drafting the article of revising it for critically important intellectual content.

Text

The manuscript should contain following subdivisions:

(1) Title page (with short running page heading, title, authors names and affiliations, corresponding author with full address, e-mail, phone and fax).

Number all manuscript pages consecutively beginning with the title page. Do not hyphenate words at the end of the lines. Do not begin sentences with abbreviations.

(2) Abstract

The main abstract should be maximum 250 words, double-spaced and on a separate page. It should briefly describe respectively the problems being addressed in the study, how the study was performed, the salient results (without abbreviations) and what the authors conclude from the results.

2.1. Key words

Immediately after the Abstract, up to six topical key words for subject indexing must be supplied.

(3) Main body (Introduction, Material and methods, Results, Discussion, Conclusion)

The headings (Introductions; Material and Methods, etc.) should be placed on separate lines.

Abbreviations should be defined at first mention and used consistently thereafter.

The Introduction should give the pertinent background to the study and should explain why the work was done. References should be numbered in the order in which they appear (1, 2 or 1–3, etc.)

Each statistical method and/or other investigation should be described in the Material and Method section. All scientific measurements must be given in SI units.

The Results should present the findings of the research. They must be free of discussion. Results should be written in the past tense. Spell out the word Figure in the text except when it appears in parentheses: Figure 3 (Figs. 2–5). Always spell out numbers when they stand as the first word in a sentence: abbreviated units cannot follow such numbers. Numbers indicating time, mass, and measurements are to be in Arabic numerals when followed by abbreviations (e.g. 1 mm; 3 ml, etc.). All numbers should be given as numerals.

The Discussion should cover, but not simply repeat the new findings and should present the author's results in the broader context of other work on the subject interpreting them with a minimum of speculation.

(4) Acknowledgements

Acknowledgments of people, grants, funds, etc. should be placed in a separate section before the reference list. The names of funding organizations should be written in full.

(5) References

The references should be limited to those relating directly to the content of the manuscript. Authors are responsible for ensuring that the information in each reference is complete and accurate. All references should be numbered in the order in which they appear in the text. Do not use footnotes or endnotes as a substitute for a reference list. At the end of the article the full list of references should give the name and initials of all authors unless there are more than six, when only the first three should be given followed by "et al". The authors' names should be followed by the title of the article, the title of the Journal abbreviated according to the style of Index Medicus, the year of publication, the volume number and page numbers. In case that more than one paper by the same author(s) published in the same year is cited, the letters a, b, c, etc., should follow the year, e.g. Bergmann (1970a) ― in the reference list.

Examples for journals and other sources are as follow:

Journals:

1. Kuroda S, Ishikawa T, Houkin K, Nanba R, Hokari M, Iwasaki Y. Incidence and clinical features of disease progression in adult Moyamoya disease. Stroke 2005; 36:2148–2153.

2. Papantchev V, Hristov S, Todorova D, et al. Some variations of the circle of Willis, important for cerebral protection in aortic surgery — a study in Eastern Europeans. Eur J Cardiothorac Surg 2007; 31:982–998.

3. Jovanović S, Gajić I, Mandić B, Mandić J, Radivojević V. Oral lesions in patients with psychiatric disorders. Srp Arh Celok Lek 2010; 138:564–569. (Serbian)

4. Valença MM, Martins C, Andrade-Valença LPA. Trigeminal neuralgia associated with persistent primitive trigeminal artery. Migrâneas cefaléias (Brasil) 2008; 11:30–32.

5. Belenkaya RM. Structural variants of the brain base arteries. Vopr neirokhir 1974; 5:23–29. (Russian)

Abstract:

6. Tontisirin N, Muangman SL, Suz P, et al. Early childhood gender in anterior and posterior cerebral blood flow velocity and autoregulation. In Abstract of Pediatrics 2007. (doi:10.1542/peds. 2006-2110; published online February 5).

Books:

7. Patten MB. Human embryology, 3rd edn. McGraw-Hill: New York, 1968.

8. Marinković S, Milisavljević M, Antunović V. Arterije mozga i kičmene moždine—Anatomske i kliničke karakteristike. Bit inženjering: Beograd, 2001. (Serbian)

Chapters:

9. Lie TA. Congenital malformations of the carotid and vertebral arterial systems, including the persistent anastomoses. In: Vinken PJ, Bruyn GW (eds) Handbook of clinical neurology, vol. 12. North Holland: Amsterdam, 1972; pp 289–339.

Unpublished data:

10. Reed ML. *Si-SiO$_2$ interface trap anneal kinetics,* PhD thesis. Stanford University: Stanford, 1987.

Online document:

11. Apostolides PJ, Lawton MT, David CA, Spetzler RF. Clinical images: persistent primitive trigeminal artery with and without aneurysm. Barrow Quarterly 1997; 13(4). http://www.thebarrow.org/Education_And_Resources/Barrow_Quarterly/204843

12. Cerebrovascular embryology, in: power point; 2000. http://brainavm.oci.utoronto.ca/staff/Wallace/2000_curriculum/index.html

(6) Tables

(7) Figure legends

Table and figure legends should be included within the text file and contain sufficient data to be understood without reference to the text. Each should begin with a short title for the figure. All symbols and abbreviations should be explained within the legend. If the magnification is quoted in a sentence, it should appear in parentheses, e.g. (x400); at the end of legend it should appear, e.g., "... fibrils. X20 000".Tables must be typed on separate pages. All tables should be simple without duplicating information given in the text. Numerical results should be expressed as means with the relevant standard errors and/or statistically significant differences, quoting probability levels (p-value).

Illustrations

All figures should be cited in the paper in a consecutive order and submitted in separated files. All figures, photographs, line drawings and graphs, should be prepared in electronic form and converted in TIFF or JPG (max quality) file types, in 300 dpi resolution, for superior reproduction. Figures, line drawings and graphs prepared using elements of MS Drawing or MS Graph must be converted in form of pictures and unchangeable. All illustrations should be planned in advance so as to allow reduction to 8 cm in column width or 16.75 cm in page width. Please review all illustrations to ensure that they are readable.

The manuscripts in above form should be submitted to the Editor-in Chief or Co-editor of the journal in electronic form prepared by MS Word for Windows (Microsoft Word 1997–2003, *.doc or higher Word, *.docx) ― font Times New Roman (12-point). The manuscript should be typed double-spaced on one side only of A4 paper. The manuscript in electronic form should be submitted through the submission portal:

http://casopisi.junis.ni.ac.rs/index.php/FUMedBiol.

Dear colleagues,

after a long pause, the journal—Facta Universitatis, Series: Medicine and Biology (FU Med Biol) of University of Niš starts in year 2014 with new manuscripts in which incorporated new or forgotten old ideas thanks to the great effort, temper and enthusiasm of authors and Editorial team.

FU Med Biol is designed as an open access peer-reviewed international journal which publishes editorials, original experimental or clinical works, review articles, case reports, technical innovations, letters to the editor, book reviews, reports and presentations from (inter)national congresses and symposiums which have not been previously submitted for publication elsewhere.

FU Med Biol will provide a platform for doctors, biologists and pharmacists all over our country and the world to promote the science, independent from the same or opposite opinions. Editorial team takes seriously the responsibility as the steward of the intellectual property to ensure the integrity of works and the sustainability of the journal.

It's my honor to invite **YOU** to contribute new articles on medicine, stomatology, biology and pharmacy to our journal—FU Med Biol in Niš, Serbia!

Editor-in-Chief

ANTERIOR CEREBRAL–ANTERIOR COMMUNICATING COMPLEX IN THE POSTNATAL PERIOD: FROM A FENESTRATION TO THE MULTIPLICATION OF ARTERIES

Ljiljana Vasović*, Milena Trandafilović, Slobodan Vlajković, Ivan Jovanović, Slađana Ugrenović

University of Niš, Faculty of Medicine, Department of Anatomy, Serbia

Abstract. *The anterior cerebral artery is a medial terminal branch of the cerebral part of the internal carotid artery on both sides. These paired arteries are connected by the anterior communicating artery. Different abnormalities of the anterior communicating–anterior cerebral arteries can include an aplasia or hypoplasia, or variable origin and/or course and/or termination, or fenestration, or duplication or multiplication or persistence of primitive or additional vessels. The aim of this manuscript was to investigate the relationships of morphological abnormalities of an anterior communicating–anterior cerebral complex in human adults of Serbian population. Material represented 266 human cadavers autopsied at the Institute for Forensic Medicine in Niš. Cerebral arteries were investigated macroscopically, under the glass; outer vessel's diameter was measured using ImageJ processing program. A total of 87 cases or 32.71% of different abnormalities of the anterior communicating–anterior cerebral complex were found and classified into six groups. The group of duplications of the anterior communicating artery with an incidence of 18.04% was the most frequent. The finding of only four aneurysms on the anterior communicating artery indicates that there was no significant difference in the rate of aneurysms in individuals of Serbian population with and without fenestrations or duplications or multiplications of the anterior cerebral–anterior communicating complex.*

Key words: *Human adult, brain base, anterior cerebral artery, anterior communicating artery, abnormalities*

Introduction

The anterior cerebral artery (ACA) is one of two terminal branches of the internal carotid artery (ICA) on the human brain base. The ACA usually courses anterior and medially to the interhemispheric fissure and passing over the optic chiasm and nerves it joins at the midline the opposite one through the anterior communicating artery (ACoA) [1]. There are two topographical parts of the ACA – precommunicating (A1) and postcommunicating (A2) segments regarding the point of ACA–ACoA junction [2]. The communicating and choroid subparts of the cerebral part of ICA with A1 segments and ACoA represent vascular components of an anterior segment of the cerebral arterial circle (CAC) [3].

The left and right A1 segments varied in diameter from 0.9 to 4.0 mm in USA population [4] or from 2.5 to 3.5 mm in Indian population [5], and in length from 7.2 to 18.0 mm [4], or from 10 to 19 mm [5], sending two to 15 perforating arterioles [4]. These (posteroinferior and posterosuperior) arterioles usually supplied the anterior cerebral commissure and globus pallidus, the optic chiasm, the anterior perforated substance, the genu of the internal capsule, the anterior hypothalamus and part of the thalamus [5].

Unpaired ACoA was commonly between 0.2–3.4 mm in caliber in USA population [4], or between 1.0 to 4.0 mm in Indian population [5], whereas it was between 0.3–7.0 mm in length [4]. Their branches (up to four) supplied the optic nerves and chiasm, suprachiasmatic area, anterior perforated substance, lamina terminalis and frontal lobe [4].

The variants and abnormalities of arteries can include an aplasia or hypoplasia, or variable origin and/or course and/or termination, or fenestration, or duplication or multiplication or persistence of primitive or accessory vessels, etc. There were anatomical descriptions of some of the ACA and ACoA abnormalities [3–12] and/or their branches [1,3–7,11]. Majority of authors reported simultaneous presence of fenestrations and (in)direct aneurysms of the ACA–ACoA complex [1,7,13–30], or arteriovenous malformation [23], but usually in case reports.

Our aim was to describe a relationship of presented fenestration and/or duplication and/or multiplication with pathological states of the ACoA and ACA in A1 and proximal A2 segments in human adult specimens of Serbian population.

Material and Methods

We defined the ACoA and ACA in A1- and neighboring subpart of the A2 segment as an ACA–ACoA complex

---

Correspondence to: Ljiljana Vasović, MD, PhD
Faculty of Medicine, Dept. of Anatomy,
81 Dr Zoran Đinđić Blvd., 18000 Niš, Serbia
Phone: +381 18 45 70 029 Fax:+381 18 42 38 770
E-mail: likica@medfak.ni.ac.rs

according to Pai et al. [5]. These vessels were explored on the brain base of 266 adult human cadavers of both genders autopsied at the Institute of Forensic Medicine in Niš because of different causes of death. The co-author (MT) investigated cerebral arteries during her academic and doctoral studies in accordance with the approval granted by our Ethics Committee (no. 01-206-1).

After the extraction of the brain from the cranium, each brain base with a ruler on it was photographed before and after the removal of the arachnoidea mater. Vessels' outer diameter was calculated using ImageJ processing program (http://rsb.info.nih.gov/ij/index.html). General data regarding the cadaver (cause of death, gender and age) and visible morphological abnormalities (additional vessels, partial or total duplication and triplication and/or fenestration) or associated aneurysm of the ACA and/or ACoA were noted for each case.

The criteria in defining the arterial abnormalities were according to the previous investigation [31]. A fenestration was defined as an abnormality that is characterized by a common origin of an artery that splits into two parallel channels, which subsequently rejoins into the same artery. Partial duplication of the artery was determined if it had a common origin on one and two separate junctions on the opposite artery. Two independent vessels' origin and termination characterized their total duplication. Three independent vessels or partially duplicated artery associated with the same single vessel characterized a triplication. A new term — anterior communicating network or the rete communicans anterior was a personal proposal for a special shape of the ACoA — a presence of two or more transverse ACoAs and at least of one vertically or obliquely oriented vessel among them. The drawings of ACoA abnormalities were modified according to Kayembe et al. [14].

Hypoplastic caliber (≤ 1.0 mm) of vessels was noted if it was only found in the group of investigated abnormalities; atheromatous plaques were noted if they were found within fenestration limbs or double or multiple vessels.

Results

We found 87 cases (32.71%) — 45 of male (25 to 90 years old) and 42 of female gender (16 to 95 years old) of single and/or associated abnormalities of the ACA–ACoA complex (Fig. 1).

Special morphological abnormalities of this complex were described within six groups:

I. *Arterial fenestration.* There were 13 cases (9 of female and 3 of male gender) of ACA fenestrations (Fig. 2). There were four cases of the single A1 fenestration (two on the right and two on the left) and six cases (five on the right and one on the left) of associated abnormalities and/or pathologies of the ACA–ACoA complex, as well as one case of single fenestration of the left A1–A2 segment and two cases (on the right and left) of its association with other abnormalities of the ACA–ACoA complex. All fenestrations were oval in the shape; a medial limb of the fenestration was smaller in six specimens, whereas a lateral limb was two times smaller. The perforating arterioles from medial limbs were constant, except in one

specimen (case 34). Large fenestrations were found three times on the left (cases 23, 47 and 53) and once (case 68) on the right side. The ACAs with fenestrations were of normal outer diameter.

Associated abnormalities were as follows: 1) rete communicans anterior (two cases); 2) duplication of the ACoA with caudally hypoplastic vessel (four cases); 3) aplasia of the left ACA and simultaneous double fenestrations of a proximal part of the right ACA (one case); and 4) persistent right primitive olfactory artery (one case). Pathological states were as follows: insular atheromatous plaques in three cases and diffuse atheromatous plaques in fenestration limbs in one case were found, as well as one simultaneous presence of the ACoA aneurysm (case 28).

II. *Arterial duplication.* This abnormality in 44 cases was found on the ACoA — partially in 21 and totally in 23 cases (Fig. 3). Partial duplication indicated that the ACoA had the shape of transversely oriented letter "V" or "Y"; their common origin was more frequent on the left ACA (n = 14) than on the right one (n = 7). Duplicated ACoAs were of different caliber in 21 cases (a caudal vessel was smaller in 19 cases and larger in two cases) and of the same caliber in two specimens. It should be noted that one of two ACoAs was hypoplastic in 23 cases; both ACoAs were hypoplastic in one specimen (case 51). Simultaneously, the left and right A1 parts were of equal outer diameters in 30 cases; the left A1 was larger in eight and smaller in six cases than the right one. Insular atherosclerotic plaques of duplicated ACoAs were found in seven cases; an aneurysm on the rostral ACoA was found twice (cases 19 and 83).

III. *Arterial triplication.* This abnormality in five cases was found on the ACoA; two specimens had independent vessels, whereas three specimens had an association of partially duplicated and single ACoA (Fig. 4). Thereby, one ACoA was hypoplastic in three cases; two ACoAs were hypoplastic in two cases (cases 55 and 58). Simultaneosly, the left A1 was dominant in one case (case 55), as well as the right A1 (case 42).

IV. *Anterior communicating network* or t*he rete communicans anterior.* This ACoA configuration was found in 22 cases (see Fig. 4). The position of anastomotic vessels indicated that the ACoA had the shape of transversely oriented letter "H" or "N" or irregular form. The left and right A1 segments were equal in 16 cases; the left was smaller in five cases and larger in one case than the right A1. Atherosclerotic plaques were found in three cases. An aneurysm of the ACoA existed in only one case (case 57; see Fig. 4).

V. *Arterial quadriplication.* This abnormality was found on the ACoA in two cases. There was an infundibular widening of ACAs at ACoA junction, whereas the outer diameters of the ACAs proximally and distally to it were relatively equal (Fig. 5).

VI. *Transverse arterial anastomoses.* These anastomoses connected bilaterally to A2 segments in three cases; in two cases there was an anastomosis rostral to the duplicated ACoA (case 10, see Fig. 2) and rostral to the rete communicans anterior (case 84; see Fig. 4), and once as multichaneled anastomoses immediately rostral to the single ACoA (case 14; see Fig. 5).

Fig 1. Drawings of 87 abnormalities of the anterior cerebral–anterior communicating (ACA–ACoA) complex.
Note: The number on each drawing will correspond to the same number on one of the next original pictures.
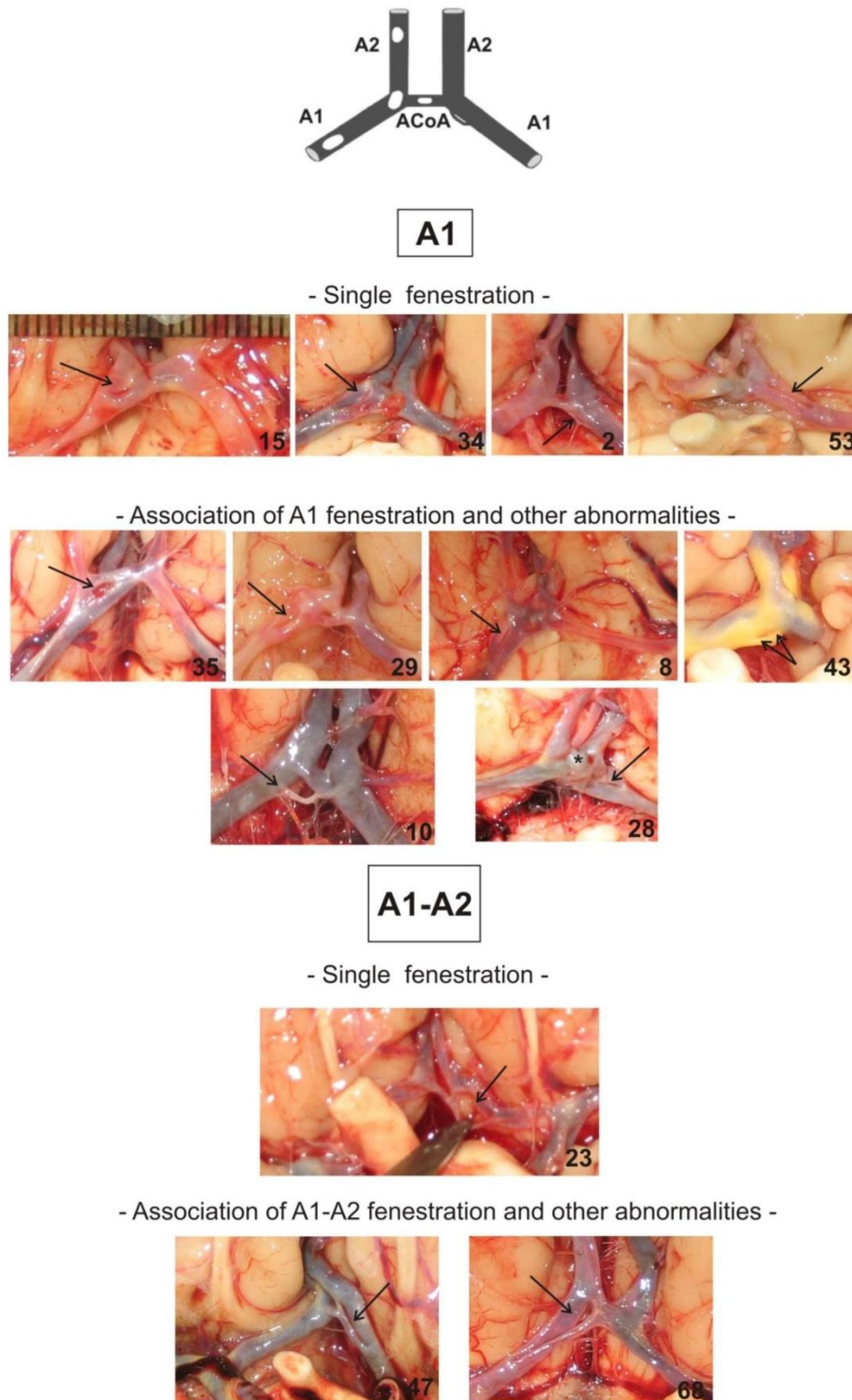
Fig 2. Fenestrations of the left or right anterior cerebral artery (ACA). Unilaterally, fenestration of the precommunicating (A1) and precommunicating–postcommunicating junction (A1–A2) was present in 13 cases. An aneurysm (*) of the anterior communicating artery (ACoA) was present in a case 28.
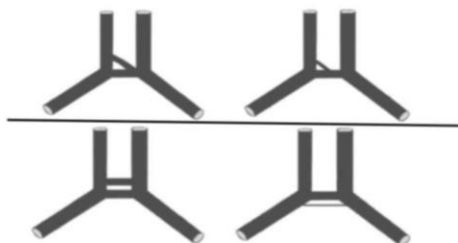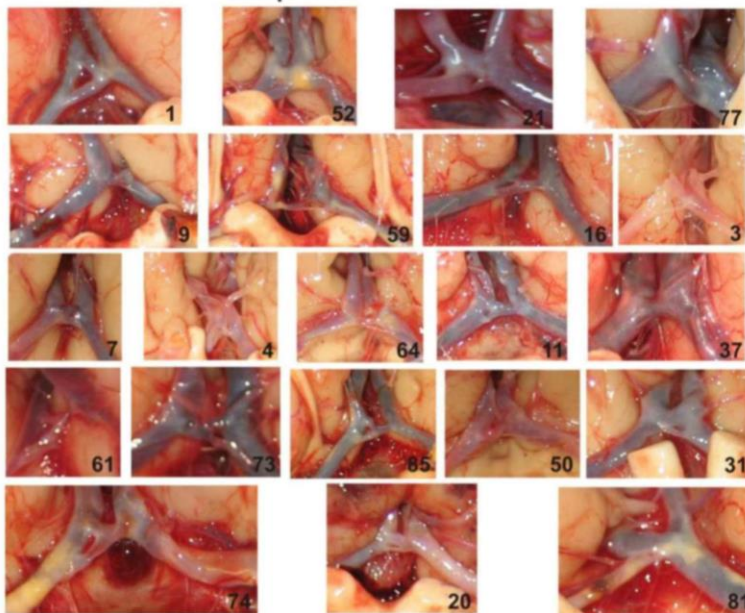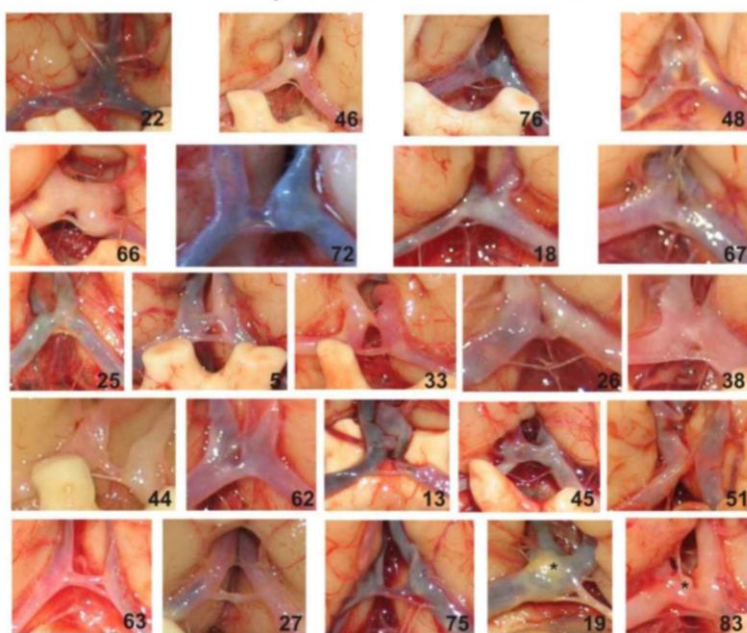
Fig. 3. Duplication of the anterior communicating artery (ACoA). Twenty one specimens characterized by single appearance of partially duplicated ACoA (a common origin on one anterior cerebral artery (ACA) and two origins on the second ACA; 23 specimens characterized by totally duplicated ACoA. An aneurysm (*) of the ACoA was present in cases 19 and 83.
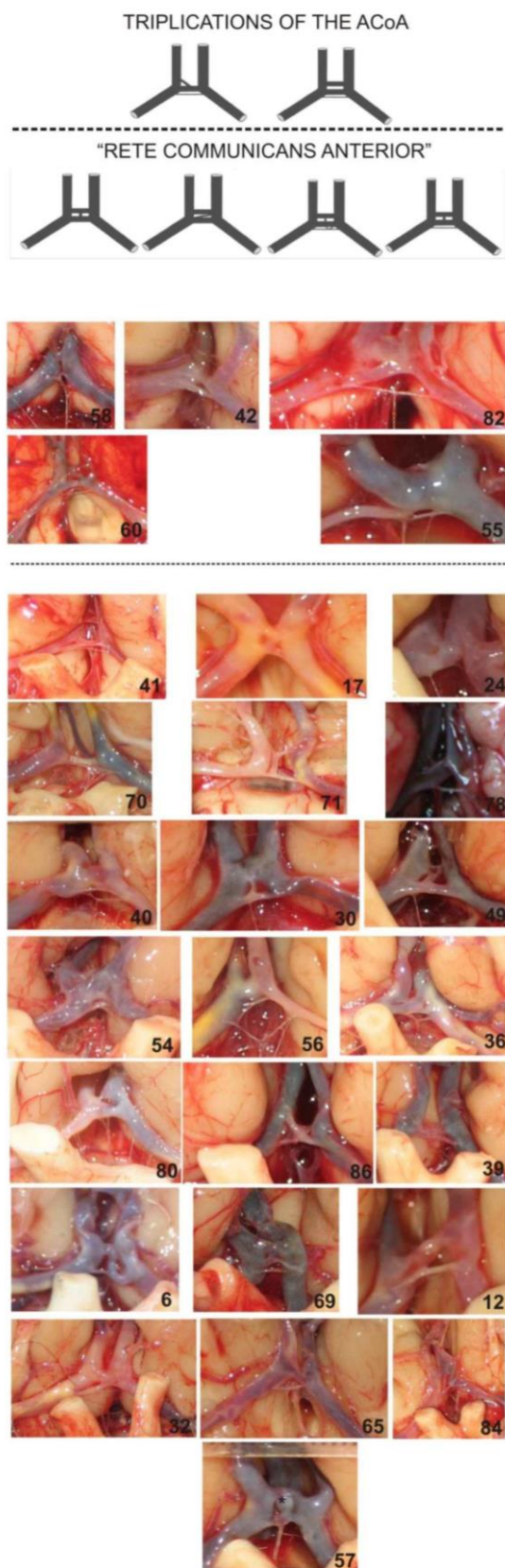
Fig. 4. Triplication of the anterior communicating artery (ACoA) and the rete communicans anterior.Five specimens of ACoA triplication and 22 specimens of the rete communicans anterior. Associated ACoA aneurysm (*) was marked in case 54.
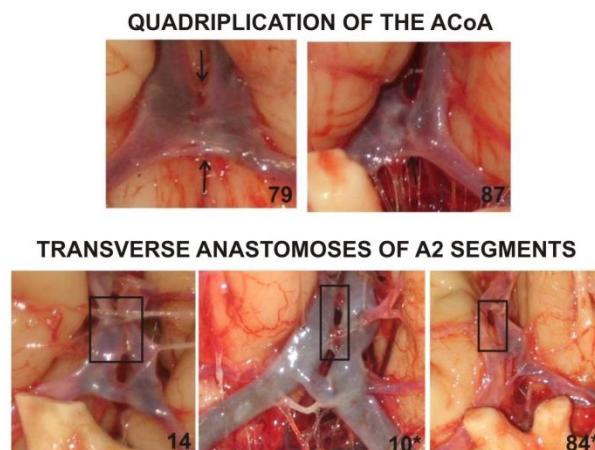
Fig. 5. Very rare abnormalities of the anterior cerebral–anterior communicating (ACA–ACoA) complex: two cases of quadriplication of the ACoA and three cases of multiple transverse anastomoses of postcommunicating parts (A2) of the ACAs; repeated instances from one of the previous images are marked with an asterisk number.

Table 1. Incidences of investigated morphological abnormalities and associated aneurysms of the anterior cerebral–anterior communicating arteries

Arterial abnormalities		A1	A1–A2	A2	ACoA	Percentage in regard to the total number of cases (n = 266)	Percentage in regard to the number of abnormalities
		Left/Right	Left/Right	Left/Right			
Fenestration	Single	3/6	2/1			4.88%	14.94%
	Double	0/1					(13/87)
	Aneurysm				1	0.37%	7.69% (1/13)
Duplication	Partial				23 (21+2*)	8.64%	55.17% (48/87)
	Total				25 (23+2*)	9.39% / 18.04%	
	Aneurysm				2	0.75%	4.16% (2/48)
Triplication	Partial and total				5	1.88%	5.74% (5/87)
	Aneurysm						
Quadriplication	Partial and total				2	0.75%	2.29% (2/87)
	Aneurysm						
Rete	Summa				24 (22+2*)	9.02%	27.58% (24/87)
	Aneurysm				1	0.37%	4.16% (1/24)
Transverse anastomoses	Summa			3 (1+1*+1**)		1.12%	3.44% (3/87)
	Aneurysm						

A1, precommunicating part of the anterior cerebral artery; A2, postcommunicating part of the anterior cerebral artery; A1–A2, junction of the A1 and A2 segments; ACoA, anterior communicating artery.
*One or two cases more in the corresponding square derived from the group of fenestration of the anterior cerebral artery.
**One case more in the corresponding square derived from the group of the rete communicans anterior.

The incidences of investigated abnormalities of the ACA–ACoA complex were summarized in the Table 1. According to the number of specimens and corresponding abnormalities, the incidences were relatively high for ACoA duplications (18.04% and 55.17%, respectively), the rete communicans anterior (9.02% and 27.58%, respectively) and fenestration of the ACA (4.88% and 14.94%, respectively).

However, we found only four aneurysms in specimens of female gender; each was unruptured and lo-
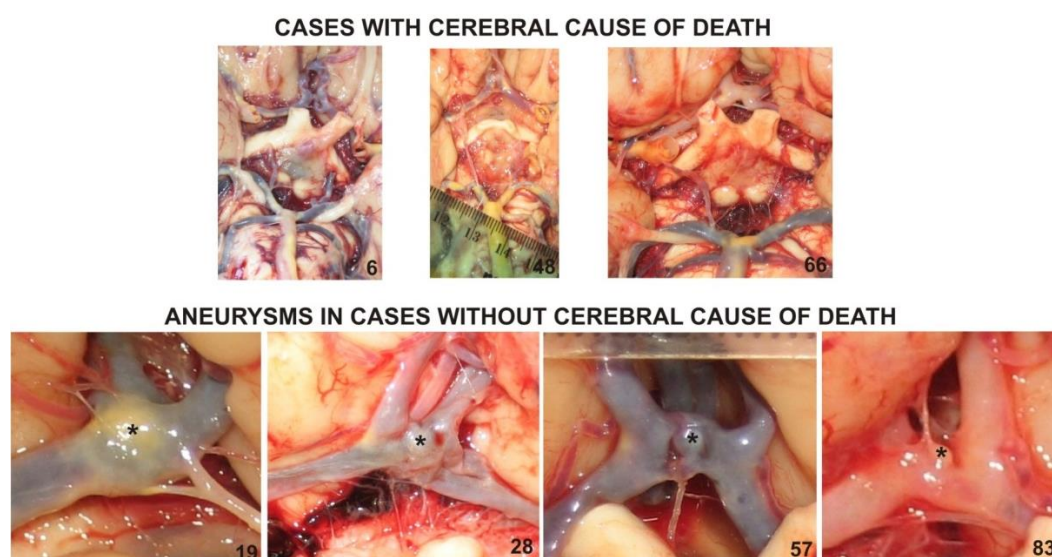
Fig. 6. Comparison of abnormalities of the anterior cerebral–anterior communicating (ACA–ACoA) complex. Three cases were autopsied because of cerebral pathology; ACoA was in the form of the rete communicans anterior (case 6) or doubled (cases 48 and 66). Four cases were without cerebral cause of death, but with a presence of the ACoA aneurysm; ACoA was also in the form of the rete communicans anterior (case 57) or doubled (cases 19, 28 and 83).

Table 2. Display of cadaveric cases with initial cerebral cause of death and cases with proven aneurysms at autopsy

				Abnormalities			
						ACA	
Groups	N^0	Diagnose	Gender/Age	ACoA	L	R	L/R outer diameter
Initial cerebral cause	6[*]	Cerebral infarction	M/82	Rete**			L=R
	48[*]	Cerebral/myocardial infarctions	M/77	Duplication		Stenosed origin	L>R
	66[*]	Cerebral apoplexy	M/68	Duplication			L=R
Anerysmatic serie at autopsy	19[*]	Massive pneumonia	F/85	Duplication Aneurysm			L<<R
	28[*]	Polytrauma	F/72	Duplication MACC Aneurysm	A1 fen		L=R
	57[*]	Respiratory insufficiency	F/95	Rete** MACC Aneurysm			L=R
	83[*]	Cardiorespiratory arrest	F/74	Duplication Aneurysm			L<R

[*] The numbers are the same as in Figures 1–4 and Figure 6
** The rete communicans anterior
ACoA, anterior communicating artery; ACA, anterior cerebral artery; M, male; F, female; L, left; R, right; MACC, median artery of the corpus callosum; A1, precommunicating part of the ACA

cated on the ACoA; its incidence was 1.50% (4/266) and 4.59% (4/87) of the cases. We emphasized that cerebral pathology (cerebral infarction or apoplexy) was the reason for the forensic autopsy in 3/87 abnormalities in which aneurysms of the ACA or ACoA did not exist (Fig. 6 and Table 2).

Discussion

As quoted by Okahara et al. [7] a fenestration or duplication of the ACA and/or ACoA is the consequence of an incomplete fusion of the embryonic plexiform anastomosis. As quoted by Koh et al. [24] fenestration of the ACA is a remnant of an embryologic anastomosis between the primitive olfactory artery and the ACA.

Some authors [7,25] described embryonic development of the ACA–ACoA complex as follows: In a 3.7 mm of embryo the primitive internal carotid artery (ICA) gives a large primitive maxillary artery and then divides into the cranial and caudal branches. The cranial branch passes dorsal to the optic stalk, and its first branch is the anterior choroidal artery. It also distributed several branches to the telencephalon, one of which will later form the middle cerebral artery.

The continuation of the cranial branch is known as the primitive olfactory artery [32]. In embryos of 11.5 to 18 mm (41–48 days) the primitive olfactory artery distributed two branches— one to the nasal fossa and the second one as the future continuation of the ACA. The latter artery is joined with opposite ACA by a plexiform anastomosis, which is a precursor of the future ACoA.

We described adult cases of some morphological arterial abnormalities of the A1, proximal A2 and ACoA as parts of ACA–ACoA complex in accordance with Pai et al. [5]. In the literature there were similar examples. So Perlmutter and Rhoton [4] investigated ACA, ACoA and Heubner's artery within the anterior cerebral-anterior communicating-recurrent artery complex. Bharatha et al. [23] included A1, communicating and proximal A2 segment as parts of an anterior communicating region.

Generally, the frequency of fenestrations for all location in the human cerebral circulation was 16% reported at the time of autopsy or 12% angiographically [33]. According to the rule in defining an arterial fenestration accepted in the literature [10,23,25,30,31], we could note the fenestration of the ACA but not ACoA. We found ACA fenestrations in 4.88% of cases, while Bharatha et al. [23] discovered fenestrations on CTAs of the anterior communicating region (A1, ACoA and proximal A2) in 6.9% of cases. Okahara et al. [7] described that their incidence ranged 0.1–7.2% in autopsies. Koh et al. [24] counted 60 cases of A1 fenestration in the literature up to year 2008.

Kim et al. [21] reported that 0.36% of patients who underwent cerebral angiography showed fenestration in A1, while 0.62% of MRA patients had a fenestration of A1 segment. As quoted by Uchino et al. [22], and Dimmick and Faulder [25], very low incidence (0.058%) of ACA fenestrations was noted on angiogram and that was lower than MRA incidence (1.2%). The reason for this was the fact that two fenestrated branches are usually divided horizontally and that they are superimposed on conventional angiographic images [22]. However, Ješić et al. [29] retrospectively reviewed cranial MR angiography images of 1000 consecutive patients and noted 0.5% of ACA fenestrations. In addition Okahara et al. [7] and Weil et al. [34] pointed to the fact that a small fenestration of ACA or partially occluded A1 segment duplication might be mistaken for ACoA aneurysm on MRA and CTA, respectively.

We found only one unruptured aneurysm of the ACoA in the group of 13 ACA fenestrations. This finding can prove the fact that aneurysms rarely develop from ACA fenestrations; untill 1988 only eight cases have been reported in the literature [16]. However, in series of 38 A1 aneurysms, Suzuki et al. [17] discovered vascular anomalies in 20.5% of the cases; 75% of these were A1 fenestrations. In addition, vascular anomalies associated with A1 fenestration were different as an ipsilateral middle cerebral artery aneurysm, an ipsilateral posterior communicating artery aneurysm, and an aneurysm at the proximal end of the fenestrated A1 [21]. Kobayashi et al. [15] reported a case of a ruptured aneurysm occurring at the bifurcation of the azygos ACA with fenestration at the right A1 segment. Ihara et al. [20] discovered an aneurysm from the fenestrated right A1 simultaneously with the presence of the azygos ACA and hypoplastic left A1 segment. Dimmick and Faulder [25] demonstrated on CTA an association of the right A2 and ACoA fenestrations with an aneurysm on the ACoA, then the presence of hypoplastic left A1 and the right persistent primitive hypoglossal artery. Kachara et al. [19] reported a rare case of fenestration of the right Al segment with a ruptured saccular aneurysm, arising from the proximal end of fenestration, associated with aplasia of the left Al segment. Bharatha et al. [23] described that aneurysms associated with fenestrations classically rose at the proximal end supported by hemodynamic stresses and by medial defect at this point. However, Koh et al. [26] reported a case of a ruptured aneurysm arising from the distal end of A1 fenestration. Some authors [21,23,33] stressed that the form of the fenestrations at both the proximal and distal edges is in response to hemodynamic forces and is analogous to branching regions of cerebral arteries. Koh et al. [24] reported an unusual case of multiple fenestrations of the right A1 segment associated with aneurysm of the left A2 segment. Independent from previous data, we agree with the findings of Kayembe et al. [14], Bharatha et al. [23] and Van Rooij et al. [27] that there was no significant difference in the rate of aneurysms in individuals with and without fenestrations, or vice-versa.

Uchino et al. [22] diagnosed that all A1 fenestrations were large, of a convex-lens-like shape, and located in the distal A1 segment with or without extension to the proximal A2 segment, whereas A2 fenestrations were small and of a slit-like shape on MRAs of Japanese population. We found 4/13 large ACA fenestrations in cadaveric specimens of our population.

We reported ACA fenestrations only unilaterally, as recently in adult cadavers as earlier in fetal ones [9, 12]. However, Friedlander and Ogilvy [18] and Aktüre et al. [30] discovered fenestration on both ACAs in two women using 3-dimensional computerized tomographic angiography (3D CTA) and autopsy, respectively. Previous authors summarized only seven cases, including their findings of bilateral A1 fenestrations between 1928 and 2011. In retrospective study by Kim et al. [21], as well as in our specimens there was no side-difference of A1 fenestration, whereas Zhao et al. [28] found it frequently on the right side. There was a dominance of female sex in our and many other reports [10,13,15,16,19, 20,22,24–26,29,30] regarding A1 fenestrations.

In evaluating cerebral angiograms, it is important to differentiate between A1 fenestration and Heubner's artery [12,16]. Perforating arterioles from the medial limb of the ACA fenestration were visible in 12/13 our cases, while Aktüre et al. [30] discovered them from both lateral and medial limbs on postmortem specimen.

Gurdal et al. [19] presented an association of the right A1 fenestration and partial duplication of the ACoA in a female cadaver. We also noted associated morphological abnormalities on the ACoA in six cases, as well an aplasia of the ACoA and opposite ACA and the persistence of the primitive olfactory artery in single cases simultaneously with ACA fenestration.

We did not find any case of ACA doubling, whereas Fawcett and Blachford [6] noted 2/700 cases of "ACA doubling on the right side within the circle". Perlmutter and Rhoton [4] noted duplication of a portion of A1 on one side in 2/50 brains.

It has been reported that the incidence of fenestration of the ACoA was 7.5–40% in autopsies [7]. However, according to the definition of the fenestration, we did not classify any case as an ACoA fenestration. Scremin [8] described that variations of the ACoA include absence, duplication, and triplication. De Silva et al. [11] classified variations of the ACoA into 12 types: single, one point fusion, long fusion, double, V shape, Y shape, H shape, N shape, triple, plexiform, presence of median anterior cerebral artery, and aneurysms. We classified investigated abnormalities of the ACoA into four groups—duplication, triplication, quadriplication and anterior communicating network. We named ACoA in the form of a network as the rete communicans anterior, while Fawcett and Blachford [6] marked similar ACoA configuration as an anterior communicating treble.

It was difficult to discuss incidences of ACoA abnormalities because the same configuration has been presented differently by different authors. This example was a review of findings of different authors or some mistakes in explanation of other results as there were in the table presented by De Silva et al. [11]. We found the anterior communicating network and total duplication of the ACoA in 9.02% and 9.39% of cases, respectively, while Fawcett and Blachford [6] noted them in legends

of their drawings in 14% and 7.2% of cases, respectively. We defined a triplication of the ACoA if there were three independent vessels or an association of partially duplicated and single ACoA, whereas Gurdal et al. [10] presented a partial triplication of the ACoA when it had a common orifice on one ACA and trifurcation on opposite ACA.

There are some our suggestions. The first is the consequence of the summation of double to multiple ACoAs and anterior communicating network (21.32% and 9.02%, respectively). We suggest including the plural for ACoAs and a new term—rete communicans anterior in Anatomical nomenclature. Another suggestion was the consequence of an indefinite distance between two or more successive ACoAs and an unspecified border for the most rostral ACoA. Because of that we included a group of transverse ACAs anastomoses as a supplementary abnormality of the ACA–ACoA complex.

Finally, we mentioned in this manuscript only one case (1/266) of absence of the left ACA and ACoA in specimens of Serbian population. However Uchino et al. [22] found 50/923 instances of unilateral A1 aplasia in Japanese population. This important abnormality, as well as possible cases of an "induced" ACoA aplasia deserves special consideration in the future article.

Conclusion

We found morphological abnormalities of the ACA–ACoA complex in 87/266 or 32.71% of cases. The finding of only four aneurysms on the ACoA indicates that there was no significant difference in the rate of aneurysms in individuals with and without fenestrations or duplications or multiplications of the ACA–ACoA complex. This fact inspired authors for additional investigation of relationships of abnormalities with or without aneurysms on other arteries of carotid and vertebrobasilar systems in our population.

References

1. Yasargil MG. Microneurosurgery, vol 1. Georg Thieme Verlag: Stuttgart, 1984.
2. Terminologia Anatomica. International Anatomical Terminology. FCAT. Georg Thieme: Stuttgart, 1998.
3. Vasović L, Trandafilović M, Jovanović I, et al. Morphology of the cerebral arterial circle in the prenatal and postnatal period of Serbian population. Childs Nerv Syst 2013; 29:2249–2261.
4. Perlmutter D, Rhoton AL. Microsurgical anatomy of the anterior cerebral-anterior communicating-recurrent artery complex. J Neurosurg 1976; 45:259–272.
5. Pai SB, Kulkarni RN, Varma RG. Microsurgical anatomy of the anterior cerebral artery - anterior communicating artery complex: An Indian study. Neurology Asia 2005; 10:21–28.
6. Fawcett E, Blachford JV. The circle of Willis: an examination of 700 specimens. J Anat Physiol 1905; 40:63–70. http://www.ncbi.nlm.nih.gov/pmc/articles/PMC1287340/

7. Okahara M, Kiyosue H, Mori H, Tanoue S, Sainou M, Nagatomi H. Anatomic variations of the cerebral arteries and their embryology: a pictorial review. Eur Radiol 2002; 12:2548–2561.
8. Scremin OU. Cerebral vascular system. In: Paxinos G, Mai JK (eds). The human nervous system, 2nd ed. Elsevier Academic Press: San Diego, 2004; pp 1326–1337.
9. Vasović L, Milenković Z, Pavlović S. Comparative morphological variations and abnormalities of circles of Willis: a minireview including two personal cases. Neurosurg Rev 2002; 25:247–251.
10. Gurdal E, Cakmak O, Yalcinkaya M, Uzun I, Cavdar S. Two variations of the anterior communicating artery: a clinical reminder. Neuroanatomy 2004; 3:32–34.
11. De Silva KRD, Silva R, Gunasekera WSL, Jayesekera RW. Prevalence of typical circle of Willis and the variation in the anterior communicating artery: A study of a Sri Lankan population. Ann Indian Acad Neurol 2009; 12:157–161.

12. Vasović L, Ugrenović S, Jovanović I. Human fetal medial striate artery or artery of Heubner. J Neurosurg Pediatrics 2009; 3:296−301.

13. Ito J, Washiyama K, Hong Kim C, Ibuchi Y. Fenestration of the anterior cerebral artery. Neuroradiology 1981; 21:277−280.

14. Kayembe KN, Sasahara M, Hazama F. Cerebral aneurysms and variations in the circle of Willis. Stroke 1984; 15:846−850.

15. Kobayashi S, Yuge T, Sugita Y, et al. Azygos anterior cerebral artery aneurysm associated with fenestration of the anterior cerebral artery. Kurume Med J 1986; 33:149−153.

16. Ogasawara H, Inagawa T, Yamamoto M, Kamiya K. Aneurysm in a fenestrated anterior cerebral artery: case report. Neurol Med Chir (Tokyo) 1988; 28:575−578.

17. Suzuki M, Onuma T, Sakurai Y, Mizoi K, Ogawa A, Yoshimoto T. Aneurysms arising from the proximal (A1) segment of the anterior cerebral artery. A study of 38 cases. J Neurosurg 1992; 76:455−458.

18. Friedlander RM, Ogilvy CS. Aneurysmal subarachnoid hemorrhage in a patient with bilateral A1 fenestrations associated with an azygos anterior cerebral artery. Case report and literature review. J Neurosurg 1996; 84:681−684.

19. Kachara R, Nair S, Gupta AK. Fenestration of the proximal anterior cerebral artery (A1) with aneurysm manifesting as subarachnoid hemorrhage--case report. Neurol Med Chir (Tokyo) 1998; 38:409−412.

20. Ihara S, Uemura K, Tsukada A, Yanaka K, Nose T. Aneurysm and fenestration of the azygos anterior cerebral artery--case report. Neurol Med Chir (Tokyo) 2003; 43:246−249.

21. Kim TH, Lee HK, Rhee JJ, Lee SJ, Lee CH, Kim MS. The incidence and clinical significance of fenestrations in the horizontal segment of the anterior cerebral artery detected by conventional angiography and magnetic resonance angiography. J Korean Neurosurg Soc 2006; 40:74−78.

22. Uchino A, Nomiyama K, Takase Y, Kudo S. Anterior cerebral artery variations detected by MR angiography. Neuroradiology 2006; 48:647−652.

23. Bharatha A, Aviv RI, White J, Fox AJ, Symons SP. Intracranial arterial fenestrations: frequency on CT angiography and association with other vascular lesions. Surg Radiol Anat 2008; 30:397−401.

24. Koh JS, Lee SH, Bang JS, Kim GK. Three-dimensional angiographic demonstration of plexiform fenestrations of the proximal anterior cerebral artery associated with a ruptured aneurysm. J Korean Neurosurg Soc 2008; 44:338−340.

25. Dimmick SJ, Faulder KC. Fenestrated anterior cerebral artery with associated arterial anomalies. Case reports and literature review. Intervent Neuroradiol 2008; 14:441−445.

26. Koh JS, Kim EJ, Lee SH, Bang JS. Ruptured aneurysm arising from the distal end of a proximal A1 fenestration: case report and review of the literature. J Korean Neurosurg Soc 2009; 45:43−45.

27. van Rooij SB, van Rooij WJ, Sluzewski M, Sprengers ME. Fenestrations of intracranial arteries detected with 3D rotational angiography. AJNR Am J Neuroradiol 2009; 30:1347−1350.

28. Zhao HW, Fu J, Lu ZL, Lü HJ. Fenestration of the anterior cerebral artery detected by magnetic resonance angiography. Chinese Med J (Engl) 2009; 122:1139−1142.

29. Ješić A, Torbica S, Marić S, Popović S, Kozić D. Anatomic variations of the anterior portion of the circle of Willis: An MR angiography study. Curr Top Neurol Psychiatr Relat Discip 2011; XIX:9−16.

30. Aktüre E, Arat A, Niemann DB, Salamat MS, Baskaya MK. Bilateral A1 fenestrations: Report of two cases and literature review. Surg Neurol Int 2012; 3:43. http://www.ncbi.nlm.nih.gov/pmc/articles/PMC3347490/

31. Vasović LP. Reevaluation of the morphological parameters according to 11 different duplications of the fetal vertebral artery at prevertebral (V1) and intracranial (V4) parts. Cells Tissues Organs 2004; 176:195−204.

32. Moffat DB. The embryology of the arteries of the brain. Arris and Gale lecture delivered at the Royal College of surgeons of England. 1962; pp 368−382. http://www.ncbi.nlm.nih.gov/pmc/articles/PMC2414182/pdf/annrcse00385-0020.pdf

33. Finlay HM, Canham PB. The layered fabric of cerebral artery fenestrations. Stroke 1994; 25:1799−1806.

34. Weil AG, Bojanowski MW, Scholtes F, Darsaut TE, Signorelli F, Weill A. Angiographic pitfall: duplicated tapered A1 segment of the anterior cerebral artery mimicking an anterior communicating artery aneurysm. Interv Neuroradiol 2011; 17:179−182.

MORPHOMETRIC CHARACTERISTICS OF JUGULAR FORAMEN AND SIGMOID SINUS GROOVE: THEIR POSSIBLE CONNECTIONS WITH HIGH JUGULAR BULB PRESENCE

Ivan Jovanović[1], Slađana Ugrenović[1], Vesna Stojanović[1], Miljan Krstić[2], Milena Trandafilović[1], Jovana Čukuranović[1]*

University of Niš, Faculty of Medicine, [1]Department of Anatomy, [2]Department of Pathology, Niš, Serbia

Abstract. *High jugular bulb represents very important variation in neurosurgery. The aim of our research was to measure certain characteristics of jugular foramen and surrounding bony structures in order to evaluate their possible significance in high jugular bulb detection. Thirty seven dried human skull sagittal sections were used as material. Sigmoid sinus groove width and depth, jugular fossa height and exocranial opening mean diameter were measured with vernier caliper. Internal auditory canal height and the distance between its inferior margin and superior margin of petrous bone, jugular foramen endocranial opening area and sino dural angle were measured with ImageJ. Cluster analysis with jugular fossa height as classification parameter was used for the classification of the analyzed skull sagittal sections. Classification analysis showed the presence of two groups: the first with predominantly low height of jugular fossa dome, the second with significantly higher values of jugular fossa dome, sino-dural angle and mean diameter of jugular fossa exocranial opening. This group predominantly included right skull sagittal sections. In addition, sigmoid sinus groove width and depth, jugular foramen endocranial opening area and jugular fossa exocranial opening mean diameter were significantly higher on the right in relation to the left side. So, it can be concluded that high jugular fossa dome is more frequently associated with sigmoid sinus groove anterior position, high values of mean diameter of jugular fossa exocranial opening and sigmoid sinus groove width and depth, especially on the right side.*

Key words: *Jugular fossa, high bulb of jugular vein, groove for sigmoid sinus, morphometry*

Introduction

Jugular foramen is hiatus located between lateral part of the occipital bone and petrous part of the temporal bone. However, today authors [1–4] more frequently describe its appearance as a canal and not as a real foramen. They describe its endocranial opening and exocranial opening, which are oriented in different planes. Its acute-angled triangular endocranial opening is by intrajugular processes divided into two or, less frequently, into three compartments. Neurovascular elements which pass through this opening are glossopharyngeal nerve and inferior petrosal sinus, which pass through its smaller anteromedial compartment, while vagus nerve, accessory nerve, posterior meningeal artery and sigmoid sinus pass through posterolateral part of the jugular foramen. Exocranial opening has alembic shape and it leads into the jugular fossa in which jugular bulb is located. The highest part of jugular fossa is its dome. Caroticojugular spine with petrosal fossula is in front, while funnel shaped pyramidal fossa with external opening of

cochlear aqueduct is anteromedially located in relation to its exocranial opening [4].

In spite of numerous previous radiological and anatomical studies, there is no agreement between authors about the jugular foramen nature, its canal like appearance and its compartments nomenclature. Jugular foramen anatomical variations, such as high bulb of jugular vein, jugular bulb bony covering dehiscence, jugular bulb diverticulum, are very frequently present. Superior jugular bulb is one of them which can influence the choice of surgical approach in the treatment of primary (glomus tumor, schwannoma), secondary (meningioma, chondrosarcoma) jugular foramen lesions [5], as well as other lesions located in posterior cranial fossa [6]. It could also be the cause of complications, like profuse bleeding and air embolism during the surgical intervention [7]. Takdemir et al. [4] considered that more frequent superior sagittal sinus drainage through right transverse, then right sigmoid sinus and right jugular foramen might be associated with its more frequent presence on the right side and, consequently, with its pathogenesis.

So, since there are indirect implications about sigmoid sinus involvement in the high jugular bulb pathogenesis and there is lack of literature data about morphological and positional relationships between

Correspondence to: Ivan Jovanović, MD, PhD
Faculty of Medicine, Dept. of Anatomy,
81 Dr Zoran Đinđić Blvd., 18000 Niš, Serbia
Phone: +381 69 23 51 980 Fax: +381 18 42 38 770
E-mail: ivanjov@sbb.rs

sigmoid sinus and jugular foramen, the aim of our research was to evaluate such relationships by the application of morphometric and statistical methods.

Material and Methods

The material included 37 sagittal sections (17 left and 20 right) of Caucasian adult dried human skulls, with completely preserved jugular foramen and sigmoid sinus groove. Skulls are the part of our Department of Anatomy collection. Petrous bones' internal auditory canal's anterior wall was removed. Vernier caliper was used for the measurement of sigmoid sinus groove ver-
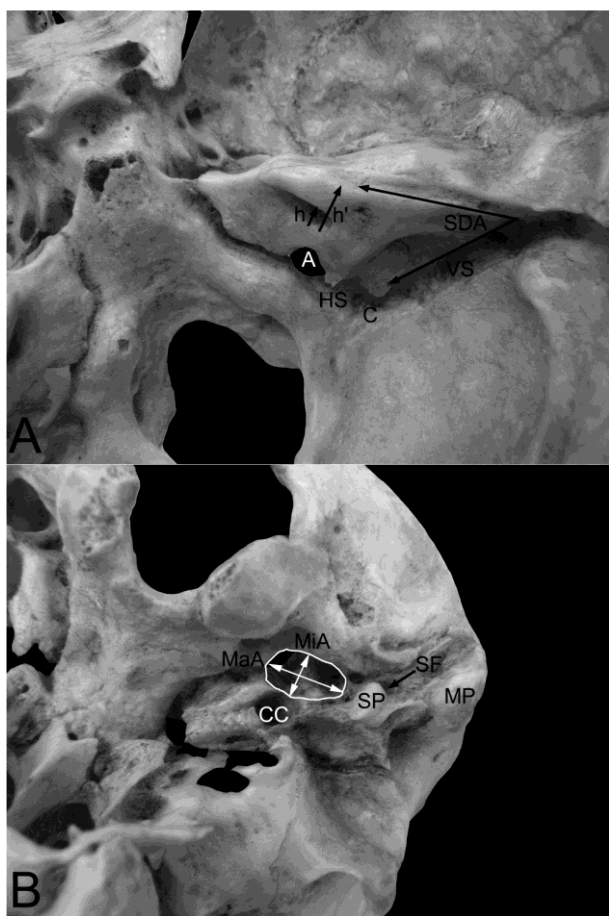

Fig. 1. View of the part of internal (A) and external (B) surfaces of cranial base. A – jugular foramen endocranial opening, sigmoid sinus groove and internal auditory canal: endocranial opening area (A), sigmoid sinus groove vertical segment (VS), curve (C) and horizontal segment (HS), sinodural angle (SDA), internal auditory canal height (h) and the distance between internal auditory canal inferior margin and petrous bone superior margin (h'); B – inferior surface of the petrous bone: mastoid process (MP), stylomastoid foramen (SF), external opening of the carotid canal (CC), styloid process (SP), and diameter of the jugular fossa external opening along the major (MaA) and minor axis (MiA).

tical segment's width and depth, sigmoid sinus groove curve width and depth and its horizontal segment width and depth (Fig. 1, A). Mean sigmoid sinus groove width (SSGw) and depth (SSGd) were calculated as average of its three segments measured corresponding values. Vernier caliper was also applied for the measurement of the jugular fossa height (FJH) as a distance between the level of its exocranial opening and its dome and two jugular foramen exocranial opening diameters: one parallel to the major and the other parallel to its minor axis (Fig. 1, B). Its mean diameter (D) was calculated as average of the latter two cited diameters. Afterwards, petrous bone posterior surface, together with vernier caliper scale, was captured with digital camera and obtained images were additionally analyzed with ImageJ (http://rsb.info.nih.gov/ij/). Vernier caliper millimeter scale was used for the system's spatial calibration. Jugular foramen endocranial opening area (A), sino-dural angle (SDA) as angle between petrous bone superior margin and sigmoid sinus groove vertical segment, internal auditory canal's height (h) and the distance between internal auditory canal inferior margin and petrous bone superior margin (h') (Fig. 1, A) were measured with this software.

Statistical analysis was performed by NCSS-PASS 2007 software (http://www.ncss.com/). Cluster analysis (k-means method), with fossa jugularis height as classification parameter, was done in order to obtain two groups of cases with its significantly different values. Significance of differences of the latter cited measured morphometric parameters of the obtained groups, as well as of the right and left skull sagittal sections, was evaluated by Student's t-test. Main effects of the side, group membership and their interaction for the evaluated morphometric parameters were analyzed by Two Way ANOVA. Additionally, the proportion of right and left skull sagittal sections as well as bony bridging in by cluster analysis obtained groups was tested with Chi-square test. Effect sizes of the established differences were calculated according to the Lipsey's and Wilson's formulas [8].

Results

Endocranial opening was in majority of the cases irregular, with approximately triangular shape and apex anteromedially directed. It was composed of two parts: smaller anteromedial and larger posterolateral, which were in most of the cases incompletely separated with temporal and occipital bones' intrajugular processes. Complete bony bridging and consequently bipartite endocranial opening was observed in 12 (5 on the left and 7 on the right side) cases (32%). Incisura which resembled glossopharyngeal recess was rarely observed. Superiorly, on the petrous bone posterior side porus acusticus internus was located. Sigmoid sinus groove beginning was placed at the level of petrous bone superior margin and transverse sinus groove junction. It extended downwards till the endocranial opening and along its course we differentiated two clearly visible segments:

longer vertical and shorter horizontal. Sigmoid sinus groove curve was located between these two segments. Generally, sigmoid sinus groove width decreased from vertical segment toward its curve and then in horizontal segment increased slightly till the endocranial opening. Exocranial opening of the jugular foramen was mostly oval in shape. Jugular fossa was above it and ended superiorly with its dome, which was present in all cases.

Morphometric and statistical analysis

The results of morphometric analysis are presented in Table 1. Generally, mean values of the internal auditory canal height, the distance between internal auditory canal inferior margin and petrous bone superior margin and sino-dural angle were not significantly different between the right and left side, respectively (Table 2). Mean jugular foramen endocranial opening area (Table 2 and Fig. 2, A), exocranial opening mean diameter

(Table 2 and Fig. 2, B), mean sigmoid sinus groove width and depth (Table 2 and Fig. 2, B) were significantly higher on the right than on the left side. Latter cited differences were characterized with medium (for A) and large effect sizes (for D, SSGw and SSGd). Mean FJH was higher on the right in relation to the left side, but this difference was not statistically significant and was characterized with small to medium effect size (Table 2). So, these results did not suggest significant lateralization of the high jugular fossa.

Cluster analysis was performed in order to obtain groups with significantly different mean jugular fossa height. Its results are showed in Table 2. Two significantly different groups are obtained. Fourteen left (56%) and 11 right (44%) sagittal sections of the skull were in the first group (totally 25 sections). Second group included 12 skull sagittal sections, from which 9 were right (75%) and 3 were left (25%). Chi-square test did not show significant predominance of right or left side

Table 1. Morphometric characteristics of jugular foramen, sigmoid sinus groove and internal auditory canal

Case	Side	Group	h (mm)	h' (mm)	A (mm^2)	D (mm)	FJH (mm)	SSGw (mm)	SSGd (mm)	SDA (^{0})
1	Left	I	3.96	6.61	67.18	8.48	11.50	6.86	4.14	59.12
2	Right	I	5.23	8.94	45.36	9.75	11.42	6.28	3.37	59.62
3	Right	I	3.92	7.46	54.40	10.53	12.06	6.54	4.48	56.28
4	Right	I	3.01	5.96	47.49	7.11	6.56	7.87	4.94	51.03
5	Left	I	3.79	7.59	39.52	8.44	9.24	8.66	5.91	61.33
6	Right	I	4.64	7.22	89.57	8.21	12.92	9.36	8.05	48.46
7	Right	I	4.83	8.03	79.75	11.32	11.48	11.10	5.34	45.64
8	Right	I	4.48	7.66	65.89	8.00	7.06	7.98	3.69	59.23
9	Left	I	4.13	7.43	41.73	5.20	10.10	5.33	2.93	66.71
10	Left	I	4.35	7.76	55.84	6.96	11.38	7.38	3.08	40.88
11	Left	I	3.92	7.82	25.59	8.72	11.48	5.79	3.98	55.57
12	Left	I	2.50	6.12	40.74	8.05	9.70	7.92	3.81	32.97
13	Right	I	4.99	8.00	50.28	6.17	10.30	6.01	5.41	53.65
14	Right	I	4.12	7.46	50.89	9.53	12.30	8.34	6.15	47.63
15	Left	I	4.32	8.05	43.25	7.11	6.60	6.33	3.75	34.97
16	Right	I	4.84	8.10	86.79	8.83	11.78	8.97	3.56	61.81
17	Left	I	3.95	5.66	57.84	9.01	13.02	7.09	5.42	39.09
18	Right	I	4.25	6.89	44.64	7.72	10.20	7.67	6.41	44.49
19	Left	I	5.45	8.50	27.99	9.87	11.78	5.70	3.95	35.85
20	Left	I	4.50	8.16	36.12	6.56	11.58	7.72	4.04	42.46
21	Left	I	2.98	6.15	37.41	6.60	12.30	6.38	5.03	58.09
22	Left	I	3.70	6.40	39.52	9.81	9.02	6.24	5.12	35.18
23	Right	I	4.17	8.75	42.41	8.35	11.42	8.43	7.09	36.63
24	Left	I	5.62	10.04	40.75	7.47	11.38	5.84	5.33	33.13
25	Left	I	5.11	9.24	79.70	4.63	12.46	4.56	3.55	50.20
26	Left	II	4.53	8.59	45.44	10.11	14.54	5.58	2.60	64.63
27	Left	II	4.72	6.69	39.96	8.47	18.12	8.29	2.73	58.83
28	Left	II	4.09	7.90	32.03	7.85	17.36	5.65	4.01	61.75
29	Right	II	4.54	8.58	66.30	9.12	14.40	6.70	2.39	68.02
30	Right	II	4.17	6.97	76.09	10.84	14.94	7.68	3.60	59.53
31	Right	II	4.01	5.88	90.89	8.64	13.80	11.92	5.04	60.69
32	Right	II	3.69	8.01	35.82	11.80	19.82	7.33	4.95	62.35
33	Right	II	4.99	8.49	38.92	9.16	14.42	7.02	5.28	45.87
34	Right	II	4.45	8.58	36.22	7.71	13.64	7.89	6.15	49.35
35	Right	II	4.01	7.96	29.67	11.25	13.82	7.38	6.11	45.41
36	Right	II	3.54	5.90	32.05	10.49	14.10	7.19	5.69	32.97
37	Right	II	5.88	8.57	60.08	7.77	20.30	8.33	6.37	47.41

Table 2. Morphometric characteristics of jugular foramen, sigmoid sinus groove and internal auditory canal in obtained groups and on the left and right side of the skull

Side	Left (n = 17)			Right (n = 20)			t-test statistics section			
Parameter	Mean	Md	SD	Mean	Md	SD	T	DF	p	d
h (mm)	4.21	4.13	0.79	4.39	4.35	0.65	0.74*	35	0.462	0.25
h' (mm)	7.57	7.76	1.18	7.67	7.98	0.95	0.28*	35	0.778	0.09
A (mm^2)	44.15	40.74	13.86	56.18	50.59	19.73	2.11*	35	0.042	0.70
D (mm)	7.84	8.05	1.55	9.12	8.98	1.55	2.49*	35	0.018	0.83
FJH (mm)	11.86	11.50	2.85	12.84	12.61	3.34	0.95*	35	0.348	0.31
SSGw (mm)	6.55	6.33	1.15	8.00	7.78	1.48	3.29*	35	0.002	1.08
SSGd (mm)	4.08	3.98	0.99	5.20	5.31	1.39	2.78*	35	0.009	0.92
SDA (^{0})	48.87	50.20	12.44	51.80	50.19	9.06	0.83*	35	0.413	0.27
Group	I (n = 25)			II (n = 12)			t-test statistics section			
Parameter	Mean	Md	SD	Mean	Median	SD	T	DF	p	d
h (mm)	4.27	4.25	0.76	4.39	4.31	0.63	0.45*	35	0.653	0.17
h' (mm)	7.60	7.66	1.07	7.68	7.98	1.05	0.20*	35	0.840	0.08
A (mm^2)	51.63	45.36	17.48	48.62	39.44	19.98	0.47*	35	0.643	0.16
D (mm)	8.10	8.21	1.60	9.43	9.14	1.43	2.45*	35	0.019	0.86
FJH (mm)	10.76	11.42	1.84	15.77	14.48	2.45	6.96*	35	<0.001	2.44
SSGw (mm)	7.21	7.09	1.47	7.58	7.35	1.63	0.68*	35	0.498	0.24
SSGd (mm)	4.74	4.48	1.30	4.58	4.99	1.46	0.35*	35	0.731	0.12
SDA (^{0})	48.40	48.46	10.43	54.73	59.18	10.35	1.73**	35	0.046	0.61

*Two – tailed T-test
**One – tailed T-test
DF, degrees of freedom; d, effect size
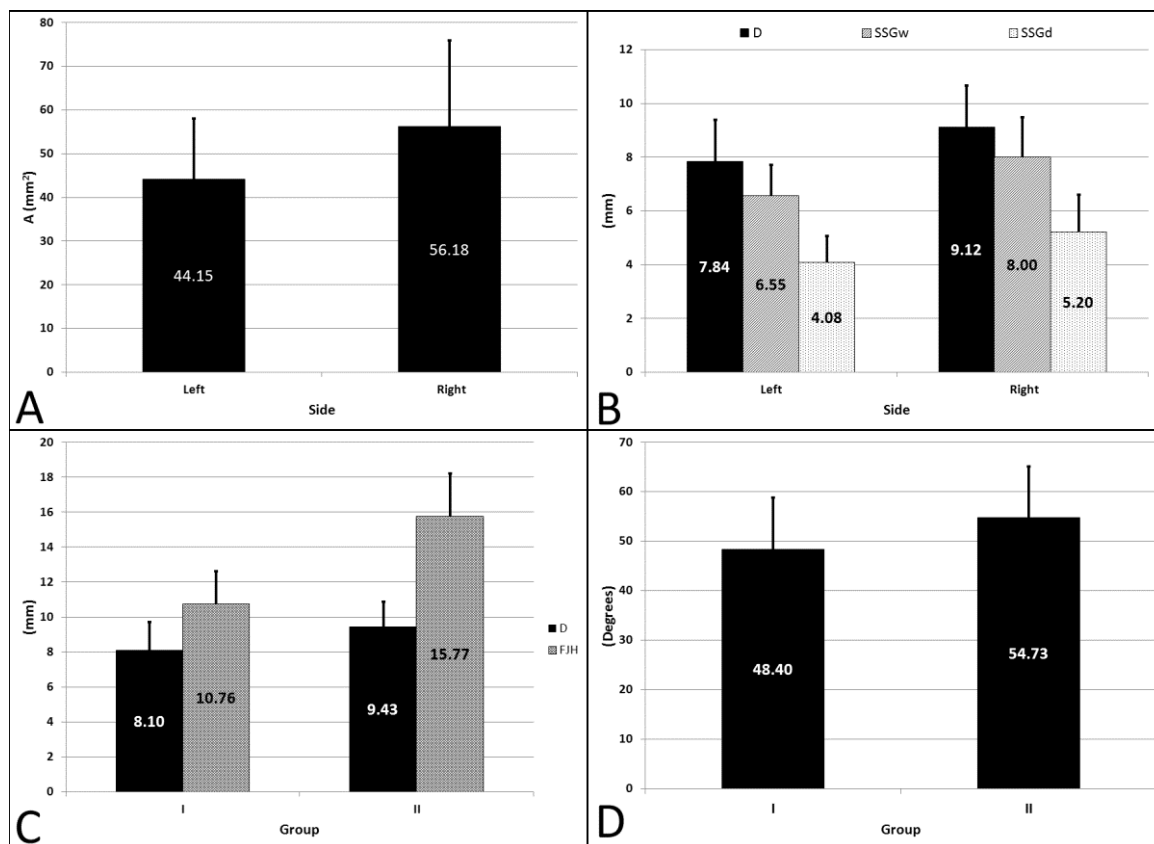
Fig. 2. Mean jugular foramen endocranial opening area on the left and right sides and sigmoid sinus groove morphometric parameters. A – jugular foramen morphometric parameters; B – mean sigmoid sinus groove width and depth and mean diameter of the jugular foramen exocranial opening on the left and on the right side; C – mean fossa jugularis height and exocranial opening diameter in by cluster analysis obtained groups; D – mean sino-dural angle in obtained groups.

in the obtained groups (H = 3.14, n = 37, DF = 1, p = 0.077). Nevertheless, obtained effect size for this test was moderate to large (d = 0.61), which might point to the conclusion that above cited absence of significance is probably due to the sample's size and that there could be mild predominance of the left in the first and right sagittal sections in the second group. Chi-square test did not show more frequent presence of complete jugular foramen endocranial opening bony bridging in the latter cited groups (H = 0.007, n = 37, DF = 1, p = 0.935, d = 0.03). As far as jugular fossa characteristics are concerned, its height and external opening mean diameter were significantly higher in the second group than in the first and these differences were characterized with large effect sizes (Table 2 and Fig. 2, C). Sino-dural angle's mean value of the second group was significantly higher than the same one of the first group and this difference was characterized by medium to large effect size (Table 2 and Fig. 2, D). Differences between all other evaluated morphometric parameters (h, h', A, SSGw and SSGd) of the above cited groups were not statistically significant (Table 2).

Finally, in order to evaluate main effects of the group membership and side, as well as their interaction for evaluated morphometric parameters, we conducted Two Way ANOVA. Results of this analysis confirmed significant main effect of the side for the mean jugular foramen endocranial opening area (F(1,33) = 3.99, p = 0.05, η = 0.33) and sigmoid sinus groove's width (F(1,33) = 7.46, p = 0.01, η = 0.43) and depth (F(1,33) = 9.89, p = 0.004, η = 0.48) with values of the right side being significantly higher than the same of the left side. Significant main effect of the group membership was established for the mean jugular fossa height (F(1,33) = 42.85, p < 0.001, η = 0.75) and sino-dural angle (F(1,33) = 4.43, p = 0.043, η = 0.34) with values of the second group being significantly higher in relation to the first group, too. Significant interaction between the side and group membership was not established for any of the evaluated morphometric parameters.

Discussion

According to Roche et al. [7] high jugular bulb presents the structure which is a connecting link between the sigmoid sinus and internal jugular vein. It is located in the jugular fossa at the inferior and medial side of the petrous bone. Jugular bulb upper extremity is at the level of jugular fossa dome. Its wall is thinner than the wall of sigmoid sinus, as well as internal jugular vein, because of the absence of sinus dural and vein's adventitial layer in it, respectively. The position of jugular bulb exhibits numerous variations. The most important variation is its high position, whose incidence varies from 6% to 65% [9]. After the development of translabyrinthine and retrolabyrinthine approaches in the cerebellopontine angle tumors exposure and surgical treatment, this variation acquired great importance. Its presence increases the possibility of the intraoperative com-

plications like profuse bleeding, or air embolism, due to its unintentional injuring [10]. High jugular bulb also impedes surgical operative area and reduces the exposure and removal of cerebellopontine tumors [7,9]. Its position can be lateral when it protrudes into the middle ear cavity above the level of inferior rim of tympanic ring. Another possibility is its high and medial position when it is in relation with internal auditory canal [7]. Different anatomical landmarks, such as inferior tympanic annulus, round window, basal turn of cochlea and internal auditory canal, were used for its definition. From the surgeon's point of view, internal auditory canal is the best landmark [9]. According to Roche et al. [7] jugular bulb is in high position when its dome is less than 6.5 mm below the inferior margin of internal auditory canal. Jugular bulb is in very high position when its dome reaches the level of internal auditory canal and overtakes its floor. This anatomical variation is termed overlapping high jugular bulb. During our research we evaluated the location and height of internal auditory canal. We did not find significant differences between obtained groups for the internal auditory canal's height and the distance from internal auditory canal inferior margin and petrous bone superior margin. In such way, we tried to exclude the possibility that internal auditory canal's lower position or its increased height could be the cause for the reduction of distance between the dome of jugular fossa and internal auditory canal inferior wall. There were numerous attempts by other authors to explain the presence of high jugular bulb by reduced mastoid pneumatization and size, but these attempts failed [11,12]. Today, general opinion is that the right jugular foramen is larger than the left one [4]. Authors also agree that the incidence of high jugular bulb increases with age and is higher on the right than on the left side [6,7,9,12,13] They considered that the large superior sagittal sinus drains through the right transverse, then right sigmoid sinus and right jugular foramen [4]. Navsa and Kramer [2] found during their jugular foramen morphometric analysis that the area of its endocranial and exocranial opening and jugular fossa dome height and jugular fossa volume were significantly higher on the right side. We also observed significantly higher values of the jugular fossa endocranial opening area and exocranial opening mean diameter on the right side, while jugular fossa dome was higher on the right side but this difference was not significant. This can be explained by differences in evaluated samples size and by different racial structure of the analyzed material. Firstly, our sample size (n = 37) was smaller than the ones of Navsa and Kramer [2]. The influence of the sample's size on our results can be additionally confirmed by the fact that in our group with significantly higher jugular fossa height the frequency of the right skull sagittal sections was higher than the left ones with medium effect size. In such way, significant right sided asymmetry of the higher jugular fossa dome cannot be excluded in our study, too. Secondly, study of Navsa and Kramer [2] included skulls of black and white racial

origin, while we used only Caucasian skulls' sagittal sections. The influence of the different racial structure in the analyzed material can be additionally supported by the finding of the latter cited authors that significantly higher right jugular fossa was observed only in skulls of black, but not in the ones of white racial origin. Wysocki [12] cited in his paper that the sigmoid sinus characteristics are very important in high jugular bulb formation. Sarmiento and Eslait [14] and Wysocki [12] also cited that the sigmoid sinus anterior position is associated with the high jugular bulb presence, while posterior position of the sigmoid sinus in the mastoid is associated with so called flat jugular bulb and its low position. Significantly higher values of sino-dural angle in the group with higher jugular fossa dome in our study may be in accordance with above cited assumption. It can be said that higher values of this angle are associated with steeper and more anteriorly positioned sigmoid sinus groove and hence might have the role in the increase of blood pressure in its terminal part and consequently high bulb formation. This is in agreement with the positions of the Sarmiento and Eslait [14] and Wysocki [12] about the mechanism responsible for the high jugular bulb genesis. Significantly higher values of the sigmoid sinus groove width and depth detected on the right side during our research may additionally support the hypothesis that together with the anterior position, larger sigmoid sinus dimensions on the right side might be responsible for the increase of the blood pressure in the jugular fossa region, which will finally

result in increased height of its dome and high jugular bulb presence.

Conclusion

It can be concluded that sigmoid sinus groove width and depth and jugular foramen endocranial opening area were higher on the right in relation to the left side. Higher jugular fossa dome was more frequent on the right side. This phenomenon was rather associated with higher values of jugular foramen exocranial opening diameter and sino-dural angle than with the latter cited sigmoid sinus groove and jugular foramen endocranial opening morphometric parameters.

In our opinion, acquisition of the sino-dural angle, jugular fossa exocranial opening diameter and additionally sigmoid sinus width and depth, could be potentially useful for more precise interpretation of *High-Resolution Computed Tomography* images in high jugular bulb preoperative diagnosis. High values of sino-dural angle, jugular fossa exocranial opening mean diameter and wider and deeper sigmoid sinus, especially on the right side may also represents signs which should draw the surgeons attention to more thoroughly evaluate the possibility of this potentially dangerous anatomical variation presence.

References

1. Chong VF, Fan YF. Radiology of the jugular foramen. Clin Radiol 1998; 53:405–416.
2. Navsa N, Kramer B. A quantitative assessment of the jugular foramen. Ann Anat 1998; 180:269–273.
3. Tekdemir I, Tuccar E, Aslan A, et al. The jugular foramen: a comparative radioanatomic study. Surg Neurol 1998; 50:557–562.
4. Tekdemir I, Tuccar E, Aslan A, Elhan A, Ersoy M, Deda H Comprehensive microsurgical anatomy of the jugular foramen and review of terminology. J Clin Neurosci 2001; 8:351–356.
5. Caldemeyer KS, Mathews VP, Azzarelli B, Smith RR. The jugular foramen: a review of anatomy, masses, and imaging characteristics. Radiographics 1997; 17:1123–1139.
6. Atilla S, Akpek S, Uslu S, Ilgit ET, Isik S Computed tomographic evaluation of surgically significant vascular variations related with the temporal bone. Eur J Radiol 1995; 20:52–56.
7. Roche PH, Moriyama T, Thomassin JM, Pellet W. High jugular bulb in the translabyrinthine approach to the cerebellopontine angle: anatomical considerations and surgical management. Acta Neurochir (Wien) 2006; 148:415–420.
8. Lipsey MW, Wilson DB. Practical meta-analysis, 1st edn. Sage Publications: London, 2001.
9. Aslan A, Falcioni M, Russo A, et al. Anatomical considerations of high jugular bulb in lateral skull base surgery. J Laryngol Otol 1997; 111:333–336.
10. Mutlu C, da Costa SS, Paparella MM, Schachern PA. Clinical-histopathological correlations of pitfalls in middle ear surgery. Eur Arch Otorhinolaryngol 1998; 255:189–194.
11. Jacob CE, Rupa V. Infralabyrinthine approach to the petrous apex. Clin Anat 2005; 18:423–427.
12. Wysocki J. Minimal distances between temporal bone structures and their mutual correlations. Med Sci Monit 2002; 8:BR80–BR83.
13. Keskil S, Gozil R, Calguner E. Common surgical pitfalls in the skull. Surg Neurol 2003; 59:228–231.
14. Sarmiento PB, Eslait FG. Surgical classification of variations in the anatomy of the sigmoid sinus. Otolaryngol Head Neck Surg 2004; 131:192–199.

MORPHOLOGICAL AND MORPHOMETRIC ANALYSIS OF FASCICULAR STRUCTURE OF TIBIAL AND COMMON PERONEAL NERVES

Slađana Ugrenović[1], Marija Topalović[2], Ivan Jovanović[1], Aleksandra Antović[3], Miroslav Milić[3], Aleksandra Ignjatović[4]

University of Niš, Faculty of Medicine, [1]Department of Anatomy, [2]Student of Faculty of Medicine, [3]Institute for Forensic Medicine, [4]Department of Medical Statistics and Informatics, Serbia

Abstract. *In clinical practice, the common peroneal nerve palsy is more frequent compared to the tibial nerve, although both are part of the sciatic nerve. The aim of our study was to analyze and compare the fascicular structure of the tibial and common peroneal nerve. For the study we used tissue samples of the sciatic nerve, 19 subjects aged 8–86 years. The samples were processed by standard histological procedures, after which were made transverse sections of 5 microns and stained with hematoxylin-eosin staining. First, we analyzed the number, size and arrangement of fascicle. After that we made photographs of each common peroneal and tibial nerve fascicules and to each the area and maximum diameter were determined. In all studied cases, a connective tissue septum that separates the fascicular groups, tibial and common peroneal nerve was detected. The tibial nerve fascicular group was numerous and medially localized while the common peroneal nerve fascicular group was less numerous and placed laterally. Morphometric analysis showed that the common peroneal nerve has statistically significantly lower number of fascicles (16.28 ± 4.39) and the total fascicular area ($2.13 \times 106 \pm 8.91 \times 106 \ \mu m2$) compared to the tibial nerve (average 35 fascicles ± 13.29 and mean fascicular area $5.05 \times 106 \pm 2.46 \times 106 \ \mu m2$). The average value of the maximum diameter and the average area of the investigated fascicle, tibial and common peroneal nerves showed no statistically significant differences. Correlation analysis of the studied parameters with the age of subjects also did not reach statistical significance. Fascicular structure with a smaller number of larger fascicles and sparse epineurial connective tissue sheath may increase susceptibility of the common peroneal nerve injury.*

Key words: *Common peroneal nerve, fascicular pattern, morphometry, aging*

Introduction

Normal conducting of electric impulses through the nerve provides connective tissue sheaths which prevent interference of electrical impulses. They are also important for the process of regeneration of fibers and provide strength and elasticity nerve. Endoneurium is a connective tissue that separates the individual myelinated fibers and groups of amyelinated nerve fibers. In addition to blood vessels in the endoneurium collagen fibers, fibronectin and laminin are present [1,2]. Perineurium is specific layer built of the concentrically arranged cell lamella (up to 15 in humans). This one connective sheath is considered to be a significant diffusion barrier which preserves constant endoneurial content [1,3]. Endoneurial content surrounded by perineurium makes the fascicle, which is a histological nerve unit. Nerves are composed of different number of fascicles, which are also of different sizes. According to the number and size of the fascicle, nerves can be divided into monofascicular

nerve with a single fascicle, oligofascicular nerve with 2–10, and polifascicular nerve with more than 10 fascicles, which can be arranged in groups or diffusely [4]. Fascicles within the nerve stem are interconnected, which contributes to resistance of the nerve stretching. Diameter of majority of fascicles ranged from 0.04 to 2 mm, although there were fascicles up to 4 mm in diameter [1]. Epineurium is the most superficial connective tissue layer that unites all fascicles in a single nerve stem. It is composed of a network of collagen fibers, loose connective tissue with blood vessels and varying amounts of adipose tissue designed to provide a loose matrix for nerve fascicles.

The sciatic nerve is the largest nerve of the human body which consists of two parts, tibial and common peroneal nerve, covered by a common connective nerve sheath. Tibial nerve arises from the anterior branches of L4–L5 and S1–S3 nerves and its motor fibers innervate the posterior compartment of muscles of the thigh (except the short head of the biceps femoris) and leg, and also the muscles of the soles. The common peroneal nerve arises from the anterior branches of L4–L5 and S1–S2 nerves and its motor fibers innervate the short head of the biceps femoris in the thigh, the muscles of anterior and lateral compartment of leg, and also the

Correspondence to: Slađana Ugrenović, MD, PhD
Faculty of Medicine, Dept. of Anatomy,
81 Dr Zoran Đinđić Blvd., 18000 Niš, Serbia
Phone: +381 69 19 67 157 Fax: +381 18 42 38 770
E-mail: sdugren@sbb.rs

muscles of dorsal region of foot [5,6]. In relation to the tibial nerve, peroneal nerve palsy was significantly more frequent in the clinical practice. It usually occurs as a result of compression, torsion and lacerations of common peroneal nerve caused by fractures to the neck of the fibula. However, the common peroneal nerve palsy can occur as a complication after fractures of the tibia, femur and acetabulum, sports injury of knee ligaments, orthopedic interventions of the knee joint and ankle joint, heart surgery, long-term immobilization and even rapid weight loss [7–9]. Having in mind that the number, size, arrangement of fascicle affects the resistance to nerve injury, the aim of our study was to analyze and compare the fascicular structure of the NT and the NPC.

Material and Methods

The study was performed on sciatic nerve tissue samples of 19 individuals (10 males and 9 females) aged from 8 to 86 years. During lifetime they had not been diagnosed with neurologic or metabolic disorder or any other kind of SNs damage. Nerve tissue was obtained during the routine autopsies performed at the Institute for Forensic Medicine in Niš. The time period from death to the autopsy was not longer than 24^h. Firstly, the cut of the skin, 5 cm long, was made at the middle part of posterior femoral region. Afterwards, the muscles of posterior femoral region were separated with blunt dissection. Then, 3 cm long SNs part was cut and afterwards fixed with 10% buffered formalin. The tissue was further embedded in the paraffin, cut into the slices 5 lm thick and then, routinely processed for the histochemical staining. Afterwards, slices were stained by hematoxylin-eosin.

Morphological and morphometric analysis of fascicular structure

First, we analyzed fascicular pattern of TN and CPN (number, size, shape and arrangement of fascicle) and the presence of fibrous-fatty Compton-Cruveilhier septum ("Co-Cu" septum). In the second part, with the help of digital cameras on the lowest magnification pictures were taken of all the fascicles of TN and CPN (1280 × 960 RGB format). Morphometric analysis was performed using the program for the analysis and processing of digital images "ImageJ". Before each measurement system calibration was performed with the help of an objective micrometer (1:100) at the same magnification. In the section "set measurements" area and Feret diameter options are checked. With the help of polygonal selections a line along the outer edge of perineurium of each fascicle is marked and using the option "measure" the values of areas and Feret diameter for each test nerve fascicles were obtained. After completing the analysis of the number, diameter and areas of TN and CPN, their average values were calculated are then statistically analyzed.

Statistical analysis

The collected data were verified by the authors, coded and entered into a special monitoring database. Statistical analysis was performed by SPSS 16.0. The results were presented in tables and graphically with a text comment. We using standard statistical methods for qualitative and quantitative assessment of the results: the absolute numbers, relative numbers (%), the arithmetic mean value ($\overline{X}$), standard deviation (SD). Normality of distribution of individual values was investigated using Shapiro-Wilk test. For the evaluation of the significance of the difference (p) between the measured values of the tested two samples used in the t-test for two independent samples, if the distribution of the parameters is normal, if the regularity is not satisfied, the comparison is performed by Mann-Whitney-U test. Correlation analysis between different variables was performed by Pearson simple linear correlation. The statistical significance of the frequency on the absolute difference between the samples was tested by χ^2 test. A statistical hypothesis was tested at the level of risk of significance $\alpha = 0.05$, the difference between the samples was considered significant if $p < 0.05$.

Results

Connective-fatty (Co-Cu) septum was detected in all examined cases. This septum divided the sciatic nerve into the two major morphofunctional fascicular groups (Fig. 1, a–b). Common peroneal nerve fascicular group was less numerous, occupied a lateral part of entire nerve cross-section (Fig. 1, b). Tibial nerve fascicular group was more numerous and occupied a medial section of the nerve (Fig. 1, b). Both fascicular groups were polifascicular types of nerves (Fig. 1). Single fascicle and fascicular groups were detected in both nerve, TN (Fig 2, a–b) and CPN (Fig. 2, c–d). Epi- and interfascicular parts of the epineurium were well developed and with noticeably greater amount of adipose tissue in older cases (Figs. 1, b; 2, d).

Morphometric analysis included 298 CPN fascicles and 644 TN fascicles. The results of morphometric analysis are presented in Table 1. Statistically significant difference (p <0.001) was detected in the average number of fascicles, and the average value of the total fascicular area between TN and CPN. The common peroneal nerve had a significantly lower number of fascicles (16.28 ± 4.39) compared to TN (35.33 ± 13.29) and a lower total fascicular area (2.13 × 106 ± 8.91 × 106 μm2) in relation to the TN (5.05 × 106 ± 2.46 × 106 μm2). Other parameters (such as average value of fascicular area and diameter) were not significantly different between NPC and NT.
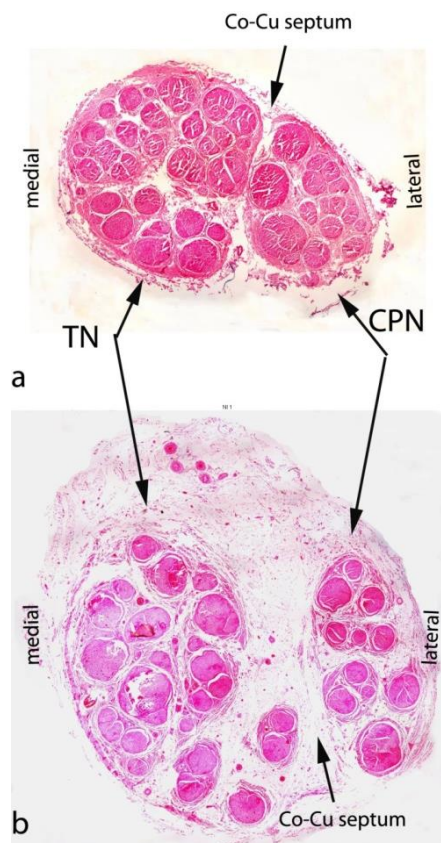
Fig. 1. The sciatic nerves cross-section of cases aged 8 (a) and 81 (b) years. In the lateral part of the cross section was observed CPN (common peroneal nerve) fascicular group; in the medial part was observed a fascicular group of TN (tibial nerve); fascicular groups were separated by Co-Cu septum. Staining with hematoxylin-eosin, photographed under magnifying glass.
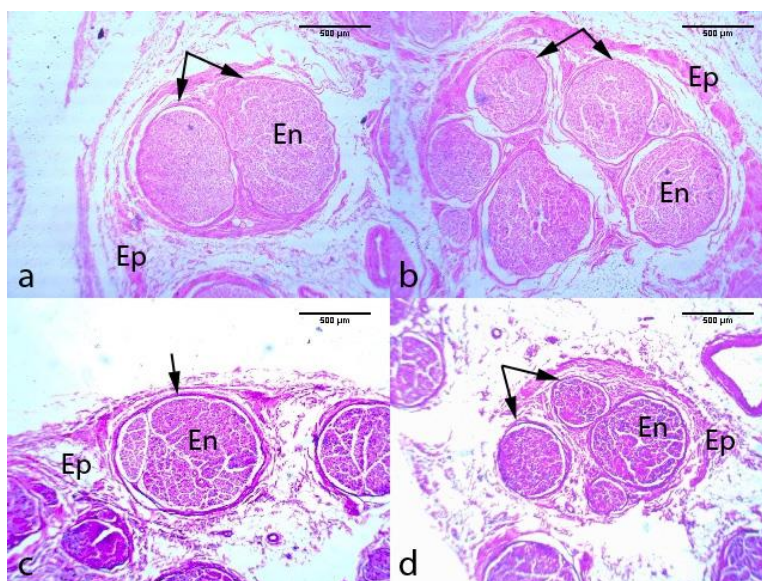
Table 1. Average value of fascicular number, total fascicular area and average value of fascicular area and diameter of CPN (common peroneal nerve) and TN (tibial nerve)

	CPN	TN	p
Fascicular number	16.28 ± 4.39	35.33 ± 13.29	<0.001
Total fascicular area (μm^2)	$2.13 \times 10^6 \pm 8.91 \times 10^5$	$5.05 \times 10^6 \pm 2.46 \times 10^6$	<0.001
Fascicular area (μm^2)	142138.99 ± 90418.28	141629.64 ± 48828.24	0.503
Fascicular diameter (μm)	476.57 ± 139.26	$481.19 \pm 73,32$	0.405

Based on the average values of fascicular diameter and area CPN and TN histogram of distribution was obtained (Figs. 1–2). Fascicles which is the average value of the diameter ranged between 350 and 450 microns where most common in both nerves (Chart 1). Also in both studied nerves, the most numerous fascicles are those whose area ranged from 50000–75000 μm2 (Chart 2). Correlation analysis of all parameters with the age of the examined cases showed no statistic significance (Table 2).

Table 2 Correlation analysis between the studied parameters: mean fascicular area and fascicular diameter of CPN (common peroneal nerve) and TN (tibial nerve) with the age of the examined cases

	Fascicular area of CPN	Fascicular area of TN	Fascicular diameter of CPN	Fascicular diameter of TN
Age (r)	-0.398	0.031	-0.293	0.094
p	0.102	0.907	0.239	0.719

r, simple linear correlation coefficient

Fig. 2. Fascicular structure of the TN with individual macro fascicle inside which can be seen intrafascicular connective septum (2a) and one of the fascicular groups (2b). Fascicular structure of the CPN (common peroneal nerve) with one large fascicle (2c) and fascicular group (2d). Ep, epineurium; En, endoneurium; arrows marked perineurium. Staining with hematoxylin-eosin; magnification × 4.

Chart 1. Histogram of CPN (common peroneal nerve) and TN (tibial nerve) fascicular distribution according to the values of their diameters
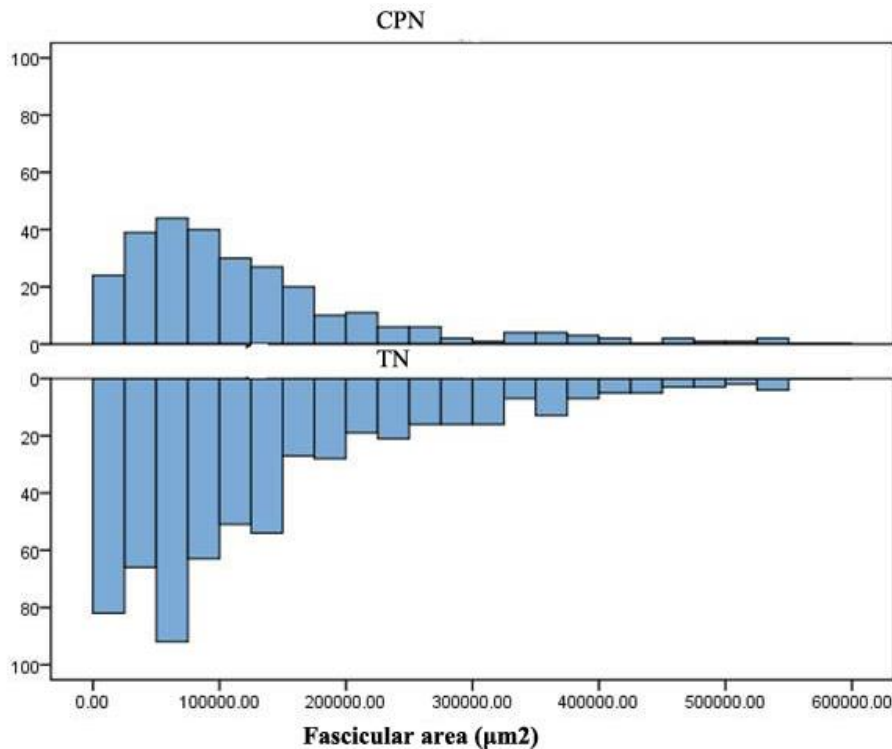
Chart 2. Histogram of CPN (common peroneal nerve) and TN (tibial nerve) fascicular distribution according to the values of their area

Discussion

Peroneal palsy often happens in clinical practice and leads to a foot drop due to paralysis of the anterior and lateral muscles compartment of the lower leg. In order to explain this problem, researchers are looking into CPN anatomical position, its relationship to neighboring structures, sparse vascularization and fascicular morphology. At the level of the gluteal region CPN makes lateral sciatic nerve division and can be compressed by the piriformis. This often

happens if CPN passes through suprapiriform foramen or through piriformis. Such anatomic variations can lead to the so-called piriformis syndrome with the appearance of ischialgia [10,11]. In the posterior femoral region TN continues in the direction of sciatic nerve vertically downwards to the popliteal fossa. Opposed to it, in the top corner of the popliteal fossa CPN changes direction and descends laterally to the neck of the fibula. Because of such direction it is believed that CPN tolerates greater tensile strength during the leg movements than NT. Fractures of the fibular neck or long-press on the nerve in this area (eg. long press of military boots) can damage the CPN [9,12]. In addition to anatomical features, it is considered that the blood supply contributes to the greater vulnerability of CPN to injury and damage. Namely, the TN receives several nutritive arteries from perforating, popliteal and posterior tibial arteries in the region of popliteal fossa. These branches form a richly anastomotic arterial chain inside the NT so it is relatively resistant to ischemic damage. On the other hand, CPN usually supplies a solitary blood vessel, most often a branch of popliteal artery in the region of popliteal fossa [13]. When the arterial nerve chain forms solitary blood vessel, establishing collateral circulation during the compression is more difficult and therefore more easily resulting of ischemic nerve damage [14]. In addition to the clinical and forensic significance, peripheral nerve fascicular pattern has a fundamental, biological significance, since it provides the necessary biomechanical resistance of peripheral nerves, especially limb nerve [4].

Analyzing the fascicular structure, we found that both investigated nerves TN and CPN were of polifascicular type with the group fascicular arrangements. Fascicles were of various sizes, so that they are described as micro-, meso-, and macro fascicles. However, a significant difference was detected in a number of fascicles. Common peroneal nerve had smaller fascicular number (approximately 16) compared to the TN (approximately 35). Also, the total CPN fascicular area was significantly lower compared to TN. There are literature data on the number of whole sciatic nerve fascicles, which ranged from 27 to 70 [13] and from 11 to 93 [1]. Đorđević-Čamba et al. [4] stated that the TN fascicular number ranged from 5–52, while the CPN fascicular number ranged from 1–8, which also confirms a significant difference in the fascicular number between two nerves. There are no literature data for total fascicular area, in particular NPC and NT. The other analyzed parameters, such as average values of fascicular area and fascicular diameter, showed no significant differences between the nerves. Diameter of the majority of fascicles ranged from 350–450 microns of both nerves. Obtained results suggest that CPN fascicular structure is characterized by a smaller number of fascicles, whose diameter and area did not differ from TN fascicles. Baima and Krivickas [9] in their findings suggest that the nerve which has a smaller number of larger fascicles and poor epineurial sheath is more sensitive to pressure and stretching. They also claim that in such fascicular structure, blood vessels are more superficially placed (in epifascicular part of epineurium) and consequently the risk of ischemia is higher (due to the compression of the blood vessels).

Conclusion

In the analysis of fascicular structure of the CPN and TN we have found that CPN has a significantly smaller number of larger diameter fascicles, which may increase its susceptibility to compression, stretching and ischemia.

References

1. Sunderland S. Nerves and nerve injures, 2nd edn. Churchill-Livingstone: New York, 1964.
2. Thomas PK, Olsson Y. Microscopic anatomy and function of the connective tissue components of peripheral nerve. In: Dyck PJ, Thomas PK (eds). Peripheral neuropathy, 2nd edn. WB Saunders Co: London, 1984; pp 97–116.
3. Thomas PK, Ochea J. Microscopic anatomy of the peripheral nervous system. In: Dyck PJ, Thomas PK (eds). Peripheral neurophathy, 2nd edn. WB Saunders Co: London, 1984; pp 39–91.
4. Đorđević-Čamba V, Stefanović B, Samardžić M. I Bazična razmatranja (histofiziologija perifernih nerava). U: Samardžić M, Antunović V, Grujičić D (urednici). Povrede i oboljenja perifernih nerava. Zavod za udžbenike i nastavna sredstva: Beograd, 1998; pp 3–47. (Serbian)
5. Williams PL, Warwick R, Dyson M, Bannister LH (eds). Gray's anatomy. Churchill Livingstone: New York, 1995.
6. Stefanović N, Antić S, Pavlović S. Anatomija donjeg ekstremiteta. Bones: Niš, 2012. (Serbian)
7. Vazquez-Jimenez JF, Krebs G, Schiefer J, et al. Injury of the common peroneal nerve after cardiothoracic operations. Ann Thorac Surg 2002; 73:119–122.
8. Weil Y, Matten Y, Goldman V, Liebergall M. Sciatic nerve palsy due to hematoma after thrombolysis therapy for acute pulmonary embolism after total hip arthroplasty. J Arthroplasty 2006; 21: 456–459.
9. Baima J, Krivickas L. Evaluation and treatment of peroneal neuropathy. Curr Rev Musculoskelet Med 2008; 1:147–153.
10. Benzon HT, Katz JA, Benzon HA, Iqbal MS. Piriformis syndrome: anatomic considerations, a new injection technique, and a review of the literature. Anesthesiology 2003; 98:1442–1448.
11. Cassidy L, Walters A, Bubb K, Shoja MM, Tubbs RS, Loukas M. Piriformis syndrome: implications of anatomical variations, diagnostic techniques, and treatment options. Surg Radiol Anat 2012; 34: 479–486.
12. Topp KS, Boyd BS. Structure and biomechanics of peripheral nerves: nerve responses to physical stresses and implications for physical therapist practice. Phys Ther 2006; 86:92–109.
13. Ugrenovic SZ, Jovanovic ID, Kovacevic P, Petrovic S, Simic T Similarities and dissimilarities of the blood supplies of the human sciatic, tibial, and common peroneal nerves. Clin Anat 2013; 26: 875–882.
14. Kadiyala RK, Ramirez A, Taylor AE, Saltzman CL, Cassell MD. The blood supply of the common peroneal nerve in the popliteal fossa. J Bone Joint Surg 2005; 87:337–342.

AGE RELATED CHANGES IN THE WALLS OF ARCUATE ARTERIES OF KIDNEY: A LIGHT MICROSCOPIC STUDY

Slobodan Vlajković[1]*, Marija Daković-Bjelaković[1], Milena Trandafilović[1], Aleksandar Petrović[2]

University of Niš, Faculty of Medicine, [1]Department of Anatomy, [2]Department of Histology and Embryology, Niš, Serbia

Abstract. *Although there are many published papers on macro- and microvascularization of the kidney, there has not been a single study that would describe the histological characteristics of the arcuate arteries in specific periods of life. Our motivation to do this study derived from the need to explain the genesis of the ischemic nephropathy and determine the morphological changes on the arcuate arteries. Tissue samples were taken from the kidneys of 50 different cadavers of both sexes. They were divided into five groups, according to their age. The kidneys were of average size and did not show any macroscopic pathological changes. After embedding in paraffin, 5 μm cross-sections through the arteries were prepared. The specimens were analyzed under standard light microscopy, after different staining. The first significant changes are characterized by the widening of the subendothelial layer and the progressive enlargement of the intima. Media gradually shows atrophy, increase of the volume of collagen fibers and reduction of cell numbers. Internal elastic lamina undergoes changes that in time make it wrinkled with denser waves to the point of multiplication. The arcuate arteries, of all the larger intrarenal arteries, undergo the biggest amount of changes. In the beginning, the arcuate arteries suffer a "JET phenomenon", and that is why the age-related mechanical changes are more prominent in them. The dynamics of the change in their walls accelerates during aging. All described changes that start as a non-atherogenous fibromatosis of the tunica intima is a prerequisite for the development of an atheromatous plaque.*

Key words: *Age changes, kidney, arcuate arteries, histology*

Introduction

Every organ works with the appropriate capacity and has a certain functional reserve, which, mainly, expresses itself in older age. The change of the functional state of each organ is caused and/or accompanied by the changes in the morphological level. Age changes lead to increased probability for the occurrence of disease or deadly outcome. They affect the parenchyma and stroma of the organ, together with the changes in blood vessels supplying it, or without them.

All parts of the vascular system are subject to the influence of aging, but most attention focuses on the changes of large distributive arteries, responsible for the development of hypertension and increased pulse pressure, and potential effects on hemodynamics of left ventricle and changes in peripheral resistance and microcirculation [1]. Changes in the renal artery are mainly examined as one of the cause of the terminal renal failure, without clear marks of their dynamics, intensity and quality. During aging, kidney becomes sensitive to many influences from the external environ-

ment (high body temperature, lack of entry of liquids, physical load, nephrotoxic drugs, etc.), as well as to the different diseases accompanied by increased body temperature, greater loss of fluids, or massive destruction of cells, which all leads to more frequent occurrence of renal diseases, which are in this age more intense, more dangerous and difficult to heal [2–5]. It often happens that older people develop chronic renal failure without clear and visible symptoms and signs of previous disease of kidneys and other organs. Recently, a renal disease called ischemic nephropathy was established. It is often present, although often overlooked syndrome that is a potentially curable cause of terminal renal failure in elderly persons and includes reduced kidney function due to inadequate flow of blood through the kidneys [3,6]. Based on the observations of many authors [7–15] that in renal cortex of elderly people there is a standard phenomenon of sclerosis and hyalinosis of glomeruli, with consecutive changes in tubules, moderate fibrosis of renal interstitium, as well as the general reduction of kidney volume, mainly in the absence of hypertension or in the presence of corrected hypertension, one can suppose that the causes of these phenomena are in the morphological as well as functional changes in the larger arteries of kidney (renal artery, segmental arteries, interlobar–arcuate arterial complex). Numerous authors suggest that ischemic nephropathy arises mainly due to

─────────────
Correspondence to: Slobodan Vlajković, MD, PhD, MS
Faculty of Medicine, Dept. of Anatomy,
81 Dr Zoran Đinđić Blvd., 18000 Niš, Serbia
Phone: +381 18 45 70 029 Fax: +381 18 423 87 70
E-mail: sloti@ptt.rs

hemodynamically significant renal artery stenosis [16–20]. However, the opinion noted that renal ischemia can be caused by a stenosis or obstruction of the main renal arteries and/or a stenosis/obstruction of intraparenchymal preglomerular arterioles [21].

The arcuate artery of kidney is any of the branches of the interlobar arteries that turn at the junction of the cortex and medulla and proceed at right angles to the parent stem and approximately parallel to the surface of the kidney. Starting from the hypothesis that the morphological changes in the larger kidney arteries during aging may be responsible for the development of ischemic nephropathy, this research is focused on examining the morphological characteristics of, in particular, arcuate arteries of kidney in various ages.

Material and Methods

The research was carried out on the cadaveric material originating from people of different ages and both sexes. The renal tissue material from Institute for Forensic Medicine in Niš, was used.

Kidney tissue samples were taken always in the same way, from 50 cadavers, of both sexes, sorted in five age groups, each containing 10 pieces, in the following way: I group — age 20–29 years, II group — age 30–39 years, III group – age 40–49 years, IV group — age 50–59 years, and V group — over 60 years. Period of time from the moment of death to sampling was not longer than 24 hours. The most common cause of death was accident or a primary malignant tumor localized far from the kidney. At the same time, there was no positive anamnesis or visible signs of diabetes and hypertension, and it were strictly observed that there are no visible signs of atherosclerosis of larger arteries. The kidneys had expected dimensions, and did not show macroscopic image of scarring process or large cyst or deformities of pyelocaliceal system. In each individual case, contralateral kidney was similar in dimensions.

Histological examination was performed on the initial part of arcuate artery, which is muscular type artery. For the purpose of examination, a sample of kidney tissue from Bertini's column in the level of bases of neighboring Malpighi's pyramids, exactly in the middle distance between the upper and lower poles of the kidney, was used. The cadaveric material was fixed in 10% neutral formalin immediately after sampling. Then, the material was molded in paraffin by standard histological procedure. After molding, the cuts with thickness up to 5 μm and normally to the long axis of vessel (cross-sec-

tion) were made. Afterwards, staining was done by following methods: Hematoxylin-Eosin (HE), elastic fibers by Weigert's resorcin-fuchsin method, Van Gieson's method for collagen, and Gomori's impregnation for reticulin [22]. By Van Gieson's method, nuclei are stained brown/black; collagen red and other tissues are yellow. According to Weigert's resorcin-fuchsin method, elastic fibers are stained brown. By Gomori, reticular fibers are stained black; collagen pale red; nuclei gray, and other tissues are stained differently, depending on the contrast. At the end, the histological analysis was done using the light microscope. All the layout and distribution of smooth muscle cells in the media, the amount and quality of collagen fibers and the presence of abnormal plaques in the arterial intima have been examined. We also evaluated the ratio of vessel lumen to the wall thickness, as well as state of endothelium, subendothelial space, internal elastic lamina, smooth muscle cells of the media (atrophic, hypertrophic, hyperplasic), interstitial space, and adventitia. On the basis of impressions, created by interpretation of the structures, using a number of staining techniques, the histological features of the arcuate arteries are contemplated.

Results

Basic information about the cadaveric materials used is shown in Table 1. It is evident that the length of the kidney slightly decreases during aging.

Within age groups, sorted by decade, there are variations in the wall structure from the youngest to the older age, so the absolute identity within a group is impossible. With some variations, the findings related to the artery within a group are as follows:

I group (*period of 20–29 years*). The intima of arcuate arteries is present only as an endothelial layer that leans on thin and real internal elastic lamina (IEL). In some arteries (24 years) the intima shows mild thickening. In the older age (28 years) of this group, in relation to the circumference, it is moderately expanded, and possessed in one quarter, mainly with collagen structures and rare smooth muscle cells (SMCs) (Fig. 1). In one branch of the arcuate artery (29 years), in circumscriptly thickened intima, the reticular network is thickened. IEL is shallowly wavy bent and sporadically duplicated. The media has the appropriate width, with well-expressed SMCs in the circular or inclined longitudinal schedule and slight partial fibrosis. In the small number of cases, SMCs are sparse and atrophic in

Table 1. Basic data about the materials used for histological examination (mean values ± standard deviation)

		Age group				
		20–29 (n=10)	30–39 (n=10)	40–49 (n=10)	50–59 (n=10)	60+ (n=10)
Mean age (years)		25.8 ± 3.6	35.1 ± 3.1	43.2 ± 1.8	54.4 ± 3.0	71.7 ± 6.9
Mean height (cm)		178.4 ± 4.8	177.8 ±13.3	174.9 ± 6.7	175.2 ± 8.5	165.8 ± 9.6
Kidney length (cm)	R	11.12 ± 0.63	11.52 ± 0.98	11.45 ± 1.17	11.38 ± 1.11	11.07 ± 1.23
	L	11.20 ± 0.91	11.87 ± 0.71	11.74 ± 0.83	11.63 ± 1.03	11.40 ± 1.14

the level of thickened intima, sporadically with collagen among them. The external elastic lamina (EEL) is hardly observable, thin, linear and aplated. The adventitia is relatively wide.

Fig. 1 Transverse section of the arcuate artery with relatively preserved structure and mild collagenization of wall (arrow). HE, × 100

II group (*period of 30–39 years*). The arcuate arteries have uneven caliber, appropriate size, well-expressed lumen, sometimes without intima or they show (older kidneys of this group) slightly partial cellular-fibrous type of thickening of the intima, with rough reticular network. In part, IEL is shallow, wavy, with uniform width, well acceptable to color, and partly duplicated and serrated. Some arteries have tortuous and partially duplicated IEL. In most cases, the media has uniform width, corresponding cellularity, and is knited by reticular fibers, with some reduction of number of SMCs in the level of fibrous thickening of the intima. One-fifth circumference of the inner part of the wall are reduced SMCs, and they are replaced by pink collagen fibers (Fig. 2), and there are collagenized reticular fibers in this level. EEL is clearly outlined, with shallowly serrated small part, and flattened in the other part. The adventitia is primarily collagenized.
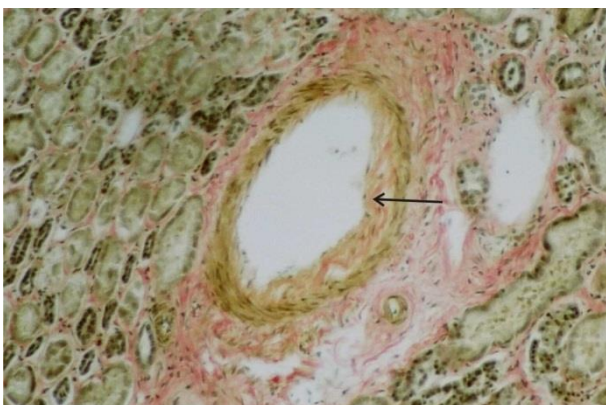

Fig. 2. Transverse section of the arcuate artery with asymmetrically widened intima in which collagen fibers (arrow) are seen. Van Gieson, × 100

III group (*period of 40–49 years*). The spectrum of arcuate arteries' caliber is wide but they show similar characteristics, depending on diameter. In the larger arteries asymmetric homogenous fibrous widening of the intima is observed, with rare spindle cells in it. These cells are periodically placed orthogonally to the lumen, and gentle and coarse elastic and collagen fibers are also present, as well as SMCs. Reticular network in intimal thickening is roughened and collagenized (Fig. 3). IEL is very shallow, wavy, in some cases partially fragmented, sometimes duplicated. In the media there is a slight reduction of cells only in places where intima is changed (homogenized), which is conditioned by changes in intima. There are no collagen fibers in the media but sometimes one can note the relative and absolute reduction of SMCs of media. EEL is clearly outlined and flattened. The adventitia in larger arcuate arteries shows the width equal to that of media, while in very small arteries it is reduced.
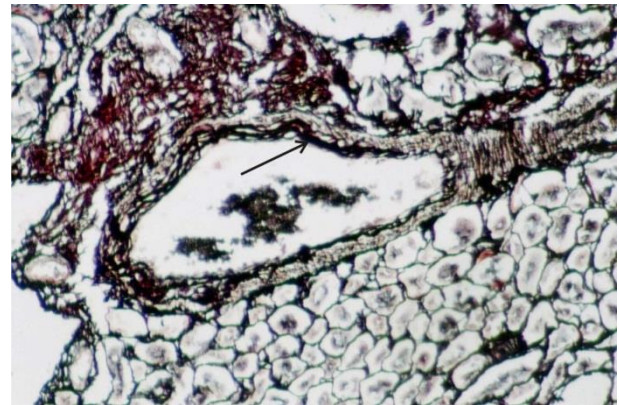
Fig. 3. Tangentially affected arcuate artery with asymmetrically fibrous intima made of rough reticular fibers (arrow), with reduction of media. Gomori, × 120

IV group (*period of 50–59 years*). The arcuate arteries do not have all the same properties. Some show complete fibrosis of the wall and visible reduction of SMCs in media. The intima is difficult to distinguish from the media; it changes more than other layers (Fig. 4). Some arteries show acellularity of inner part of wall, where there are asymmetrically affected parts of the intima and media (Fig. 5). Some arcuate arteries, however, have a minimal expansion of the intima with thickened reticular fibers. The intima is relatively broad, as well as media, and collagenized. SMCs are attended, as well as wavy and coarse reticular fibers. IEL is slightly wavy, partially indistinct. The media is partially to almost completely acellular. Some arteries have wide media and moderately reduced SMCs. In relatively atrophic media there are rough reticular fibers. EEL is the right circular line. It outlines media under broader adventitia and at some places it is wavy above collagenized intima. The adventitia is emphasized and collagenized.

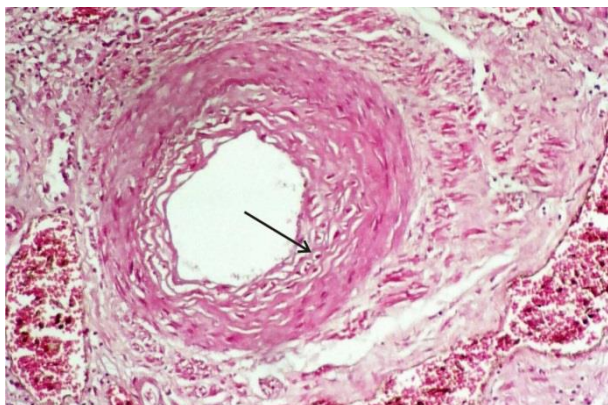**Fig. 4.** Transverse section of the arcuate artery. Loosely widened intima (arrow) with a moderate number of cells asymmetrically suppresses atrophic media. HE, × 120
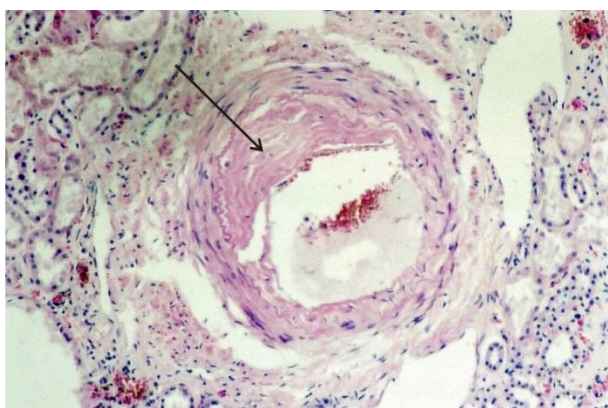

Fig. 5. Transverse section of the arcuate artery. Asymmetrically markedly widened hyaline-collagen intima (arrow) partially reduces media and makes subocclusion of lumen. HE, × 120

V group (*over 60 years*). The arcuate arteries are of unequal size and morphological characteristics, most of them are overall highly increased and with thickened walls. In two thirds of the expanded intima the arcuate arteries show markedly asymmetric fibrocollagen thickening with homogenized content and rare spindle cells, sometimes with the SMCs (Fig. 6). Cuts along the length of the vessel show the minimal and slightly asymmetric thickening of intima. The intima has the fibrocollagen and belongs to suboclusive type. In the broader intima, the reticular network is roughened (thickened) and replaced by collagen (Fig. 7). In the level of intimal thickening, IEL is sometimes multiply decomposed (Fig. 8), in other cases is suppressed by intimal widening, condensed and shallow wavy, and in many cases it is duplicated. The media is in some cases droningly wide, but it is narrowed in the level of fibrous thickening of the intima, until complete fibrocollagenization of the entire wall, with the ultimate reduction of its cells. Where fibrosis has overtaken the inner zone of media, SMCs are sporadic, rarely bundled and drowned in collagen mass (see Fig. 6). In third type of cases, the
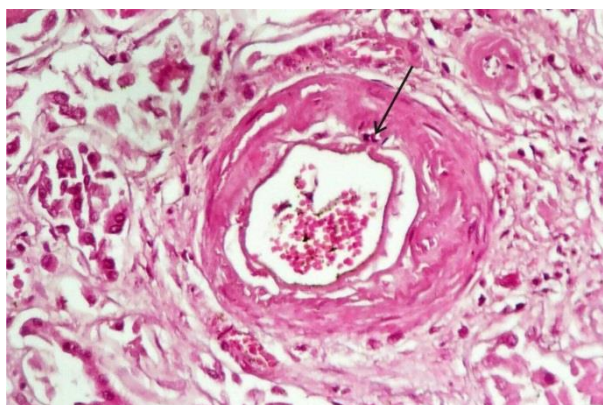
Fig. 6. Transverse section of the arcuate artery. Lumen stenosis and thickening of the arcuate artery wall due to subtotal fibrosis and hyalinization of its wall, with rare atrophic smooth muscle cells (arrow). HE, × 120
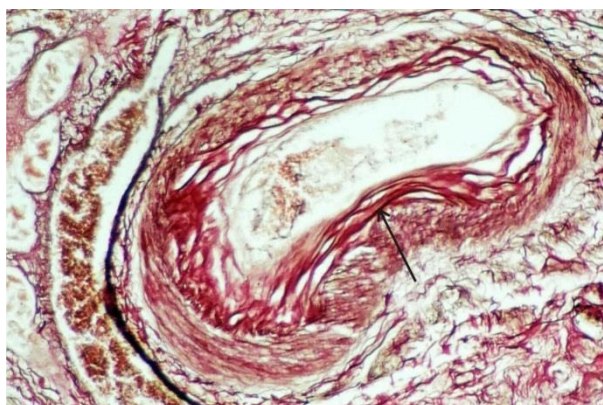
Fig. 7. Tangential section of the arcuate artery shows coarsening of reticular fibers (arrow) and their collagenization in the intima and part of media. Gomori, × 150

Fig. 8. Transverse section of the arcuate artery. Assymetrical multiplication of IEL (arrow), which reduces media. IEL, internal elastic lamina; Weigert, × 100

media is in general slightly asymmetric, its two-thirds are widened, and one third is narrower, with fewer cells due to moderate atrophy and reduction of SMCs number, only slight fibrous fibers can be seen through the media. Reticular network is gentler or slightly thickened in the media (see Fig. 7). EEL is almost completely absent or is well outlined, with wavy monotonous rhythm. The adventitia is narrow, loose, partially with areas of arteriolohyalinosis.

Discussion

The kidney has an essential role in hypertension, taking into consideration that its blood vessels are sensitive to different types of pathological changes that are directly associated with increased blood pressure. At the same time and independently of that, the progressive reduction of blood flow through the kidney arteries has significant influence on atrophy of renal parenchyma. These changes need not always be directly related to pathological processes, but may be an expression of aging events [23–25]. In the above-mentioned processes, extreme sensitivity reflects, first of all, in the small arteries and arterioles, especially in preglomerular vessels. Narrowing of kidney blood vessels leads to glomerular sclerosis, tubular atrophy and interstitial fibrosis (nephrosclerosis).

Despite numerous works about the macro- and microvasculature of the kidney in the world literature, until now, no studies have described the histological characteristics of arcuate arteries of kidney for certain periods of life, starting from the time when the kidney is fully ripe for all of its functions, to the old age. According to our results, one of the characteristics of aging by years, if the age shows changes such as fibrous thickening of intima, is that they first appeared focal, then spread in circumference, i.e. increased the width (thickness) of the intima and enriched the content. Haemodynamical factor in the process of aging changes is significant, in addition to positional situations (branching blood vessels and platelet aggregation) in normal conditions, due to duration. This means that in relation to duration, i.e. elapsed time, the effects of this factor are evident. This excludes pathological factors.

Within age groups there are variations in the composition of the wall from the youngest to older age, so that the absolute identity of the findings within a particular group is impossible. On the other hand, although there are regularities in the appearance of certain changes, they are subject to variation, too, so that some appear inadequate in relation to time and blood vessel, but this can be attributed to unequal genetic texture of the people, and to the existence of individual difficulties and physical burdens of the people who are unknown to us. Of course, the body height of a person, its constitution, obesity and other variations affect the changes to the structure of the wall of blood vessels. Therefore, the number of seemingly unusual findings within a group should not be surprising, because it is a wide range of time (range 10 years), with

unequal genetic potential, type of diet, physical form of the load, and more.

There is no doubt that all layers of the vessel wall "suffer" age changes, but we believe that the initial, primary and most visible changes are taking place in the intima, IEL and media (in some cases even EEL suffers changes). According to this, one can consider three questions: the question of the intima, IEL and media.

The question of the intima. Due to diffusional supplying of internal half of the media, the intima is presented only by the endothelium, which is close to IEL. The example is the case of the aorta that is going to 10th year [26]. From that period its thickening begins by creating subendothelial layer, which is a prerequisite for further compromising of nutrition and developing further changes in the intima, and consecutive repercussions to the media, through the development of atheromatous changes. The intima of most segments of all artery types is mainly reduced to the endothelial layer lying close to the IEL, which means that it is in principle almost absent, except in some cases where it shows initial partial thickening in the form of cushion widening, where the reticular network is well expressed about SMCs, but even outside them, at the earliest age groups. In older age there are increased values of parameters of intimal fibroplasia [27]. Changes in the composition of the intima reduce diffusional process which is reflected in the ingredients of vessel's wall. With aging, the endothelial cells become heterogeneous in size, shape and orientation, resulting in reduction of laminar flow and increasing receptivity to lipid deposits, and this endothelium becomes more sensitive to oxidative stress and damage by free radicals [13].

It appears that changes in the properties of IEL are dependent on state of the intima i.e. that are only in close correlation with its thickening (increased jaggedness of IEL, its duplication and fragmentation). In places where thickening of intima starts, one can see strong reinforcement of amplitude and density "plication" of IEL, probably due to the increased need for communication between the intima and media. This happens through the IEL, which, we assume, increases the surface exchange of communication between the media and intima, which is growing, initially only in the form of mucopolysaccharides, and later the cell contents.

Morphogenesis of the intima secondarily depends on the action of the media: in the beginning, it is possible that the subendothelial layer is possessed by diffusion of polysaccharide content, eventually by lymphocytes, but in the further course, media fills the content of the intima, because the former affects the condition of IEL, which is its product, sending the SMCs into the subendothelial layer. For these reasons, cell content near the IEL is much more common than below the endothelium.

The question of the IEL. Elastic lamina of arteries is the organizational structure whose role is primarily supportive, not only for the maintenance of lumen contours, but also for support of the main parenchymatous functioning part, i.e. media. So, it significantly follows changes of the lumen diameter and on the other hand it

maintains the media. SMCs of media are fixed for IEL and EEL and they are, among other things, the structural support of the media and its product. IEL is undoubtedly an important component in the narrowing and widening of the walls of blood vessels, but on the post mortem microscopic preparations, in normal circumstances, it is more or less aplated or slightly wavy [28]. We observed that the existence of larger or smaller amplitudes (waves) is an equivalent of age changes, often associated with changes in the intima. One possible presumption is that in this way it is trying to increase the area of exchange between progressively expanded intima and inner parts of the media. It is understandable that, with increasing width of intima and its "dramatic" events during the formation of larger fibromatous or atheromatous plaques, there is a duplication of IEL, decreasing the wall properties (loss of receptivity to color, fragmentation), which is a sign that, under these circumstances, the mechanisms of adaptation and compensation are absent.

It is interesting that the IEL is most commonly one-pieced, ie. homogenous, evenly broad structure. During the aging, i.e. by the influence of long acting hemodynamic factors (through time, with age), it is among the first structures which opposes damaging factors of duration of circulation, and begins to change. As an expression of its damage or attempt to confront the present long-term burden of mechanical pulse wave, it shows compensatory duplication or triplication [28]. This is often observed in places of strong shock, such as initial segments of arcuate arteries which stand at right angles to the shock wave from interlobar artery. These changes are slightly reduced with the reduction of caliber of arcuate artery in the horizontal position. It looks like some form of vessel's defense to load, because it can not produce these effects in a short-term action. This raises the question: does the blood current – blood blow provoke production of growth factors?

The continuity of the presence of changes in the IEL (such as low receptivity to color, thinness, duplication, possibly fragmentation) in the level of cushion widening of intima testifies about insufficiency of process of diffusion, which is reperonced to the morphofunctional state of SMCs at this level and its inner part, as well as to the reduction of production of IEL. These age changes may not be accompanied with changes of its thickness and may include increased number of collagen fibers that overlap fenestrae of IEL and/or reduction of total surface area of these fenestrae by changes in the structure of elastic layers [29]. IEL of arcuate arteries in the kidney in old age particularly acts — multiplies, divides into layers. This phenomenon may be called the multiplication of IEL.

The question of the media. Tunica media is adapted adequately to distribution of blood vessels, in fact, it is adapted according to hemodynamic wave - prevalently it is elastic in conductive types and muscular in distributive type. Media content is appropriate to topographic location: in elastic arteries — elastic fibers, in muscular arteries — SMCs. The tunica media is mainly formed by SMCs and elastin, and the latter is

arranged in fenestrated lamellae between which are collagen fibers, extracellular matrix, and SMCs [30]. These parenchymatous components almost contain a minimum of collagen fibers. In relation to time we have observed directly and indirectly that there is a change in their content. In arcuate (muscular) arteries there occurs reduction of their SMCs or their deterioration due to atrophy, especially in the level of thickened intima (nutritional factor). However, in the process of aging it was progressively noted that reticular network knitting SMCs can be collapsed, bold or collagenized. The question of the presence of collagen fibers in a larger quantity is interesting considering that the media does not have fibroblast cells. It is possible that collagen fibers arise from reticular network which got coarse. It could be stated under the presumption that the influence of growth factors induces the development of fibroblast cells from undifferentiated mesenchymal cells of intima.

Eventual thickening of the media could be relative, due to the presence of edema and lipid content in the case of atheromatosis, but absolute widening of the media was not often observed. So, we can say that in the process of aging there occurs reduction of functional part of the vessel, ie. media, probably and primarily due to intima fibrosis and consecutive atrophy of SMCs, with accompanying coarsening of reticular network, which in turn further reduces nourishment of cells because it prevents access of nutritious substances to the muscle cells due to the creation of "armor" from the bolded reticular network. In the level of bold intima, the media is easily reduced. Media repairs and maintains the quality or permanence of IEL structural integrity.

One can pose a question about proliferative capacity of SMCs of media, i.e. the existence of stem cells. A number of SMCs, under the influence of cytokines and growth factors in the process of intimal fibrosis, migrate from media to intima [31]. It is clear that, under the influence of chronic hemodynamic stimuli, the SMCs of media experience changes. These changes resemble "dedifferentiation". With the loss of capacity for contraction, SMCs acquire the ability to divide and synthesis of extracellular matrix increases. SMCs in the intima lose their thickness and filaments containing myosin, and increase the amount of organelles involved in protein synthesis [31]. So, there is a phenotypic modulation from "contractile" phenotype to the "synthetic-proliferative" phenotype. Therefore, it is considered that mutations and phenotypic modifications of SMCs of media reach the intima [32]. This transformation happens in atherosclerosis, where SMCs synthesize collagen in the scale characteristic for fibroblast cells [33]. SMCs, which migrate from the media, are primarily proliferative cells in the intima, though in some cases, their proliferation may arise from ancestral myointimal cells [32]. There is no doubt that, in some cases, migrations of SMCs are very numerous.

Considering the normal age changes, all under the influence of hemodynamic factors, it seems that among the major intrarenal arteries, arcuate arteries show the largest changes. The arcuate arteries are damaged be-

cause of their position and effect of hemodynamic factors, which is described by other authors [34]. The arcuate arteries at the beginning suffer "JET phenomenon" – a stronger shock wave pulse, because they are at a right angle to the straight interlobar arteries, and therefore, age "mechanical" changes are more expressed in them. However, in the further course, due to the depreciation of shock pulse wave, they have fewer changes. Many textbooks show uniformity of arcuate artery's caliber which is almost impossible, because this artery is shown as a continuing arc of the interlobar artery in a flat section, and the question arises: where are their side branches in terms of space (stereometrically) in the corticomedullary border in a light of the total thickness of the kidney? Therefore, it is necessary to perform a comprehensive research of arcuate arteries and standardization of their size, because, undoubtedly, they are not all of equal caliber or thickness of the wall.

Conclusion

The first significant changes are recorded in the third decade in the form of enhancement of subendothelial layer and progressive widening of the intima, which is gradually possessed by an amorphous mass; then the cells appear in it.

With aging, the internal elastic lamina (IEL) becomes less susceptible to color and wrinkled with larger and denser extent, to the fragmentation and multiplication. With the weakening of the media, IEL suffers changes, which means that the media maintains morphological integrity and permanence of IEL.

Media shows atrophy and gradual reduction of SMCs, and increased collagen content. Reticular network which initially gently knits each smooth muscle cell but with aging it gets coarse and collagenizes. A universal finding is the existence of circumscriptive reduction of media in the level of thickened intima.

The dynamics of changes in the layers of the arcuate artery wall accelerates and becomes difficult with age. All described changes that begin as non-atherogenic fibromatous plate of intima, are a prerequisite for the development of atheromatous plate. All these changes reduce the diameter of the lumen, i.e. they lead to narrowing of the arcuate arteries in older age.

Age changes in the wall of arcuate arteries of kidney in the elderly, combined with other factors in the external and internal environment, may be responsible for the occurrence of ischemic kidney disease.

References

1. Plante GE. Impact of aging on the body's vascular system. Metabolism 2003; 52:31–35.
2. Porush JG, Faubert PF. Renal disease in elderly patients. Rev Clin Gerontol 1997; 7:299–307.
3. Rodger RS. Renal function in the elderly. Br J Urol 1998; 82:65-70.
4. Rodrigez-Puyol D. The aging kidney. Nephrology forum. Kidney Int 1998; 54:2247–2265.
5. Mulder WJ, Hillen HFP. Renal function and renal disease in the elderly: Part I. Eur J Int Med 2001; 12:86–97.
6. Zucchelli P, Zuccala A. Ischaemic nephropathy. In: Davison AM (ed). Oxford textbook of clinical nephrology, vol. 2. Oxford University Press, 1998; pp 1445–1456.
7. Takazakura E, Wasabu N, Handa A, Takada A, Shinoda A, Takeuchi J. Intrarenal vascular changes with age and disease. Kidney Int 1972; 2:224–230.
8. McLachlan MSF, Guthrie JC, Anderson CK, Fulker MJ. Vascular and glomerular changes in the aging kidney. J Pathol 1977; 121:65–78.
9. Kappel B, Olsen S. Cortical interstitial tissue and sclerosed glomeruli in the normal human kidney, related to age and sex. Virchows Arch A Path Anat Histol 1980; 387:271–277.
10. Barton M. Ageing as a determinant of renal and vascular disease: role of endothelial factors. Nephrol Dial Transplant 2005; 20:485–490.
11. Baylis C, Schmidt R. The aging glomerulus. In: Martinez-Maldonado M (ed). Renal disease in the elderly. Semin Nephrol 1996; 16:265–276.
12. Bos WJW, Demircan MM, Weening JJ, Krediet RT, van der Wal AC. Renal vascular changes in renal disease independent of hypertension. Nephrol Dial Transplant 2001; 16:537–541.
13. Wei JY. Understanding the aging cardiovascular system. Geriatrics Gerontol Int 2004; 4:S298–S303.
14. Labropoulos N, Leon LR, Brewster Jr LP, et al. Are your arteries older than your age? Eur J Vasc Endovasc Surg 2005; 30:588–596.
15. Long DA, Mu W, Price KL, Johnson RJ. Blood vessels and the aging kidney. Nephron Exp Nephrol 2005; 101:e95–e99.
16. Breyer JA, Jacobson HR. Ischemic nephropathy. Curr Opin Nephrol Hypertens 1993; 2:216–224.
17. Bax L, van der Graaf Y, Rabelink AJ, Algra A, Beutler JJ, Mali WP; SMART Study groop. Influence of atherosclerosis on age-related changes in renal size and function. Eur J Clin Invest 2003; 33:34–40.
18. Ilkay E, Gunal AI, Yavuzkir M, et al. Effect of renal artery stenting on renal function in patients with ischemic nephropathy. Jpn Heart J 2004; 45:637–645.
19. Olin JW. Renal artery disease: diagnosis and management. Mt Sinai J Med 2004; 71:73–85.
20. Fujii H, Nakamura S, Kuroda S, et al. Relationship between renal artery stenosis and intrarenal damage in autopsy subjects with stroke. Nephrol Dial Transplant 2006; 21:113–119.
21. Zuccala A, Zucchelli P. Ischemic nephropathy: diagnosis and treatment. J Nephrol 1998; 11:318–324.
22. Bancroft JD, Stevens A. Theory and practice of histological techniques. Churchill Livingstone: Edinburgh, 1977; pp 103, 107, 110.
23. Meyer BR. Renal function in aging. J Am Geriatr Soc 1989; 37:791–800.
24. Palmer BF, Levi M. (1996). Effect of aging on renal function and disease. In: Brenner BM (ed). The kidney. WB. Saunders Co: Philadelphia, 1996; pp 2274–2296.
25. Gomez Campdera FJ, Luno J, Garcia de Vinuesa S, Valderrabano F. Renal vascular disease in the elderly. Kidney Int 1998; 54:S73–S77.
26. Anestiadi VH, Nagornev VA. [Patho- and morphogenesis of atherosclerosis (clinico-experimental aspects)]. Arkh Patol 1984; 46:10–18. (Russian)
27. Tracy RE, Parra D, Eisaguirre W, Torres Balanza RA. Influence of arteriolar hyalinization on arterial intimal fibroplasia in the renal

cortex of subjects in the United States, Peru, and Bolivia, applicable also to other populations. Am J Hypertens 2002; 15:1064−1073.

28. Datta BN. Textbook of pathology, 2nd edn. Jaypee Brothers Medical Publishers: New Delhi, 2004.

29. Lee K, Forudi F, Saidel GM, Penn MS. Alterations in internal elastic lamina permeability as a function of age and anatomical site precede lesion development in apolipoprotein E-Null mice. Circ Res 2005; 97:450−456.

30. Wagenseil JE, Mecham RP. Vascular extracellular matrix and arterial mechanics. Physiol Rev 2009; 89:957−989.

31. Louis SF, Zahradka P. Vascular smooth muscle cell motility: From migration to invasion. Exp Clin Cardiol 2010; 15:e75−e85.

32. Schoen FJ. Blood vessels. In: Cotran RS, Kumar V, Robbins SL (eds). Robbin's pathologic basis of disease. WB Saunders Co: Philadelphia, 1994; pp 467−516.

33. Shekhonin BV, Domogatsky SP, Rudin AV, Rukosuev VS. [Immunomorphological characteristics of collagen distribution of the I, III, IV, V types in normal intima and in atherosclerosis of the human big arteries and aorta]. Arkh Patol 1984; 46:18−24. (Russian)

34. Lastić-Maletić S. Krvni i limfni sudovi. U: Atanacković M (ed). Patologija. Medicinski fakultet: Beograd, 2003; pp 277−296. (Serbian).

HISTOCHEMICAL AND MORPHOMETRIC ANALYSIS OF CONNECTIVE TISSUE IN HUMAN GLOMERULES DURING AGING

Vesna Stojanović[*]*, Ivan Jovanović, Slađana Ugrenović, Braca Kundalić, Miljana Pavlović*

University of Niš, Faculty of Medicine, Department of Anatomy, Serbia

Abstract. *During aging there are alterations in human glomerules followed by increase of the connective tissue amount, accumulation of glomerular basal membrane and mesangial matrix on account of the rest of cell population. The aim of the study was quantification of the present connective tissue in mesangium of glomerules which morphologically did not show signs of sclerosis and determination of its part in glomerular structure. Investigation included 30 tissue samples of human kidneys of cadavers of both sexes, aged 20-85. Tissue samples were routinely stained with Mallory trichrome stain and analyzed by light microscope under 400× magnifications. Images were analyzed with ImageJ software. Statistical analysis was performed with NCSS-PASS software. Cluster analysis was performed for the classification of glomeruli into 3 age groups, first with average age of 29, second with 44 and third with average of 71 years old. Histochemical investigations indicated the growth of connective tissue in mesangium of human glomerules during aging. It was also demonstrated morphometrically showing significant increase (p<0.05) of mean connective tissue area and its percentage in glomerule. In first, the youngest group the connective tissue was present in 17.33%, while in second group there was statistically significant increase (32.11%). The most significant growth compared to other age groups appeared in third group, where there was 40.66% of connective tissue in glomerule. Results of morphometrical and statistical analysis suggest that during aging process there is significant increase of area and percentage of connective tissue in the glomerule followed by reduction of cell size.*

Key words: *Human glomerules, mesangium, connective tissue, aging*

Introduction

Aging may be considered as gradual deterioration of cell function which is based on biophysical and biochemical changes of cell content, gradual loss of cell capacity for reproduction and regeneration of structural elements [1–3]. Very important problem in studying the aging process is also how to distinguish aging from disease. Aging is connected with physiological, morphological and functional changes in the kidney. Many of these changes, such as loss of nephrons, may be interpreted as an attempt of protection in aging process which influences renal homeostasis. The disorders call into question renal backup and reduce renal capacity which leads to new insults [4,5]. Etiological and other factors such as cytokines, growth factors, proliferation, pro-apoptotic, transcription and other factors [6,7], are involved in renal aging.

Age-related changes in kidney are similar to those verified in chronic renal disease and experimental models with chronic renal deficiency. Old age in humans is followed with renal mass loss. The loss is primarily developed in cortex, while medulla is relatively spared,

which is shown by some studies whose results suggest that even half of neurons may disappear until old age [8–10]. It is known that a man is born with definitive number of nephrons (except in premature birth), and that its morphological and functional maturation lasts till sexual maturity, on account of corpuscle's size, amount of vascular and connective tissue and increased length and tortuosity of tubules [4,5,11–13]. Aging is accompanied with nephron loss [4,11,13,14], increase of sclerotic glomerules percentage, changes in blood vessels with obliteration of the lumen, decrease of glomerular cells number and higher interstitial tissue content in cortex and medulla [15,16]. All of these changes which appear during aging affect function of corpuscles and kidney. Human glomerular aging includes progressive loss of glomerules which is directly related to birth mass, presence of shunts between the afferent and efferent arteriole, growth of mesangial matrix followed with onset of glomerulosclerosis and increase in number of globally sclerotic glomerules [17–20]. Previous studies showed that "physiological" deterioration of glomerules normally begins during intrauterine life and continues during child's growth and development.

The aim is to quantify the presence of connective tissue in the mesangium of the glomerules which do not show morphological signs of sclerosis and to determine its part in glomerular structure during aging.

Correspondence to: Vesna Stojanović, MD, PhD
Faculty of Medicine, Dept. of Anatomy,
81 Dr Zoran Đinđić Blvd., 18000 Niš, Serbia
Phone: +381 18 45 70 029 Fax: +381 18 423 87 70
E-mail: vesna@medfak.ni.ac.rs

Material and Methods

The material was human right kidney tissue of 30 cadavers, obtained during routine autopsies at the Institute for Forensic Medicine in Niš. Their age ranged from 20 to 85 years. During autopsy kidney damage or congenital anomalies were not observed. Cadavers were without previously diagnosed kidney disease, diabetes, hypertension, or any other systemic disease.

Tissue specimens were fixed in 10% buffered formalin for 12 hours and then embedded in paraplast. The tissue was then cut into 5 μm thick sections and routinely stained with Mallory trichrome stain. Histological slices were analyzed under 400× magnification. Images of histological slices were captured with digital camera (5 megapixels resolution).

Glomerules were analyzed with ImageJ software (http://rsbweb.nih.gov/ij/) which was spatially calibrated with object micrometer (1:100). Glomerular tuft area (AG), Feret's diameter (DF), perimeter (BG), diameter along main (DM) and secondary axis (Dm), total number of cells per glomerular area unit (Nn), and glomerular connective tissue area (ACT) were measured. Seven sclerotic glomeruli, if noticed, then non-sclerotic glomeruli located subcortically, juxtamedullary and columnary, seven of each, selected by unbiased method, were analyzed per one case, therefore there was a maximum of 28 glomeruli per one case. In total, 743 glomeruli were analyzed in all 30 cases. Glomerular images were additionally processed for connective tissue area measurement. Glomerular tuft image was first manually selected by polygonal selection tool and extracted from the other parts of histological slice image. Selection of its connective tissue, which was green stained on Mallory trichrome stained sections, was performed by "color-based tresholding" option. Its application was based on green colored sample of glomerular tuft image. Afterwards, only green stained parts of glomerule remained on image, which was further converted into binary image. Binary image was used for connective tissue area measurement. Green colored samples were taken at three different localizations in each glomerular tuft image. Connective tissue area was measured for each sample. Average connective tissue area was then calculated from three obtained values for each glomerular tuft. Glomerular connective tissue percentage was obtained from the ratio between glomerular connective tissue area and total glomerular area. Average values of morphometric parameters were calculated for each of all 30 evaluated cases.

Statistical analysis was performed with NCSS-PASS software (http://www.ncss.com/). Cluster analysis by the k-means method was performed for the classification of glomeruli into age groups according to their morphometric characteristics. One-way ANOVA was used for the comparison of more than two groups. In cases where data did not have normal distribution Kruskal-Wallis one-way ANOVA was used for the comparison of more than two groups. Statistical significance test was performed for $p < 0.05$.

Results

Morphological analysis

During histological analysis of renal preparations stained by trichrome staining – modification by Mallory, renal corpuscles are classified into three groups based on size, cellularity and presence of connective tissue. The first group includes sclerotic corpuscles, the second group includes morphologically normal ones and the third is composed of hypertrophic corpuscles.

In the group of sclerotic renal corpuscles (Fig. 1, A–B) we noticed collapse of capillaries, intensive accumulation of extracellular matrix, while the glomerular capillary network almost disappeared and was replaced by connective tissue. Inside of sclerotic glomerule rare capillaries (Fig. 1, A) and scarce nuclei (Fig. 1, B) may be seen. External leaf of Bowman's capsule was not clearly separated from internal leaf so there was relatively narrow urinary space only in places. Around described corpuscles there were numerous proximal and distal tubules, while in the interstitial connective tissue there were poorly observable capillaries with clearly expressed interstitial sclerosis. Majority of these corpuscles was noticed in the oldest persons.
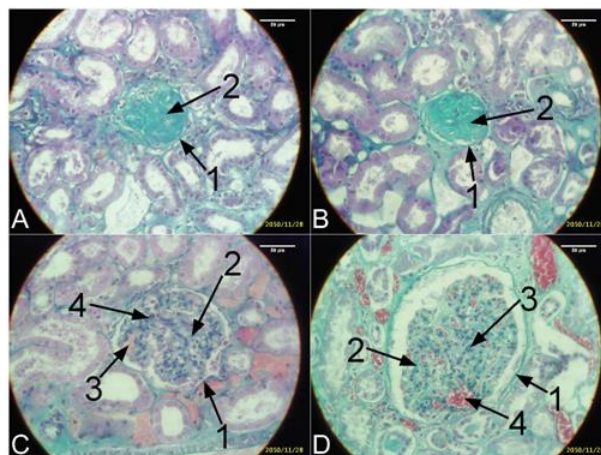

Fig. 1. A — Sclerotic renal corpuscle of a male, aged 48; B — Sclerotic renal corpuscle of a female, aged 39; C — Normal renal corpuscle of a male, aged 48; D — Hypertrophic renal corpuscle of a male, aged 78. 1, Bowman's capsule; 2, connective tissue; 3, blood vessels; 4, nuclei. Mallory's trichrome staining, 400×.

Morphologically normal corpuscles (Fig. 1, C) were the most numerous in the middle-aged and the youngest persons. They possess clearly defined external and internal leaf of Bowman's capsule which lies next to glomerular capillary network. Between these two leaves there is urinary space with relatively constant width in all parts of glomerule. Glomerular capillary network consists of clearly visible capillary loops surrounded by mesangial matrix with scarce connective tissue and numerous nuclei of mesangial cells which are small, dark and centrally positioned. There are proximal and distal

tubules around glomerules, with relatively narrow interstitial space and clearly noticeable capillaries inside.

Hypertrophic capillaries (Fig. 1, D) were considerably larger than previous ones. The external leaf of Bowman's capsule was thickened in almost all parts, while the internal one was sporadically discontinuous and urinary space was much expanded in some parts. Glomerular capillaries were multiplied; mesangial matrix was considerably replaced by connective tissue, while cellularity in glomerule was increased. In interstitial space there were tubules, capillaries and increased content of connective tissue. The presence of these corpuscles is higher in middle-aged and older persons.

Morphometric analysis of glomerules

As a result of the analysis we obtained three groups of cases. The first group consists of the youngest cases, six in total, who were aged 24–33 years, average 29. Eleven older cases, aged 40–49 years, average 44, were in the second group. In the third group there were 13 oldest cases aged 65–76 years, average 71 (Table 1).

Mean glomerular area of investigated cases shows changes which were not statistically significant, while mean connective tissue area and its percentage in glomerule rise significantly (p<0.05) during aging (Table 1; Fig. 2). In the first, the youngest group mean connective tissue area is 2601.18 μm², which is 17.33% of glomerular area. In the second, older group, there was statistically significant increase of connective tissue area. Its value is 4468.52 μm², which makes up 32.11% of glomerule. The most significant increase of connective tissue area is present in the third, the oldest group, compared to other two (p<0.05). Its mean value is 4468.52 μm², or 40.66% of glomerular area (Table 1; Fig. 3).

Mean perimeter, mean diameter along main axis of glomerule and mean Feret's diameter show the same trend, as well as mean glomerular area during human aging, while mean diameter along secondary axis of glomerule shows continuous decrease from first to third age group (Table 1; Fig. 4). Changes of these parameters are not statistically significant which indicates that size and shape of investigated glomerules are not in correlation with aging process.
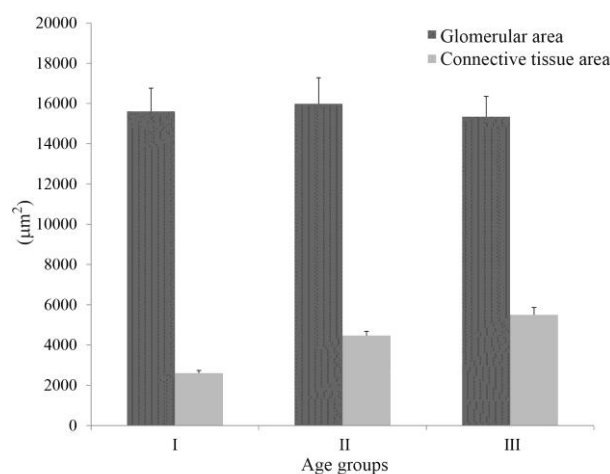

Fig. 2 Mean glomerular area and mean glomerular connective tissue area of groups obtained by cluster analysis
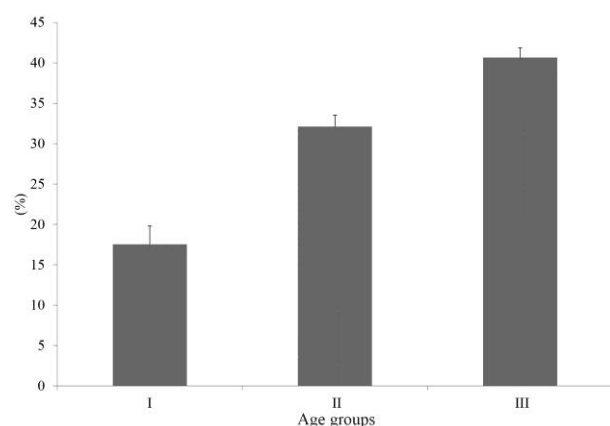

Fig. 3 Mean percentage of connective tissue per glomerule of groups obtained by cluster analysis

Table 1. Morphometric features of glomerular groups obtained by cluster analysis

	A_G (μm²)		B_G (μm)		D_M (μm)		D_m (μm)		D_F (μm)		A_{VT} (μm²)		VT%		$N_n(1/μm^2) \times 10^{-3}$	
Cluster							I (n = 114)									
Parameter	$\bar{X}$	Md	$\bar{X}$	Md	$\bar{X}$	Md	$\bar{X}$	Md	$\bar{X}$	Md	$\bar{X}$	Md	$\bar{X}$	Md	$\bar{X}$	Md
Value	22478.81	21894.61	564.24	556.76	189.36	185.69	149.84	149.53	197.22	193.01	6774.02	6406.87	30.66	31.49	5.9	5.9
SE	314.27		4.69		1.53		1.30		1.58		115.15		0.45		0.1	
95% LCL	21859.05	21188.06	554.99	546.10	186.36	183.13	147.27	146.19	194.11	189.62	6546.94	6207.42	29.76	30.54	5.7	5.8
95% UCL	23098.56	22664.15	573.50	568.77	192.37	189.62	152.40	151.94	200.33	197.60	7001.10	6588.96	31.55	32.46	6.0	6.1
Cluster							II (n = 430)									
Parameter	$\bar{X}$	Md	$\bar{X}$	Md	$\bar{X}$	Md	$\bar{X}$	Md	$\bar{X}$	Md	$\bar{X}$	Md	$\bar{X}$	Md	$\bar{X}$	Md
Parameter	22478.81	21894.61	564.24	556.76	189.36	185.69	149.84	149.53	197.22	193.01	6774.02	6406.87	30.66	31.49	5.9	5.9
Value	314.27		4.69		1.53		1.30		1.58		115.15		0.45		0.1	
SE	21859.05	21188.06	554.99	546.10	186.36	183.13	147.27	146.19	194.11	189.62	6546.94	6207.42	29.76	30.54	5.7	5.8
95% LCL	23098.56	22664.15	573.50	568.77	192.37	189.62	152.40	151.94	200.33	197.60	7001.10	6588.96	31.55	32.46	6.0	6.1
Cluster							II (n = 430)									
Parameter	$\bar{X}$	Md	$\bar{X}$	Md	$\bar{X}$	Md	$\bar{X}$	Md	$\bar{X}$	Md	$\bar{X}$	Md	$\bar{X}$	Md	$\bar{X}$	Md
Parameter	22478.81	21894.61	564.24	556.76	189.36	185.69	149.84	149.53	197.22	193.01	6774.02	6406.87	30.66	31.49	5.9	5.9
Value	314.27		4.69		1.53		1.30		1.58		115.15		0.45		0.1	
SE	21859.05	21188.06	554.99	546.10	186.36	183.13	147.27	146.19	194.11	189.62	6546.94	6207.42	29.76	30.54	5.7	5.8
95% LCL	23098.56	22664.15	573.50	568.77	192.37	189.62	152.40	151.94	200.33	197.60	7001.10	6588.96	31.55	32.46	6.0	6.1

Mean perimeter, mean diameter along main axis of glomerule and mean Feret's diameter show the same trend, as well as mean glomerular area during human aging, while mean diameter along secondary axis of glomerule shows continuous decrease from first to third age group (Table 1; Fig. 4). Changes of these parameters are not statistically significant which indicates that size and shape of investigated glomerules are not in correlation with aging process.
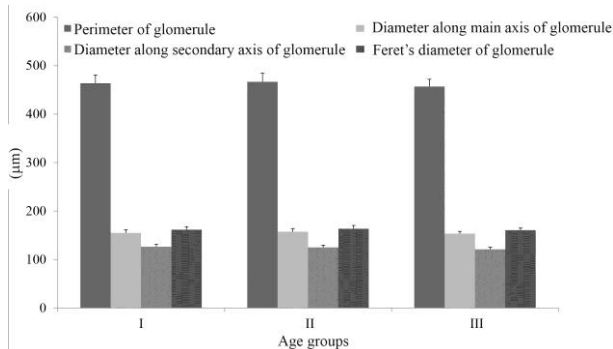

Fig. 4   Mean perimeter, mean diameter along main axis, main diameter along secondary axis and mean Ferret's diameter of glomerules of groups obtained by cluster analysis

Mean cell number per area unit significantly increases ($p < 0.05$) during aging (Table 1; Fig. 5). There is decrease of 11.60% in the second group compared to the first, decrease of 16.39% and 26% in the third compared to the second and the first, respectively. During aging process the glomerules show higher values of mean connective tissue area and percentage which is followed by decrease of cell number.
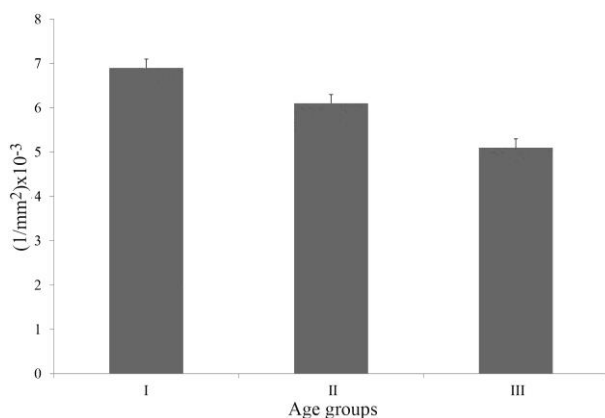

Fig. 5   Mean cellularity of glomerules of groups obtained by cluster analysis

Discussion

On the basis of abundant literature data about the changes in glomerules which precedes either focal (FSGS) or global glomerulosclerosis of kidney [10,13,21], in the first part of our study we estimated the increase of glomerular

connective tissue area, as well as its areal fraction (percentage) per one glomerule. Additionally, we analyzed the relationship between the age and latter cited parameters in order to determine dynamics of connective tissue production during the aging and its influence on glomerular cellularity. Opposed to earlier investigations which mostly suggest the increase of sclerotic glomerules percentage during aging [22–24], our results showed increase of connective tissue even in the glomerules with non-manifested morphologically visible sclerosis and intensity of that increase. In the third, the oldest group connective tissue occupied 40.66% of total glomerular area, in the second 32.11%, and only 17.33% in the first group, whereby this process was at the same time followed with significant decrease of glomerular cell number which was the most prominent in the third group and somewhat milder in the second age group. Similar attempts of quantification of connective tissue were not found in available literature, but we tried to link it with the data about age-related alterations of the structural elements of the glomerule which might take part in the production of glomerular connective tissue. It was Vechner [25] who determined the rise of mesangial cells part up to 6.2% of glomerular volume in middle age and 10.4% in old age. Sorensen [26] investigated relation between mesangial cells, mesangial matrix, endothelial cells and other glomerular structures. His results showed that mesangial and endothelial cells occupied proportionally largest part of glomerule. If we take into account that proliferation of these cells leads to increased production of extracellular matrix and its connective tissue, then we can find correlation between age and increased percentage of connective tissue that we obtained. However, decreased cell number per area unit, followed by increased connective tissue percentage, may indirectly indicate that the glomerules may enter the process of global sclerosis, especially after age of 50, according to our results. One of the most interesting current findings is discovery of extreme variability in number of the glomerules in different individuals. Research by Neugarten et al. [17] showed that number, size of glomerules and kidney weight decreased with aging. Numerous researchers determined that the growth of mesangial matrix caused by collagen deposition, capillary obliteration and immune-mediated glomerular inflammation lead to progressive reduction of total cell number, particularly after age of 60 [13,20–22], which is also in accordance to our results. Mesangial matrix changes its protein structure and proliferates in initial phase enlarging the size of the glomerule that eventually leads to the accumulation of connective tissue in the glomerule and decrease in its size. All these alterations significantly affect development of age-related glomerulosclerosis [13]. The results of Kasiske's [23] morphological study demonstrated positive correlation between number, i.e. percentage of sclerotic glomerules and aging, as well as intrarenal vascular disease. Aging and intrarenal vascular disease together (with or without hypertension) directly correlate with glomerulosclerosis, particularly in outer parts of the cortex.

Glomerular hypertrophy is an important feature of FSGS, diabetic nephropathy, membranous glomerulonephritis, hypertension and obesity-related nephropathy. While glomerular hypertrophy may be useful for renal function in the short term, it seems that its presence becomes detrimental over a long period of time [27,28]. It is supposed that enlarged glomerules increase the risk of the onset of sclerosis as a consequence of hyperperfusion and high glomerular capillary pressure. Considering the inflammatory nature of glomerusclerosis in many renal diseases, it would be rational to expect that glomerular hypertrophy precedes glomerulosclerosis and that it also appears in the population that does not suffer from renal disorders.

Conclusion

From this point of view, our results, which suggest significant growth of connective tissue in glomerules during aging in the individuals that have not developed the signs of renal diseases, gain in importance.

References

1. Kalinovskaia EG. Močevidateljnaia sistema. Biologia starenia. Nauka: Leningrad, 1982. (Russian)
2. Kowald A, Kirkwood TB. A network theory of ageing: the interactions of defective mitochondria, aberrant proteins, free radicals and scavengers in the ageing process. Mutat Res 1996; 316:209–236.
3. Lata H, Walia L. Ageing: Physiological aspects. JK Science 2007; 9:111–115.
4. Mackenzie HS, Taal MW, Luyckx VA, Brenner BM. Adaptation to nephron loss. In: Brenner BM (ed) Brener and Rector's the kidney, 6th ed. Saunders: Philadelphia, 2000; pp 1901–1942.
5. Zhou XJ, Rakheja D, Yu X, Saxena R, Vaziri ND, Silva FG. The aging kidney. Kidney Int 2008; 74:710–720.
6. Percy C, Pat B, Poronnik P, Gobe G. Role of oxidative stress in age-associated chronic kidney pathologies. Adv Chronic Kidney Dis 2005; 12:78–83.
7. Peppa M, Uribarri J, Vlassara H. Aging and glycoxidant stress. Hormones (Athens) 2008; 7:123–132.
8. Palmer BF, Levi M. Effect of ageing on renal function and disease. In: Brenner BM (ed) Brener and Rector's the kidney. Saunders: Philadelphia, 1996; pp 2274–2296.
9. Rodríguez-Puyol D. The aging kidney. Kidney Int 1998; 54: 2247–2265.
10. Martin JE, Sheaff MT. Renal aging. J Pathol 2007; 211:198–205.
11. Lindeman RD. Overview: renal physiology and pathophysiology of aging. Am J Kidney Dis 1998; 16:275–282.
12. Beck LH. Changes in renal function with aging. Clin Geriatr Med 1998; 14:199–209.
13. Silva FG. The aging kidney: A review – Part I. Int Urol Nephrol 2005; 37:185–205.
14. Mimran A. [Renal function and aging]. Nephrologie 1990; 11: 275–280 (French)
15. Epstein M. Aging and the kidney. J Am Soc Nephrol 1996; 7: 1106–1122.
16. Long DA, Mu W, Price KL, Johnson RJ. Blood vessels and the aging kidney. Nephron Exp Nephrol 2005; 101:95–99.
17. Neugarten J, Gallo G, Sibiger S, Kasiske B. Glomerulosclerosis in aging humans is not influenced by gender. Am J Kid Dis 1999; 34:884–888.
18. Tracy ER, Parra D, Eisaquirre W, Torres Balanza RA. Influence of arteriolar hyalinization on arterial intimal fibroplasia in the renal cortex of subjects in the US, Peru, and Bolivia, aplicable also to other populations. Am J Hypertens 2002; 15:1064–1073.
19. Marcantoni C, Ma LJ, Federspiel C, Fogo AB. Hypertensive nephrosclerosis in African Americans versus Caucasians. Kidney Int 2002; 62:172–180.
20. Stojanović V, Jovanović I, Ugrenović S, Pavlović S. Quantification of sclerotic renal glomeruli during the aging process in humans. Med Pregl 2010; 61:775–778.
21. Korbet SM. Primary focal segmental glomerulosclerosis. J Am Soc Nephrol 1998; 9:1333–1340.
22. Zheng F, Plati AR, Potier M, et al. Primary focal segmental glomerulosclerosis in B6 mice disappears after menopause. Am J Pathol 2003; 162:1339–1348.
23. Kasiske BL. Relationship between vascular disease and age-associated changes in the human kidney. Kidney Int 1987; 31: 1153–1159.
24. Schwartz MM, Churchill M, Bidani A, Churchill PC. Reversible compensatory hypertrophy in rat kidneys: Morphometric characterization. Kidney Int 1993; 43:610–614.
25. Wehner H. Stereologiche Untersuchungen am Mesangium normaler menschlicher Nieren. Wirchows Arch Abt A Pathol Anat 1968; 344:286–294.
26. Sorensen FH. Quantitative studies of the renal corpuscles III: The influence of postmortem delay before taking renal tissue samples and of the duration of tissue fixation. Acta Path Microbiol Scand A 1975; 83:251–258.
27. Basgen JM, Rich SS, Mauer SM, Steffes MW. Measuring the volumen density of the glomerular mesangium. Nephron 1988; 50:182–186.
28. Fogo AB. Progression versus regression of chronic kidney disease. Nephrol Dial Transplant 2006; 21:281–284.

RELATIONS OF THE INITIAL SEGMENT OF THE OCULOMOTOR NERVE AND ADJACENT ARTERIES IN FETAL AND ADULT PERIOD

Milena Trandafilović[1], Ljiljana Vasović[1], Slobodan Vlajković[1], Ivan Jovanović[1], Slađana Ugrenović[1], Miroslav Milić[2]*

University of Niš, Faculty of Medicine, [1]Department of Anatomy, [2]Institute for Forensic Medicine, Serbia

Abstract. *The relationship between the initial part of the oculomotor nerve and the posterior cerebral and superior cerebellar arteries is well understood, but there is still insufficient data about details of these relationships. The aim of this work was to examine the relationships of the initial segment of the oculomotor nerve with adjacent arteries in fetal and adult period. The examination was performed on 259 human brains (191 adults and 68 fetuses). Arteries in fetal brain were perfused with Micropaque and examined by photo film. Adult cases were examined during the forensic autopsy and then basis of the brain was photographed. The close relationship of the initial segment of the oculomotor nerve with basilar artery in 8.3%, with superior cerebellar artery in 17.3%, with posterior cerebral artery in 68.6% of cases was noted. The root of the nerve appeared above postcommunicating part of the posterior cerebral artery in 1.3% of cases and under the level of superior cerebellar artery in 1.6% of cases. The oculomotor nerve with two roots was noted in 2.6% of cases. Neurovascular relationship between oculomotor nerve and adjacent arteries, as morphological characteristic on the ventral side of the brain trunk, has pathoanatomical meaning by the nerve disfunction caused by compression.*

Key words: *Human cadavers, brain base, oculomotor nerve, cerebral arterial circle, vertebrobasilar system*

Introduction

The oculomotor nerve (III) controls the most of the sceletal and two smooth eye muscles. The third nerve is divided into four segments: initial (cisternal), supracavernous, intracavernous and orbital [1].

The root of the oculomotor nerve converges and leaves the midbrain in the posterior part of the interpeduncular fossa, proximately anteriorly and laterally to the posterior perforated substance. The roots of the oculomotor nerve continue their course transversally through the interpeduncular fossa, change their course ventrolaterally around medial surface of the cerebral peduncle and pass between the superior cerebellar artery (SCA) and the posterior cerebral artery (PCA) [2]. The oculomotor nerve passes further ventrally, laterally and rostrally, reaching the lateral wall of the cavernous sinus and, finally goes into the orbit [1].

The posterior cerebral artery, terminal branch of the basilar artery, Zeal and Rhoton [3] divided into four segments. These segments are named by Terminologia Anatomica [4] as the precommunicating part (P1 segment), the postcommunicating part (P2 segment), the lateral occipital artery (P3 segment) and the medial occipital artery (P4 segment). The superior cerebellar artery is the branch of the basilar artery that supplies the

numerous structures of the cerebellum. The posterior communicating artery (PCoA) is the branch of the cerebral segment of the internal carotid artery and posteriorly, it communicates with the posterior cerebral artery separating P1 and P2 segments [5,6].

Boeri and Passerini [7] examined clinical manifestations caused by trunk extension and elongation of the basilar artery (BA). Guy and Day [8] analysed intracranial aneurysms that caused the oculomotor nerve palsy. Marinković and Gibo [1] investigated neurovascular relations and blood supply to the initial segment of the oculomotor nerve. Schumacher-Feero et al. [9] analysed the causes of the oculomotor nerve palsy in children. Birchall et al. [10] described recovery after the endovascular treatment of the posterior communicating artery aneurysm that caused the oculomotor nerve palsy.

Zhang et al. [11] emphasized variations among the neurovascular relations of the oculomotor nerve and adjacent arteries. Uz and Tekdemir [12] paid attention to relation between the oculomotor nerve and the PCA. Mulderink et al. [13] described the oculomotor nerve palsy caused by the PCoA compression, but Lee et al. [14] and Chen et al. [15] analysed the third nerve palsy caused by the PCoA aneurysm. Takahashi et al. [16] reported the case of the incomplete oculomotor palsy caused by the PCoA aneurysm.

The previous facts define the presence of the close relationships between the oculomotor nerve, the PCA and the SCA, but there is still insufficient data about peculiarities of those neurovascular relations [12]. Importance of the relations of the oculomotor nerve and

Correspondence to: Milena Trandafilović, MD, postgraduate student
Faculty of Medicine, Dept. of Anatomy,
81 Dr Zoran Đinđić Blvd., 18000 Niš, Serbia
Phone: +381 18 45 70 029 Fax: +381 18 423 87 70
E-mail: mitra018@yahoo.com

adjacent arteries can be discussed in the light of the compressive lesions, vascular penetrations, arteriovenous malformations, and the arterial aneurysms [1].

The aim of this study was to examine neurovascular relationships of the initial segment of the oculomotor nerve with the adjacent arteries in fetal and adult period.

Material and Methods

We performed a retrospective analysis of digital images of 68 fetal and 191 adult cases respectively, dissected at the Department of Anatomy and Institute for Forensic Medicine in Niš. The study included cases with 9 vascular components in the circle of Willis in which the oculomotor nerve was detected bilaterally. For that reason, 36 fetal cases and 120 adult cases were statistically observed and reported.

Fetuses of both genders, from 17 to 24 weeks of gestation were a part of the collection of our Department of Anatomy, and they were used in the preparation of doctoral thesis [16]. All fetuses were obtained legally from the Clinic of Gynecology and Obstetrics in Niš. The Council for Postgraduate Study of the Faculty of Medicine in Niš at this time gave permission to investigate the fetal material. The arteries of fetuses were injected with Micropaque or latex through the left cardiac ventricle or through the common carotid artery. All fetuses were fixed in 10% formalin for 2 weeks. Fetal brains were removed and kept in individual calvarias.

The dissected brains originated from cadavers of both genders and different ages (from the neonate to 95 years) and different causes of death in the period between 2006 and 2013. Investigation of these cases was in accordance with the rules of the internal Ethics Committee (no. 01-9068-4) of our Faculty of Medicine. Morphological features of structures at the base of brain and their relationships were observed through a magnifying glass and recorded on a film and in workbook. Measurement of distances between the oculomotor nerve and adjacent arteries was performed with ImageJ (http://rsb.info.nih.gov/ij/index.html).

Results

Results were presented in four phases.

I. *Typical symmetry in neurovascular relationships*
In 3 adult cases, the oculomotor nerve left the midbrain in the level of the basilar bifurcation bilaterally (Fig. 1, a). In 17 adult and 3 fetal cases, the third nerve appeared bilaterally at the ventral side of the midbrain in the level of the P1 segment (Fig. 1, b), but in 18 adult and 6 fetal cases in the level of the P1–P2 junction (Fig. 1, c). The oculomotor nerve bilaterally left the midbrain in the level of P2 segment in 15 adult and 11 fetal cases (Fig. 1, d).

In summary, bilateral symmetry in relationships between the oculomotor nerve and the BA or segments of the PCA was noted in 55.6% of fetal and 44.2% of adult cases. Among adult cases, the most frequent pattern of the neurovascular relations was bilateral relation with the P1 segment (16.7%). In fetal period, that was bilateral relation of the oculomotor nerve and P2 segment, with the presence in 30.6% of cases (Table 1).
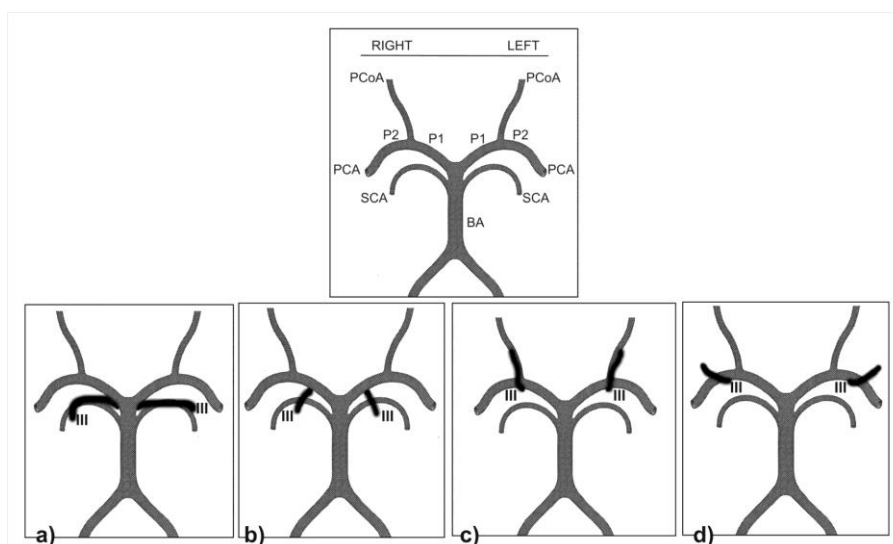

Fig. 1. Different examples of symmetrical neurovascular relationships between the oculomotor nerve and adjacent arteries. a) Bilateral relationship of the oculomotor nerve and the basilar bifurcation; b) bilateral relationship of the oculomotor nerve and the precommunicating segment of the posterior cerebral artery; c) bilateral relationship of the oculomotor nerve and the junction of the precommunicating and postcommunicating segment of the posterior cerebral artery; d) bilateral relationship of the oculomotor nerve and the postcommunicating segment of the posterior cerebral artery.
PCA, posterior cerebral artery; P1, precommunicating part of the PCA; P1–P2, junction of the pre- and postcommunicating parts of the PCA; P2, postcommunicating part of the PCA; SCA, superior cerebellar artery; BA, basilar artery; PCoA, posterior communicating artery; III, oculomotor nerve.

Table 1. Rewiev of the neurovascular relation of the initial part of the oculomotor nerve and the posterior cerebral artery (PCA) related to the side orientation

The PCA segments		Number of cases					
Right	Left	Adult cases		Fetal cases		Summa	
		120	(100%)	36	(100%)	156	(100%)
P1	P1	20	(16.7%)	3	(8.3%)	23	(14.7%)
P1	P1–P2	8	(6.7%)	1	(2.8%)	9	(5.8%)
P1	P2	12	(10%)	2	(5.6%)	14	(9%)
P1–P2	P1	15	(12.5%)	2	(5.6%)	17	(10.9%)
P1–P2	P1–P2	18	(15%)	6	(16.7%)	24	(15.4%)
P1–P2	P2	8	(6.7%)	4	(11.1%)	12	(7.7%)
P2	P1	14	(11.7%)	2	(5.6%)	16	(10.3%)
P2	P1–P2	10	(8.3%)	4	(11.1%)	14	(9%)
P2	P2	15	(15%)	11	(30.6%)	26	(16.7%)

P1, precommunicating part of the posterior cerebral artery; P1–P2, junction of the pre- and postcommunicating parts of the PCA; P2, postcommunicating part of the PCA.

II. *Typical asymmetry in neurovascular relationships*

The third nerve was related to the level of the P1–P2 junction at the right, but at the level of P1 segment at the left side, in 15 adult and 2 fetal cases (Fig. 2, a). The oculomotor nerve had a relation with the P1 segment at right side and with the P1–P2 junction at left side in 8 adult and in 1 fetal case (Fig. 2, b). The third nerve left the midbrain in the level of the right P1 and the left P2 segment of PCA in 12 adult and 2 fetal cases (Fig. 2, c). Relation of the oculomotor nerve with the left P1 segment and right P2 segment was noted in 14 adult and 2 fetal cases (Fig. 2, d). Relation of the third nerve with the P2 segment at right and the P1–P2 junction at left was noted in 10 adult and 4 fetal cases (Fig. 2, e). The opposite neurovascular relation, the third nerve in the level of the P1–P2 junction at the right and in the level of the P2 segment at the left side, was noted in 8 adult and 4 fetal cases (Fig. 2, f).

Asymmetry of the typical neurovascular relationships of the initial segment of the oculomotor nerve was noted in 55.8% of adult and 41.7% of fetal cases (Table 1).
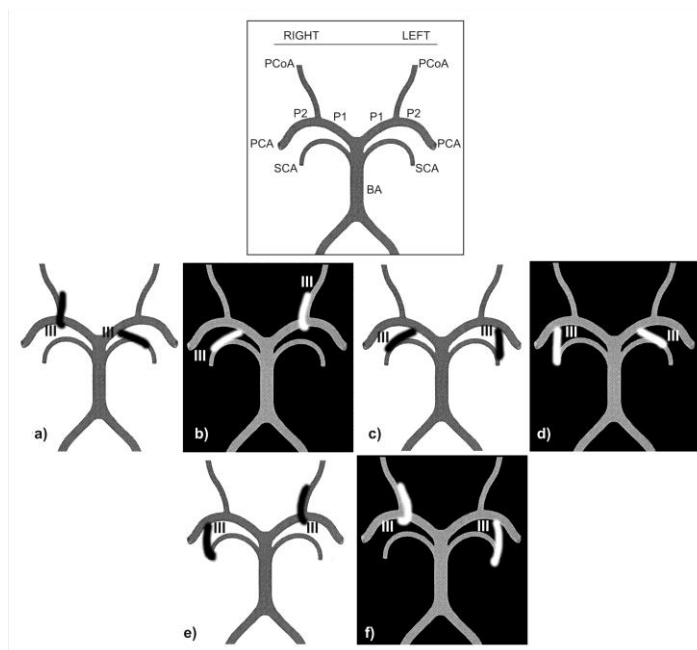

Fig. 2. Review of examples of asymmetrical neurovascular relationships between the oculomotor nerve and adjacent arteries. a) Relationship of the oculomotor nerve and the precommunicating–postcommunicating (P1–P2) junction at the right side and the P1 segment at the left; b) relationship of the oculomotor nerve and the P1 segment at the right side and the P1–P2 junction at the left side; c) relationship of the oculomotor nerve with the P1 segment at the right and the P2 segment at the left side; d) relationship of the oculomotor nerve and the P2 segment at the right and the P1 segment at the left side; e) relationship of the oculomotor nerve and the P2 segment at the right and the P1–P2 junction at the left side; f) relationship of the oculomotor nerve and the P1–P2 junction at the right side and the P2 segment at the left side.
PCA, posterior cerebral artery; SCA, superior cerebellar artery; BA, basilar artery; PCoA, posterior communicating artery; III, oculomotor nerve.

III. *Specific neurovascular relationships*

These cases were found in 14 cases (Fig. 3). In one adult case, the oculomotor nerve left the midbrain rostral in relation to the P2 segment bilaterally (Fig. 3, a) and in two more adult cases this phenomenon was noted unilaterally. The frequence of this phenomenon was 1.3% of all cadaveric cases. In one adult case (0.3% of all examined cases), the third nerve appeared ventrally in relation to the left P2 segment and passed parallel and compressed with the PCA to the point of nerve cutting (Fig. 3, b). In 3 adult cases, the initial segment of the third nerve went caudally crossing the dorsal, caudal and ventral surface of the SCA, and after the curve around the SCA, run rostrally. In adult cases, this pattern was noted unilaterally. In one fetal case, the oculomotor nerve appeared at the ventral side of the midbrain caudally of the SCA at the both sides (Fig. 3, c). In summary, this pattern of the neurovascular relationship

was noted in 1.6% of cases. The oculomotor nerve had two big roots unilaterally at the ventral surface of the midbrain in 7 adult cases and one fetal case that is 2.6% of cases (Fig. 3, d).

IV. *Rewiev of the neurovascular relationships distribution*

Irrespective of the side orientation, the oculomotor nerve mostly had the relationship with the P1 segment at one and some part of the PCA at the other side in adult period (57.5%).

In fetal period, the oculomotor nerve had the most frequent relation (63.9%) with the P2 segment at one, and some part of the PCA at the other side (Fig. 4 and Table 2).

The oculomotor nerve was in close proximity with the PCA in 77.9% of adult cases. In distribution of the PCA segments, the P1–P2 junction and the P2 segment had an equal presence (28.9%) and were more frequent
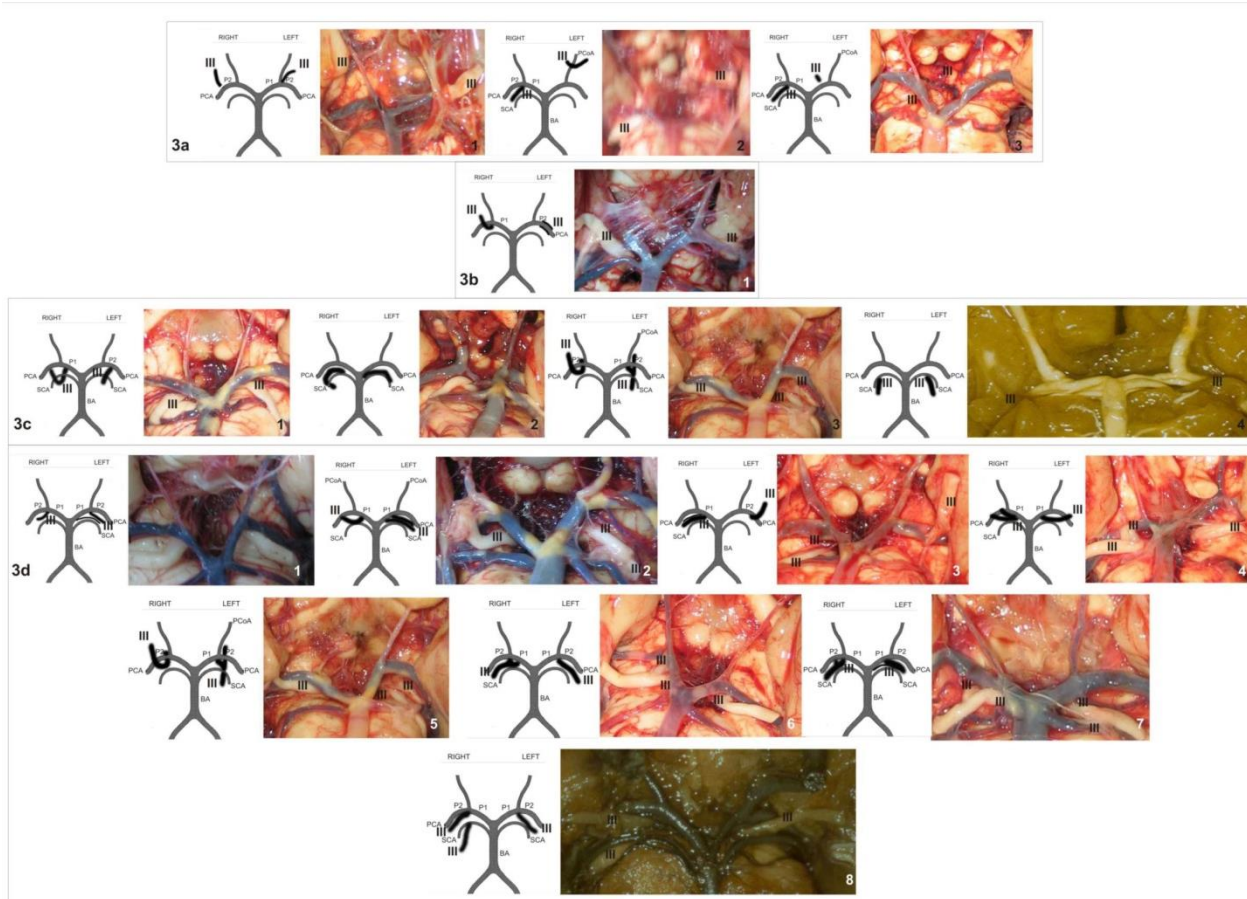

Fig. 3. Review of specific neurovascular relations of the oculomotor nerve and adjacent arteries in 14 cases: a) the oculomotor nerve left the midbrain rostral in relation to the postcommunicating (P2) part of the posterior cerebral artery (PCA) bilaterally in three cases; b) third nerve appeared dorsal in relation to the left P2 segment and passed parallel and compressed with the PCA in one case; c) the initial segment of the third nerve went caudally crossing the superior cerebellar artery (SCA), and after the curve around the SCA, ran rostrally in three adult cases, and the oculomotor nerve appeared at the ventral side of the cerebral trunk caudally of the SCA bilaterally in a fetal case; d) the oculomotor nerve had two big roots unilaterally in seven cases and bilaterally in one case.

PCA, posterior cerebral artery; P1, precommunicating part of the PCA; P1–P2, junction of the pre- and postcommunicating parts of the PCA; P2, postcommunicating part of the PCA; SCA, superior cerebellar artery; BA, basilar artery; PCoA, posterior communicating artery; III, oculomotor nerve.

Table 2. Review of the neurovascular relation of the initial part of the oculomotor nerve and segments of the posterior cerebral artery (PCA) irrespective of the side orientation

PCA segments		Number of cases					
		Adult cases		Fetal cases		Total	
		120	(100%)	36	(100%)	156	(100%)
P1	P1	20	(16,7%)	3	(8.3%)	23	(14.7%)
P1	P1–P2	23	(19,2%)	3	(8.3%)	26	(16.7%)
P1	P2	26	(21,7%)	4	(11.1%)	30	(19.2%)
P1–P2	P1–P2	18	(15%)	6	(16.7%)	24	(15.4%)
P1–P2	P2	18	(15%)	8	(22.2%)	26	(16.7%)
P2	P2	15	(12,5%)	11	(30.6%)	26	(16.7%)

P1, precommunicating part of the PCA; P1–P2, junction of the pre- and postcommunicating parts of the PCA; P2, postcommunicating part of the PCA.

than the P1 segment (20.1%). The third nerve was in close relationship with the SCA in 18.6%, and with the basilar bifurcation in 9.3% of adult cases (Table 3).

Average relations between the oculomotor nerve and adjacent arteries in adult cases were presented in Table 4. The biggest average distance (2.75 mm) was noted between the third nerve and the basilar bifurcation at the right side. At the left side, this distance was 2.62 mm. Average neurovascular distance with the SCA was 1.48 mm at the right, and 1.52 mm at the left side. The closest artery to the oculomotor nerve was the PCA with all its segments, and measured distances varied from 0.01 mm related to the P2 segment at the right side to 0.19 mm related to the P1 segment at the right side.

Discussion

The initial segment of the oculomotor nerve is in close relationship with the basilar artery distal segment branches. These arteries are two PCAs (as the terminal branches), two SCAs and many lateral branches of the previous arteries [1]. Also, the oculomotor nerve can form close neurovascular relationship with the PCoA, but it depends on the size and location of the PCA [11].
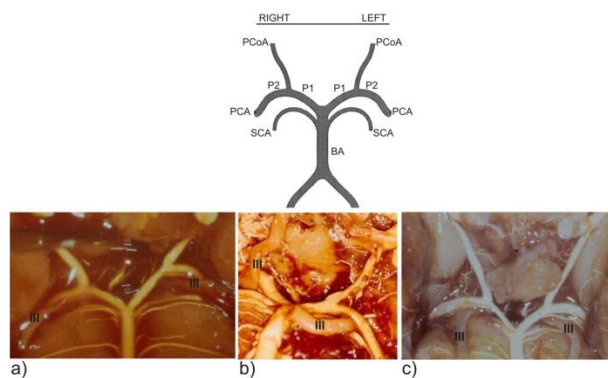

Fig. 4. Relationship of the oculomotor nerve and postcommunicating part of the posterior cerebral artery — bilaterally (a), on the left (b) and right (c) sides.
PCA, posterior cerebral artery; P1, precommunicating part of the PCA; P2, postcommunicating part of the PCA; SCA, superior cerebellar artery; BA, basilar artery; PCoA, posterior communicating artery; III, oculomotor nerve.

Location of nerves and blood vessels is mostly unchanged in adult period in comparison with prenatal state [18]. For that reason, it was possible to summarize the results, irrespective of life period.

Zhang et al. [11] analysed MRI images of 140 individuals and 3 adult cadavers, and found that the oculomotor nerve had a close relationship with the BA in almost 50% of cases. The third nerve had a close relationship with P1 segment in 98.6% of cases (56.8% with the posterior third, and 41.8% with the medial third of the P1). In most of cases, the oculomotor nerve was located in the proximity of the SCA, too. The most frequent type of relationship made by the PCA, the SCA and the oculomotor nerve, is so-called a "sandwich-like" structure. This study described that the oculomotor nerve runs dorsally and ventrally around the SCA, making the curve, in one case. Only in 3.6% of cases, the third nerve had the close relationship with the PCoA, and in 0.7% of cases compression by this artery was noted. Authors emphasized that the state of PCoA was significantly associated with the state of the PCA and its relationship to the oculomotor nerve.

Esmer et al. [19] analysed neurovascular relationships of the oculomotor nerve and adjacent arteries in 140 adult hemispheres, and found the close relationship between the oculomotor nerve and the PCA in 97.9%. In our study, this type of the neurovascular relationship was noted in 68.6% of cases (77.9% in adults and 76.4% in fetal cases).

The close relationship between the oculomotor nerve and the BA was described in cases of the nerve root appearance in the level of the basilar bifurcation. This neurovascular pattern has 8.3% of cases (9.3% of adults and 9.7% of fetal cases) in our study. The third nerve has close proximity with the SCA in cases of the close relations with the basilar bifurcation or in cases of the nerve course and/or appearance under the SCA. This neurovascular relationship was found in 17.3% of cases. The neurovascular relationship with the P1 segment was noted in cases of the nerve appearance in the level of P1 segment, but in the cases of close relationsip with the basilar bifurcation, too; it was noted in 17.3% of cases.

Pai et al. [9] emphasized that position of the oculomotor nerve between the SCA and PCA is almost constant. Liang et al. [20] analysed 392 oculomotor nerves

via MRI and found that the SCA was situated superior and compressed only one nerve. Hardy et al. [21] and Uchino et al. [22] also reported that the SCA or some of its branches can run superior to the oculomotor nerve.

The route of the oculomotor nerve below the SCA and crossing its trunk in the further course of the nerve were noted in one fetus bilaterally and in three adults unilaterally, and that is more frequently in comparison to the data from the available literature.

In some of our cases, the neurovascular pattern was different in relation to literature description. In one adult case, the oculomotor nerve left the midbrain rostral in relation to the P2 segment bilaterally, and in two adult cases more, this phenomenon was noted unilaterally. In these cases, the oculomotor nerve runs parallel with the PCoA. We did not find the similar description of the oculomotor relation with the P2 segment in the available literature.

Importance of the close relations of the oculomotor nerve and adjacent arteries can be discussed by the clinical importance of the compressive lesions, vascular penetrations, arteriovenous malformations, and the arterial anurysms [1].

In general, it is possible to discuss about two types of the compressive lesions. The first is associated with the third cranial nerve disfunctions, manifested by diffrerent clinical signs. This phenomenon is caused by a crossing compression of the nerve at the level of its root exit. Mostly, the oculomotor nerve root has a close relationship only with small arteries, as the collicular artery, the accessory collicular artery, the medial posterior choroidal artery and the perforating diencephalic arteries. Some of these arteries can compress the nerve root and cause hyperactive disfunction and, further, the spasm of bulbomotors. The second type of compressive lesions is the simple vascular compression of the distal part of the initial segment of the oculomotor nerve, which results in the conductional block and the intraneural circulatory disturbance. This part of the nerve is often in contact with the SCA and the P2 segment, and not so often with the BA, the P1 segment, the PCoA, and their variants or embrional arterial forms (duplicated arteries, fenestrations of the arterial trunk and the persistent trigeminal artery) [5]. According to Liang et al. [20], it is postulated that detection of neurovascular compression would have high sensitivity and low specificity for nerve paralysis. Also, the compression of the oculomotor nerve can be asymptomatic when it is compressed sufficiently and form a curve by the PCA, SCA, PCoA or BA.

Vascular penetration of the oculomotor nerve is described only in some papers [1,5]. As shown in the reports of the previous authors, the roots of the oculomotor nerve, which range in number between 20 and 25, can leave the midbrain in various parts. In 8% of cases, the oculomotor nerve has two roots – the main root, which leaves the midbrain through the medial sulcus of the crus cerebri, and accessory root, which leaves the midbrain through the middle part of the crus cerebri. The rarity of the oculomotor nerve penetration is not clear in the close relationship of the nerve and adjacent small arteries, and having in mind the possibility of appearance of the numerous nerve roots in the interpeduncular fossa, but this neurovascular relation is the possible reason for the frequent cross-compression of the nerve roots. In our study, 2.6% of cases (7 adult and 1 fetal) have the oculomotor nerve with two roots at one side.

Aneurysms of the terminal part of the basilar artery are located between the beginning of the SCA and the PCA. They are almost always in contact with the initial segment of the oculomotor nerve and this state can cause the partial or complete oculomotor neve palsy. Aneurysms of the basilar bifurcation make 5% of intracranial aneurysms and almost 50% of all vertebrobasilar saccular aneurysms. Saccular aneurysms are mostly situated in the interpeduncular fossa where they can compress the initial segment of the oculomotor nerve, the crus cerebri and the most of the interpeduncular blood vessels. Aneurysms of the PCA make up 2.2% of all saccular aneurysms, and 7-15% of all vertebrobasilar aneurysms. In Yasargil's [5] cases, aneurysms of the P1 and P2 segments were usually in close proximity with the initial segment of the third nerve. In the presence of the clinical manifestation of the superior oculomoror division paresis, aneurysm was sited at the SCA-PCA junction [8]. Vascular compression of the oculomotor nerve by the PCoA without pathological changes of the arterial wall is possible only in case of parallel course of the nerve and artery. It is more frequent in young persons. In older persons, compression of the oculomotor nerve is more possible besause of the atherosclerotic changes that cause elongation and dislocation of the arteries. This possibility has to be considered in cases of the oculomotor nerve palsy with unknown etiology [13]. Absence of the oculomotor nerve palsy in the cases of arterial aneurysms that are in close relationships with the third nerve, indicate small aneurysms or specific location of aneurysms without the nerve compression [14]. Boeri and Passerini [7] presented the cases with the oculomotor nerve palsy caused by the megadolichobasilar artery, anomaly that implies the extreme length and width of the BA. They emphasized atherosclerotic changes as the cause of that anomaly, and further, the palsy. Our study included cases with atheromatous changes. Among adults, 40% of cases had atheromatous plaques in the cerebral arteries which were related to the age of cases.

Conclusion

Bilaterally symmetrical neurovascular relationship of the initial segment of the oculomotor nerve and surrounding arteries was noted in 46.8% of cases. Asymmetrical relationship between the initial segment of the oculomotor nerve and surrounding arteries in the majority of cases is characterized by a direct relationship to the P1–P2 junction on one side, and the P1 segment, on the other. The case of the oculomotor nerve with two

roots was noted in 2.6% of cases and this pattern was unilateral. The route of oculomotor nerve below the superior cerebellar artery and crossing its trunk in the further course of the nerve was noted in one fetus bilaterally and in three adults unilaterally.

References

1. Marinković S, Gibo H. The neurovascular relationships and the blood supply of the oculomotor nerve: the microsurgical anatomy of its cisternal segment. Surg Neurol 1994; 42:505–516.
2. Pedroza A, Dujovny M, Ausman JI, et al. Microvascular anatomy of the interpeduncular fossa. J Neurosurg 1986; 64:484–493.
3. Zeal AA, Rhoton AL. Microsurgical anatomy of the posterior cerebral artery. J Neurosurg 1978; 48:534–559.
4. Terminologia Anatomica. International Anatomical Terminology. FCAT. Georg Thieme: Stuttgart, 1998.
5. Yasargil MG. Microneurosurgery, vol I. Thieme Med Pub: Stuttgart, 1984.
6. Pai BS, Varma RG, Kulkarni RN, Nirmala S, Manjunath LC, Rakshith S. Microsurgical anatomy of the posterior circulation. Neurol India 2007; 55:31–41.
7. Boeri R, Passerini A. The megadolihobasilar anomaly. J Neurol Sci 1964; 1:475–484.
8. Guy JR, Day AL. Intracranial aneurysms with superior division paresis of the oculomotor nerve. Ophtalmology 1989; 96:1071–1076.
9. Schumacher-Feero LA, Yoo KW, Solari FM, Biglan AW. Third cranial nerve palsy in children. Am J Ophthalmol 1999; 128:216–221.
10. Birchall D, Khangure MS, McAuliffe W. Resolution of third nerve paresis after endovascular management of aneurysms of the posterior communicating artery. AJNR Am J Neuroradiol 1999; 20:411–413.
11. Zhang WG, Zhang SX, Wu BH. A study on the sectional anatomy of the oculomotor nerve and its related blood vessels with plastination and MRI. Surg Radiol Anat 2002; 24:277–284.
12. Uz A, Tekdemir I. Relationship between the posterior cerebral artery and the cisternal segment of the oculomotor nerve. J Clin Neurosci 2006; 13:1019–1022.
13. Mulderink TA, Bendok BR, Yapor WY, Batjer HH. Third nerve paresis caused by vascular compression by the posterior communicating artery. J Stroke Cerebrovasc Dis 2001; 10:139–141.
14. Lee KC, Lee KS, Shin YS, Lee JW, Chung SK. Surgery for posterior communicating artery aneurysms. Surg Neurol 2003; 59:107–113.
15. Chen PR, Amin-Hanjani S, Albuquerque FC, McDougall C, Zabramski JM, Spetzler RF. Outcome of oculomotor nerve palsy from posterior communicating artery aneurysms: comparison of clipping and coiling. Neurosurgery 2006; 58:1040–1046.
16. Takahashi M, Kase M, Suzuki Y, Yokoi M, Kazumata K, Terasaka S. Incomplete oculomotor palsy with pupil sparing caused by compression of the oculomotor nerve by a posterior communicating posterior cerebral aneurysm. Jpn J Ophthalmol 2007; 51:470–473.
17. Vasović L. Morphological characteristics of the cerebral arterial circle with different origin of the vertebral arteries, PhD Thesis. Faculty of Medicine: University of Niš 1990. (Serbian)
18. Benninghoff A, Goerttler K. Lehrbruch der Anatomie des Menschen. Urban & Schwarzenberg: München und Berlin, 1960.
19. Esmer AF, Sen T, Comert A, Tuccar E, Karahan ST. The neurovascular relationships of the oculomotor nerve. Clin Anat 2011; 24:583–589.
20. Liang C, Du Y, Lin X, Wu L, Wu D, Wang X. Anatomical features of the cisternal segment of the oculomotor nerve: neurovascular relationships and abnormal compression on magnetic resonance imaging. J Neurosurg 2009; 111:1193–1200.
21. Hardy DG, Peace DA, Rhoton AL Jr. Microsurgical anatomy of the superior cerebellar artery. Neurosurgery 1980; 6:10–28.
22. Uchino A, Abe M, Sawada A, Takase Y, Kudo S. Extremely tortuous superior cerebellar artery. Eur Radiol 2003; 13:L237–L238.

ISOLATION, CHARACTERIZATION AND ANTIBACTERIAL ACTIVITY OF ACTINOBACTERIA FROM DYE POLLUTED SOILS OF TIRUPUR

Ramasamy Vijayakumar[1], Rajendran Malathi[2]

[1]*Department of Microbiology, Bharathidasan University Constituent College, Kurumbalur, India*
[2]*Department of Microbiology, Dr. G.R. Damodaran College of Science (Autonomous), Coimbatore, India*

Abstract. *The study revealed that the 31 actinobacterial isolates were isolated from dye polluted soils. The 31 actinobacterial isolates were grouped into 6 genera, among which Streptomyces was the predominant genera. Actinobacterial isolates were screened for their antibacterial properties. Only 2 isolates, namely RMS3 and RMS6, showed promising antibacterial activity against bacterial pathogens. The antibacterial activity of the antagonistic actinobacteria RMS3 and RMS6 showed maximum on Bacillus subtilis and Klebsiella pneumoniae. The potent actinobacteria were identified as Streptomyces sp. RMS3 and Nocordia sp. RMS6 on the basis of their phenotypic properties, and their antibacterial compound was similar to cephalexin and spiramycin respectively.*

Key words: *Actinobacteria, textile effluent polluted soil, antibacterial activity, HPLC*

Introduction

Actinobacteria are the most widely distributed group of microorganisms in nature. They are attractive, bodacious filamentous Gram positive bacteria having high GC content in their DNA. Actinobacteria are considered to be an intermediate group between bacteria and fungi. Majority of actinobacteria are free living, saprophyte found in soil, water and colonizing in plants. Actinobacteria are noteworthy as antibiotic producers, making three quarters of all known products; especially streptomycetes produced many antibiotics and other class of biologically active secondary metabolites, they cover around 80% of total antibiotic product, with other genera. It is anticipated that the isolation, characterization and the study on actinobacteria can be useful in the discovery of antibiotics from novel species of actinobacteria [1].

Streptomycetes is the largest antibiotic producing genus in the microbial world. The number of antimicrobial compounds reported from streptomycetes has increased almost exponentially in the last two decades. About 4,000 antibiotic substances have been discovered from bacteria and fungi, many of them are produced by streptomycetes. Most of the streptomycetes produce a diverse array of antibiotics including aminoglycosides, anthracyclins, glycopeptides, polyether and tetracycline [2]. Screening of microorganisms for the production of novel antibiotics has been intensively pursued for many years. Antibiotics have been used in many fields including, veterinary and pharmaceutical industry. Actinobacteria have the capability to synthesize many different biologically active secondary metabolites such as antibiotics, herbicides, pesticides, anti-parasitic compounds and enzymes like cellulose and xylanase used in waste treatment [3].

The abundance of terrestrial actinobacteria and their antibiotic productivity are known. The terrestrial actinobacteria would be an important source for the discovery of new antibiotics. Unfortunately, the rate of discovery of new compounds from existing genera obtained from terrestrial sources has decreased, while the rate of re-isolation of known compounds has decreased. Moreover, the rise in the number of drug-resistant pathogens and the limited success of strategies in proceedings new agents indicate an uncertain forecast for future antimicrobial therapy [4,5]. Thus, it has been emphasized that new group of microbe from unexplored habits be pursed as sources of novel antibiotics and other small therapeutic agents [6]. The perusal of the literature proved that there are not many reports of actinobacteria from textile effluent polluted soils. Keeping these points in view, the present study has been undertaken to isolate and screen the antibiotic producing actinobacteria from dye polluted soils of Tirupur, Tamil Nadu. Further, the identified antagonistic actinobacteria were characterized based on morphological, biochemical, cultural and physiological characteristics.

Material and Methods

Collection of soil sample. The soil samples were collected from textile dye polluted areas of Tirupur. The top layer soil samples were collected aseptically in ster-

---

Correspondence to: Ramasamy Vijayakumar
Dept. of Microbiology, Bharathidasan University Constituent College
Kurumbalur – 621 107, Perambalur Dt., India
E-mail: vijayakumar1979@gmail.com

ile polythene bags. Samples were brought to the laboratory and stored at 4ºC for further assay.

Isolation of actinobacteria. Starch casein nitrate (SCN) agar medium (Himedia, Mumbai) was used for isolation and enumeration of actinobacteria. The medium was supplemented with 10 μg/ml amphotericin and 25 μg/ml streptomycin (Himedia, Mumbai) to prevent fungal and bacterial contamination respectively. Using conventional dilution plate technique, 10g of soil samples were suspended in 100 ml of distilled water and 0.5 ml of suspension from this was spread over starch casein agar medium and incubated for 7–9 days at 28ºC. After incubation, the actinobacterial colonies were purified and sub-cultured on SCN agar plates and stored for further assay.

Screening for antibacterial activity. Antibacterial activities of isolates were tested   preliminarily by cross streak method [7]. Actinobacteria isolates were streaked across diameter on starch casein agar plates. After incubation at 28ºC for 6 days, 24 h cultures of *Bacillus subtilis* and *Klebsiella pneumoniae* were streaked perpendicular to the central strip of actinobacteria culture. All plates were again incubated at 30ºC for 24 h and zone of inhibition was measured.

Characterization of antibacterial compounds

Extraction of antibacterial compounds. The antagonistic actinobacteria RMS3 and isolate RMS were inoculated into starch casein broth. They were then incubated at 28ºC for 10 days in a shaker at 200-250 rpm. After incubation the culture filtrate was obtained by filtering through Whatmann No.1 filter paper and Millipore filter (Millipore Millex-HV Hydrophilic PVDF 0.45 μm). To the culture filtrates, equal volume of solvents (ethyl acetate, acetone, butanol, chloroform and distilled water) was added and centrifuged at 5000 rpm for 10 min to extract the compounds [8]. The compounds obtained from different solvents were tested for their antibacterial activity against the test organisms (*Bacillus subtilis* and *Klebsiella pneumoniae*) by 'well diffusion' method. The lawn cultures of bacteria on the Muller-Hinton agar plates were prepared. The 5 mm diameter well was made using sterile cork borer. The mixture (solvent and antibacterial compound) was poured into the well separately and incubated at 37ºC for 24 h. The solvents alone were used as control. After incubation the zone of inhibition was measured. The maximum antibacterial effect shown in solvent extracts were selected for further assay.

Antibacterial compound analysis by HPLC. The chromatographic separation of antibacterial compound was carried out on a LC-10 AT vp model HPLC using 250 x 4.60 mm Rheodysne column (C-18). The solvent system used was methanol (HPLC grade) and water (HPLC grade) in the ratio of 88:12. The operating pressure was 114 kgf, at a flow rate 0.8 ml/min and the temperature was set at 30ºC. The UV-Vis (SPD-10 A vp) detector was set at 210 nm. The sample was mixed with

the solvent in the ratio of 50:50 and filtered using Millipore filter before injection. About 25 μL of the sample filtrate was injected into the column. The sample was run for 10 min. and the retention time was noted. The elution time was compared with the standard and the compound was determined [9,10].

Characterization of actinobacteria. Colony morphology of actinobacteria were recorded with respective colour of aerial and substrate mycelium, size and nature of colonies reverse side colour and pigmentation on starch casein agar medium as recommended by International *Streptomyces* Project (ISP) [11]. Microscopic characterization was carried out by cover slip culture method [12]. Actinobacteria culture plates were prepared on starch casein agar medium and 5-6 sterile cover slips were inserted at an angle of 45º. The plates were incubated at 28ºC for 4–8 days. The cover slips were removed and observed under high power magnification. The morphological features of spores, sporangia and aerial and substrate mycelia were observed. Actinobacteria were identified using standard manuals (Bergey's Manual of Systematic Bacteriology and Bergey's Manual of Determinative Bacteriology). The formation of aerial and substrate mycelia and arrangement of spores on mycelium were observed under high power objective of light microscope. Cultural characteristics (growth, colouration of aerial and substrate mycelia, formation of soluble pigment) were tested. Actinobacterial isolates were inoculated onto different media, starch casein agar, nutrient agar, yeast extract malt extract agar (ISP2), oat meal agar (ISP3), inorganic salt agar (ISP4), glycerol asparagine agar (ISP5). The plates were incubated at 28ºC for 7 days. After incubation the colony morphology with respect to colour, aerial mycelium, size and nature of colony, reverse side colour and pigmentation on different media were recorded.

Biochemical tests including H_2S production, catalase, oxidase, urease, nitrate reduction, starch, lipid, gelatine and casein hydrolysis, haemolysis, melanin pigment production and triple sugar iron (TSI) were also performed as recommended by ISP. Chemo-taxonomical properties, such as analysis of whole cell sugars [13] and cell wall amino acid analysis [14] were analyzed. Physiological characterization, such as the effect of pH (3–11), temperature (10–50ºC) and salinity (NaCl concentrations 1–16%) and antibiotic sensitivity against ten different antibiotics (Himedia, Mumbai) [cloxacillin, amikacin, ampicillin, tobramycin, ciprofloxacin, nitrofurantoin, nalidixic acid, trimethrioprim, streptomycin, tetracycline and trimethoprin] were also tested. Utilization of carbon sources, such as starch, dextrose, fructose, maltose and mannitol, and nitrogen sources namely L-arginine, L-aspargine, L-cystine, L-histidine and L-tyrosine were tested on starch casein agar medium.

Results

A total of 297 actinobacterial colonies were isolates from 25 dye polluted soil samples of Tirupur, India.

Among 297 colonies, based on the actinobacteria colony morphology, 31 morphologically distinct isolates were purified, sub cultured and maintained on cultivation medium (SCA) for further characterization. The actinobacterial isolates showed a distinguished array of macroscopic features such as aerial and substrate mycelium and diffusible extra cellular pigments. These isolates formed white and yellow coloured aerial mycelium, reverse side colour was yellow, white and dark yellow.

Under light microscope, actinobacterial isolates showed formation of aerial and substrate mycelium, spore mycelium and various structures like spiral, filamentous, spirally twisted and elongated aerial mycelium. Based on the colony morphology and microscopic characterization, the actinobacteria were identified to generic level. Among 31 isolates, 21 (68%) isolates belonged to the genus *Streptomyces, Nocordia* 3 (10%), *Actinopolyspora* 3 (10%), *Kitasatosporia* 2 (6%), *Catellospora* 1 (3%) and *Glycomyces* 1 (3%). Among the genera recorded, *Streptomyces* was the most predominant and frequently occurred in soil when compared to other genera.

All the 31 isolates were screened for their antibacterial activity against *Bacillus subtilis* and *Klebsiella pneumoniae*. Among 31 isolates, 17 (54.84%) isolates showed activity against test bacteria. All the 17 isolates showed activity on Gram-positive bacteria, whereas seven isolates inhibited Gram-negative bacterial growth, and 7 isolates had both Gram positive and negative bacteria. The isolates which possessed strong antibacterial activity against both Gram positive and negative were selected for further study. Culture filtrates of 7 isolates (both Gram positive and Gram negative activity) were tested for their antibacterial activity by well diffusion method. Among the 7 isolates only 2 showed maximum activity against all the pathogens tested. Hence, these two potent isolates were selected for further characterization.

The antibacterial activities of the actinobacterial extracts were tested against two bacteria. The maximum inhibition effect was showed with ethyl acetate extract of *Streptomyces* sp. RMS3 against *K. pneumoniae* (26 mm) and *B. subtilis* (22 mm). Similarly, the maximum antibacterial activity of *Nocardia* sp. RMS6 was showed with ethyl acetate extract against *B. subtilis* (30 mm) and *K. pneumoniae* (26 mm). Further, methanolic extracts of both isolates showed maximum activity, whereas other solvent extracts showed moderate to minimum inhibition effect against all the pathogens tested (Table 1).

The antibacterial compounds were analyzed by HPLC analysis. The absorption peak values of *Streptomyces* sp. RMS3 compound showed at 3.587 and 6.520 min. whereas the compound of *Nocardia* sp. RMS6 showed absorption peaks at 3.677 and 6.573 min. Both antibacterial compounds showed single major compound. On the basis of retention time and absorption peaks the antibacterial compounds were compared with the standard antibacterial compounds. Retention time of RMS3 compound was found similar to cephalexin, when compared with the HPLC pattern of standard antibacterial compound (Fig. 1). Similarly, retention time of RMS6 compound was found to be spiramycin, when compared with the HPLC pattern of standard antibacte-

Table 1. Antibacterial efficacy of actinobacteria

Name of the Strain	Name of the pathogen	Zone of inhibition (mm)				
		Alcohol	Chloroform	Distilled water	Ethyl acetate	Methanol
Streptomyces sp. RMS3	*B. subtilis*	14 (4)	12 (7)	12 (0)	22 (8)	14 (5)
	K. pneumoniae	13 (5)	14 (3)	13 (0)	26 (8)	15 (6)
Nocardia sp. RMS6	*B. subtilis*	12 (4)	14 (7)	15 (0)	30 (8)	18 (5)
	K. pneumoniae	15 (5)	16 (3)	12 (0)	26 (8)	20 (6)

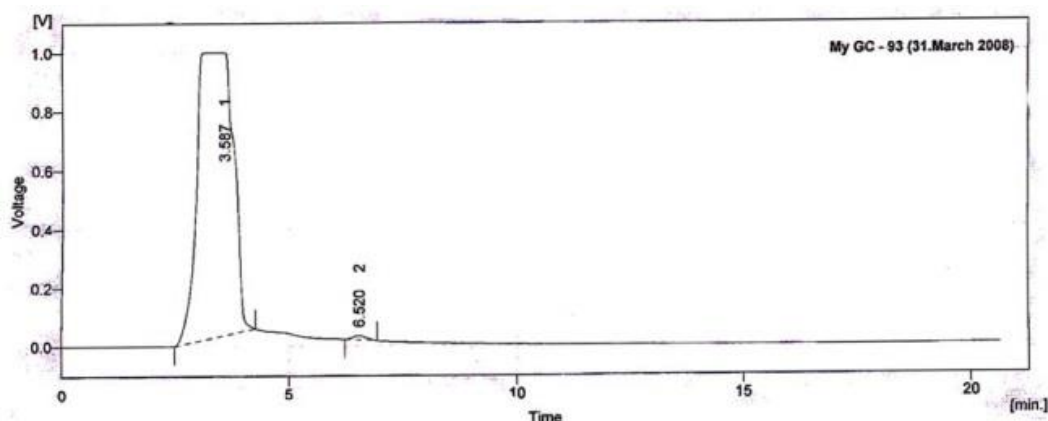(Control values were presented in parentheses)

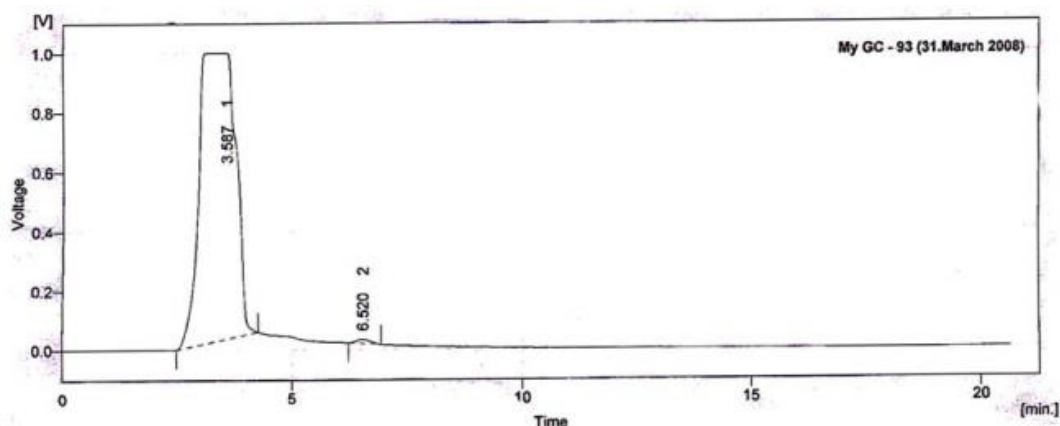**Fig.e 1.** HPLC chromatogram of antimicrobial compound RMS3

Fig. 2. HPLC chromatogram of antimicrobial compound RMS3

Table 2. Summary of chromatogram results on retention time

Name of the compound	No. of Major compound	No. of double bond	Carboxyl / hydroxyl groups	No. of methyl group	Carbon ring	Retention time
Cephalexin	One	6	2/-	-	13	3.3
Spiramycin	One	4	11 / 3	11	16	3.6

- Absence

Table 3. Cultural characteristics of the potential producers

S. No.	Name of the medium	*Streptomyces* sp. RMS3	*Nocardia* sp. RMS6
Starch nitrate agar			
	Aerial mycelium	White	White
	Substrate mycelium	Dark yellow	Light yellow
	Pigmentation	Nil	Nil
Nutrient agar			
	Aerial mycelium	White	White
	Substrate mycelium	White	White
	Pigmentation	Nil	Nil
Yeast extract malt extract (ISP 2)			
	Aerial mycelium	White	White
	Substrate mycelium	Dark yellow	Dark yellow
	Pigmentation	Nil	Nil
Oat meal agar (ISP 3)			
	Aerial mycelium	White	White
	Substrate mycelium	Dark yellow	Dark yellow
	Pigmentation	Nil	Nil
Inorganic salt agar (ISP 4)			
	Aerial mycelium	Yellowish White	White
	Substrate mycelium	Yellowish White	White
	Pigmentation	Nil	Nil
Glycerol asparagines agar (ISP 5)			
	Aerial mycelium	White	White
	Substrate mycelium	White	White
	Pigmentation	Nil	Nil

rial compound (Fig. 2). Cephalexin contains 6 double bonds, two carboxyl groups and 13 carbon rings at retention time 3.3 min. whereas, spiramycin contains 4 double bonds, 11 carboxyl groups and 3 hydroxyl groups, and showed 11 methyl groups 16 carbon rings at retention time of 3.6 min (Table 2).

Both isolates formed aerial and substrate mycelia. The strain RMS3 produced spirally twisted spores on aerial mycelium, whereas strain RMS6 produced branched vegetative mycelium. The potent isolates RMS3 and RMS6 were cultured on different media namely starch nitrate agar, nutrient agar, yeast extract malt extract agar (ISP2), oat meal agar (ISP3), inorganic salt agar (ISP4), and glycerol asparagine agar (ISP5). After incubation, white colour series of aerial and yellow colour series of substrate mycelium was produced by both RMS3 and RMS6 and no diffusible pigment was produced. Based on the colony morphology, microscopic structure, cultured, biochemical, physiological and chemotaxonomic properties of the potent two antagonistic actinobacterial isolates were identified to generic level as *Streptomyces* sp. RMS3 and *Nocordia* sp. RMS6. The cultural and other phenotypic properties like biochemical, chemo-taxonomical (whole cell sugars and cell wall amino acids) physiological (carbon and nitrogen source utilization, effect of pH, temperature and NaCl) on the growth of potential producers were recorded in Tables 3 and 4.

Discussion

Actinobacteria have been routinely screened for their high industrial value novel bioactive metabolites. These searches have been remarkably successful, approximately two thirds of naturally occurring antibiotics, including many of medical importance, have been isolated from actinobacteria [15]. In the present study, 31 morphologically distinct isolates with white and yellow coloured aerial mycelia, and yellow, white and dark yellow coloured substrate mycelia were isolated. Among

Table 4. Phenotypic properties of the potential producers

Properties	*Streptomyces* sp. RMS3	*Nocardia* sp. RMS6
Biochemical properties		
H$_2$S production	+	-
Nitrate reduction	-	+
Urease	-	+
TSI	Alkaline slant/ alkaline bud	Alkaline slant alkaline bud
Gelatin hydrolysis	+	-
Catalase	+	+
Oxidase	-	-
Starch hydrolysis	+	-
Casein hydrolysis	+	+
Haemolysis	+	+
Lipid hydrolysis	+	-
Melanin production	-	-
Whole cell sugar	-	-
Cell wall amino acid	-	+
Carbon source utilization		
Starch	+++	+++
Dextrose	++	-
Fructose	+	-
Maltose	++	+
Mannitol	+++	+++
Nitrogen source utilization		
L -arginine	+++	+
L -aspargine	+++	+++
L -cystine	+++	+++
L -histidine	+++	-
L -tyrosine	+++	+++
Effect of temperature (°)		
4	+++	+++
18	+++	+++
28	++++	++++
38	++	++
48	+	++
pH		
5	++	-
6	+++	+
7	+++	+++
8	+++	+++
9	+++	+++
Effect of NaCl		
Without NaCl	+++	+++
1%	++	++
2%	+	+
3%	-	-
4%	-	-

31 isolates, *Streptomyces* was the most predominant (68%) and frequently occurred in soil when compared to other genera. The dominance of *Streptomyces* among the actinobacteria especially in various soils has also been reported by many workers [16–19].

Among 31 isolates, 54.84% isolates showed antibacterial activity against Gram positive bacteria, whereas seven isolates only inhibited Gram negative bacterial growth, and 7 isolates had both Gram positive and Gram negative bacteria. From these, only 2 isolates with maximum antibacterial activity were selected for further work. The solubility of the antibacterial compounds from both the isolates were observed mostly in ethyl acetate solvent, whereas in other solvents they showed moderate to minimum solubility. It was evidenced by the antibacterial activities. In the same way, Vijayakumar et al. [20,21] tested the antimicrobial activity pattern of the marine actinobacteria against various human pathogenic bacteria and fungi, and reported that the inhibitory effect was varied depends on the pathogenic microorganisms.

High pressure liquid chromatography is being routinely used for the analytical estimation of various antibiotics [18]. In the present study, the antibacterial compounds were analyzed by HPLC analysis. Based on the retention time and absorption peaks, the antibacterial compounds were compared with the standard antimicrobial compounds [9,10,19–21]. Retention time of RMS3 compound was found similar to cephalexin, when compared with the HPLC pattern of standard antibacterial compound. Similarly, retention time of RMS6 compound was found to be spiramycin, when compared with the HPLC pattern of standard antibacterial compound. Correspondingly, similar type of HPLC analysis has been reported by Sethi [10]. For the identification of actinobacteria, ISP provided essential basic tools. In the present study, based on the colony morphology, microscopic structure, cultural, biochemical, physiological and chemotaxonomic properties of the potent two antagonistic actinobacterial isolates was identified to generic level as *Streptomyces* sp. RMS3 and *Nocordia* sp. RMS6.

Conclusion

Many of the antimicrobial drugs could not express their efficiency on all the pathogens in a same manner. Because the complexity of the cell wall of the microorganisms was different, they would protect the microorganisms from the antimicrobial drugs. Further, the productions of antimicrobial compounds have often been influenced by the components of medium, culture conditions, pH, temperature, time course etc. Extraction and purification of the compounds are essential processes for the characterization of antimicrobial compounds. Further investigation is needed in order to determine the structure of active compound and to scale up the production of metabolites.

References

1. Williams ST, Cross T. Actinomycetes. Appl Microbiol 1971; 4:471–473.
2. Sahin N, Ugur A. Investigation of the antimicrobial activity of some isolates. Turk J Bio 2003; 27:79–84.
3. Oskay M, Tamer AÜ, Azeri C. Antibacterial activity of some actinomycetes isolated from farming soils of Turkey. Afr J Biotechnol 2004; 3:441–446.
4. Projan SJ. Infectious diseases in the 21st century: increasing threats, fewer new treatments and a premium on prevention. Curr Opin Pharmacol 2003; 3:457–458.
5. Projan SJ, Youngman PJ. Antimicrobials: new solutions badly needed. Curr Opin Microbiol 2002; 5:463–465
6. Bull AT, Ward AC, Goodfellow M. Search and discovery strategies for biotechnology: the Paradigin shift. Microbiol Mol Biol Rev 2000; 64:573–606.
7. Lemos ML, Toranzo AE, Barja JL. Antibiotic activity of epiphytic bacteria isolated from intertidal seaweeds. Microb Ecol 1985; 11:149–163.
8. Gandhimathi R, Arunkumar M, Selvin J, et al. Antimicrobial potential of sponge associated marine actinomycetes. J Med Mycol 2008; 18:16–22.
9. Swami MB, Sastry MK, Nigudkar AG, Nanda RK. Correlation of HPLC Retention time with structure and functional group of macrolide polyene. Hind Antibiot Bull 1983; 25:81–99.
10. Sethi PD. High performance liquid chromatography: Quantitative analysis of pharmaceutical formulations, first ed. CBS Publishers and distributors: New Delhi, 2001.
11. Shirling EB, Gottlieb D. Methods for characterization of Streptomyces species. Int J Syst Evol Bacteriol 1966; 16:312–340.
12. Kawato M, Shinolue R. A simple technique for the microscopical observation. In: Memoirs of the Osaka university liberal arts and education. 1-1 Yamadaoka Suita: Osaka Japan, 1959; p 114.
13. Lechevalier MP, Lechevalier H. Chemical composition as a criterion in the classification of aerobic actinomycetes. Int J Syst Evol Bacteriol 1970; 20:435–443.
14. Becker B, Lechevalier MP, Lechevalier HA. Chemical composition of cell-wall preparations from strains of various form-genera of aerobic actinomycetes. Appl Microbiol 1965; 13:236–243.
15. Pandey A, Shukla A, Majumdar SK. Utilization of carbon and nitrogen sources by Streptomyces kanamyceticus M27 for the production of an antibacterial antibiotic. Afr J Biotechnol 2005; 4:909–910.
16. Moncheva P, Tishkov S, Dimitrova N, Chipeva V, Nikolova SA, Bogatzevska N. Characteristics of soil actinomycetes from Antartica. J Cul Coll 2002; 3:3–14.
17. Vijayakumar R, Muthukumar C, Thajuddin N, Panneerselavam A. Studies on the diversity of actinomycetes in the Palk Strait region of Bay of Bengal, India. Actinomycetologica 2007; 21:59–65.
18. Remya M, Vijayakumar R. Isolation and characterization of marine antagonistic actinomycetes from West Coast of India. Facta Universitatis 2008; 15:13–19.
19. Cholarajan A, Vijayakumar R. Isolation, identification, characterization and screening of antibiotic-producing actinobacteria from the crop fields of Thanjavur district, Tamilnadu, India. Int J Recent Sci Res 2013; 4:55–60.
20. Vijayakumar R, Panneer Selvam K, Muthukumar C, Thajuddin N, Panneerselvam A, Saravanamuthu R. Optimization of antimicrobial production by the marine actinomycetes Streptomyces afghaniensis VPTS3-1 isolated from Palk Strait, East Coast of India. Indian J Microbiol 2012; 52:230–239.
21. Vijayakumar R, Panneer Selvam K, Muthukumar C, Thajuddin N, Panneerselvam A, Saravanamuthu R. Antimicrobial potentiality of a halophilic strain of Streptomyces sp. VPTSA18 isolated from the saltpan environment of Vedaranyam, India. Ann Microbiol 2012; 62:1039–1047.

THE APPLICATION OF BISPHOSPHONATES IN THE TREATMENT OF PATIENTS WITH DISTURBED RENAL FUNCTION—CASE REPORT

Danijela Tasić

Clinic of Nephrology, Clinical Center, Niš, Serbia

Abstract. *Renal osteodystrophy and osteoporosis are related to chronic renal disease. In the present research and clinical dilemmas, indications have been proposed concerning the possible application of bisphosphonates in patients suffering from renal insufficiency. The aim of the study is to present a patient with disturbed renal function who was treated with parenteral bisphosphonates. The patient is a 56-year old male who was receiving hemodialysis for 29 years. In order to estimate risk for further bone fractures and to evaluate possible indication for intravenous bisphosphonates a bone mineral densitometry was performed, as well as transiliac biopsy with histological examination of the bone. The etiology of bone fractures in renal patients is multifactorial and cannot be fully explained only with the aid of pathohistological examination. After the thorough diagnostics, it could be possible to apply bisphosphonates in the treatment of patients with renal osteodystrophy on chronic hemodialysis or peritoneal dialysis.*

Key words: *Bisphosphonates, renal failure, dialysis*

Introduction

Bisphosphonates are inhibitors of osteoclastic bone resorption and are commonly used for the treatment of osteoporosis, bone resorption and hypercalcemia of different etiology [1]. Because of the adverse side-effects bisphosphonates are not used in the treatment of patients with terminal renal failure [2]. They are studied for possible use in the treatment of renal osteodystrophy and have not been approved for use yet in patients with renal failure [3]. Approximately 80% of the bisphosphonate is eliminated by the kidneys, with the remaining 20% taken up by the bone. Because of the risk of accumulation, elevated serum creatinine is listed in the manufacturers' literature as a contraindication to bisphosphonates use [4]. However, they have been safely used in dialysis patients and after renal transplantation for the treatment of high turnover bone disease, as well as vascular calcification and osteoporosis [5].

Case Report

Among 120 peritoneal dialysis (PD) patients, the study describes a 56-year old male who had been on hemodialysis (HD) since 1977 and started peritoneal dialysis in 2001. In 2006 he had an episode of syncope when he fell down and got left femoral neck fractures with low mechanical impact. Dual energy x-ray absorptiometry of the spine (L1–L4) was used to measure bone mineral density (BMD) in range of osteoporosis: 0,878 g/cm², T score -2,5. Furthermore, BMD was also measured in left femur in a range osteoporosis: total left femur BMD 0,631 g/cm², T score -3,1. We have been using cyclically one intravenous infusion of clodronate 300 mg/weekly during 6 months. After 6 months of therapy bone densitometry was repeated and it revealed deterioration in BMD of the spine (L1–L4) 0,847g/cm² with T score -2.78; on left femur BMD (total femur was 0,592 g/cm², T score -3,4). The therapy was terminated although the desired effect of the inhibition of osteoclast activity was not achieved due to the inability to determine the cumulative
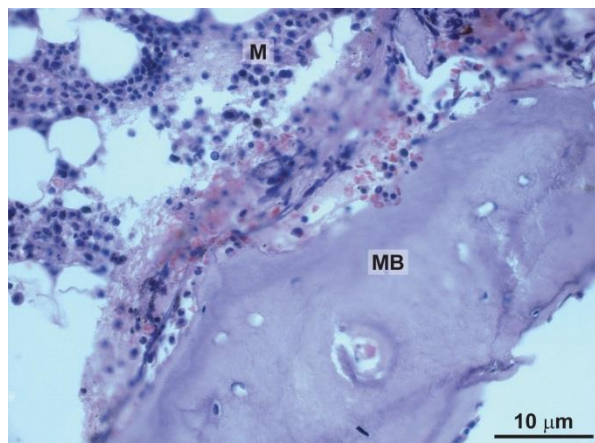

Fig. 1. Bone biopsy; hematoxylin and eosin, original magnification ×200. H & E staining of a biopsy sample for general histology (MB, mineralized bone; M, marrow). Scale bar = 10 μm

Correspondence to: Danijela Tasić MD, MSc
Clinic of Nephrology, Clinical Center Niš
48 Dr. Zoran Đinđić Blvd., 18000 Niš, Serbia
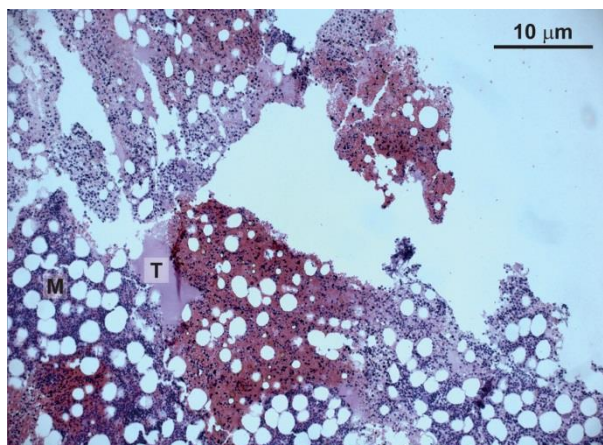Phone: +381 18 45 30 856
E-mail: danijeladt@yahoo.com

Fig. 2. Bone marrow medulla; hematoxylin and eosin, original magnification ×200. H & E staining of a biopsy sample the ratio of cells to fat about 50% (T, trabeculae; M, marrow). Scale bar = 10 μm

Fig. 3. X –ray; anteroposterior radiograph of the hands. Subperiosteal bone resorption is visible.

dose and because of the concern of possible side effects of the medication [6]. In order to exclude low bone turnover iliac biopsy was performed which excluded other mechanisms except osteoporosis.

Discussion

In the present research, indications have been proposed concerning the possible application of bisphosphonates in patients suffering from renal insufficiency The national guidelines have no recommendations on the treatment of renal rapid turnover osteodistrophy and osteoporosis using bisphosphonates in renal patients [7]. Previous clini-

cal studies have shown that bisphosphonates can be safely used in preventing complications and preserving bone mass in a population of renal patients. Bisphosphonates can be used with caution and in especially treatment of malignant hypercalciemia [8]. The dose of drug, the length of treatment (delayed complications) should be adapted to dialysis modality and residual renal function [9].

Conclusion

There is no clear beneficial effect of bisphosphonate treatment that outweighs possible side-effects in patients with renal failure at the moment. Positive result can be expected, but we need more clinical data regarding efficacy and safety of bisphosphonates in dialysis patients.

References

1. Hawley C, Elder G; Caring for Australasians with Renal Impairment (CARI). The CARI guidelines. Biochemical targets. Nephrology (Carlton) 2006; 11:S198–216.
2. Saadi H, BoobesY, Bernieh B, Abouchacra S. Osteoporosis in renal failure: how accurate is the diagnosis and is there any role for bisphosphonates? Int J Diabetes & Metab 2005; 13:99–102.
3. Body JJ, Pfister T, Bauss F. Preclinical perspectives on bisphosphonate renal safety. Oncologist 2005; 10:3–7.
4. Jackson HG. Renal safety of ibandronate. Oncologist 2005; 10:14–18.
5. Tasić D. Mogući korisni aspekti bisfosfonata u lečenju bolesnika sa bubrežnom insuficijenciom. I Internacionalni kongres Lečenje osteoporoze sa međunarodnim učešćem: Niška Banja, 2006. (Serbian)
6. Tasić D, Avramović M, Veličković R, Veličković Lj. The application of bisphosphonates in the treatment of patients with disturbed renal function. 8th BANTAO Congress: Belgrade, 2007. (Serbian).
7. Cunningham J. Bisphosphonates in the renal patient. Nephrol Dial Transplant 2007; 22:1505–1507.
8. Toussaint ND, Elder JG, Kerr PG. Bisphosphonates in chronic kidney disease: balancing potential benefits and adverse effects on bone and soft tissue. Clin J Am Soc Nephrol 2009; 4:221–233.
9. Courtney AE, Maxwell AP. Chronic kidney disease and bisphosphonate treatment: are prescribing guidelines unnecessarily restrictive? Postgrad Med J 2009; 85:327–330.
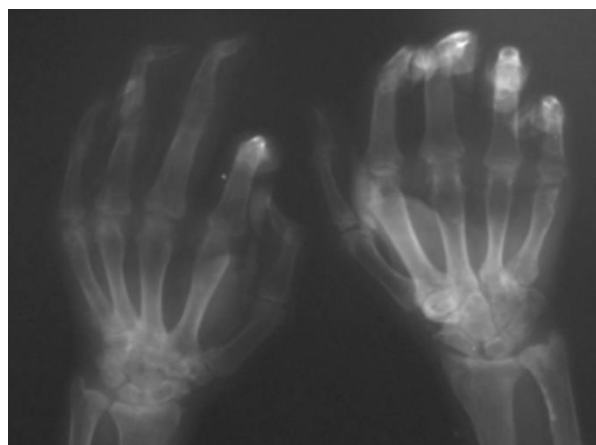
MOYAMOYA PHENOMENON IN SERBIAN POPULATION

*Aleksandar Kostić[1], Milena Trandafilović[2*], Ivan Stojanović[3]*

University of Niš, Faculty of Medicine, [1]Clinic for Neurosurgery, [2]Department of Anatomy, [3]Institute for Forensic Medicine, Niš, Serbia

To the editor:

We want to provide a detailed description of the case of Moyamoya phenomenon that was recently noted in the paper about the morphology of cerebral arterial circles (CACs) in Serbian population [1]. We found that the first paper about Moyamoya phenomenon referring to Serbia was published almost twenty years ago [2].

The word "moyamoya", taken from a Japanese dictionary, in translation means a puff of smoke; in scientific literature it refers to the network of fine collaterals around and distal to the CAC due to progressive unilateral (Moyamoya syndrome) or bilateral (Moyamoya disease) stenosis of the intracranial part of the internal carotid artery (ICA) and its proximal branches [3].

Moyamoya syndrome was found in a 55-years-old male, who died due to pulmonary thromboembolism.
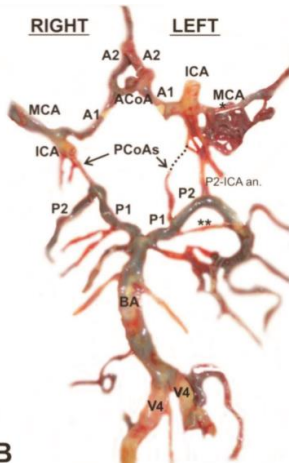
Brain arteries			Outer diameter [mm]	Length [mm]
Left M1	Proximal end		1.73	3.65
	Convoluted vessels	Rete mirabile	0.43–1.49	
		Stenosed vessel part	0.75	5.69
	Distal end		1.63	
Left C4			3.36	
Left A1	Vessel trunk		2.52	11.55
	(Proximal) saccular aneurysm		1.79	
	(Distal) saccular aneurysm		Width of the aneurysm wasn't measured (left optic nerve partly covers this aneurysm)	5.11
Left A2	Vessel trunk		2.38	
	Berry aneurysm		2.30	2.53
ACoA			1.40	4.45
Right A1			1.66	17.11
Right A2			1.69	
Right M1			2.59	
Right C4			2.57	
Right PCoA			0.66	6.79
Right P1			2.51	14.78
Right P2			2.42	
Left P1			2.47	7.12
"Bridge" artery between the left P1 and P2			0.45	10.97
Left P2			2.42	
Left P2–ICA anastomosis	PCA end		1.26	
	ICA end	Medial branch	0.58	
		Lateral branch	1.19	
BA	Below the basilar bifurcation		4.24	
	Middle part		4.24	31.47
	Rostrally to the VBJ junction		3.83	
Left V4			3.21	
Right V4			3.76	

Fig. 1. Arteries on the brain base of a male cadaver. **A**, Convoluted blood vessels (Moyamoya pattern) in the sphenoid part of the left middle cerebral artery (circle), and three aneurysms (arrows) in the left anterior cerebral artery. **B**, Brain arteries and persistent primitive anastomoses are marked on modified image. **C**, Outer diameters of brain arteries and anastomoses are noted in the table. C4, choroid and communicating subparts of the cerebral part of the internal carotid artery (ICA); M1, sphenoid part of the middle cerebral artery; *stenosed M1 subpart; A1, precommunicating part of the anterior cerebral artery (ACA); A2, postcommunicating part of the ACA; ACoA, anterior communicating artery; PCoA, posterior communicating artery; P1, precommunicating part of the posterior cerebral artery (PCA); P2, postcommunicating part of the PCA; P2–ICA an., P2–ICA anastomosis; **bridge artery between the left P1 i P2; BA, basilar artery; V4, intracranial part of the vertebral artery.

Correspondence to: Milena Trandafilović, MD
Faculty of Medicine, Dept. of Anatomy,
81 Dr Zoran Đinđić Blvd., 18000 Niš, Serbia
Phone: +381 18 45 70 029 Fax: +381 18 423 87 70
E-mail: mitra018@yahoo.com

The research of cadaveric brain vessels was performed at the Institute of Forensic Medicine in Niš during co-author's (MT) academic and postdoctoral studies. An approval for doctoral investigation was granted by the

Research Ethics Committee (No. 01-206-1) of our Faculty of Medicine. The vessels were photographed on the brain base; their outer diameters were studied from the digital images, using the ImageJ program (http://rsb.info.nih.gov/ij/index.html). Summarizing pathoanatomical findings, we will indicate six features: 1) a partial stenosis of the left middle cerebral artery (MCA) at its sphenoid part and a presence of a network of the MCA collaterals medially to the limen insulae; 2) the presence of three (one saccular and two berry) aneurysms in the left anterior cerebral artery (ACA); 3) the presence of atheromatous plaques in the basilar artery, and internal carotid and vertebral arteries; 4) the presence of a "bridge" artery between the left precommunicating (P1) and post-communicating (P2) parts of the posterior cerebral artery; 5) the presence of the left P2–ICA anastomosis; and 6) left-right caliber asymmetry of arteries on the brain base (Fig.1).

As cited by Scott and Smith [3], the incidence peaks were in five-year children and adults in their mid-40s and the incidence among all patients with Moyamoya in Europe appears to be about 1/10 of that observed in Japan. Case reports in the Balkan journals were related to the case of Moyamoya disease in a 13 year-old girl in Serbia [2], and the case of Moyamoya syndrome of a 71-year-old male in Slovenia [4]. In a retrospective study by Borota et al. [5] over a period of 22 years in the former Yugoslavia, Moyamoya pattern of cerebral vessels was discovered only in 31 patients of both genders. We accepted the definitions of Moyamoya syndrome and Moyamoya disease given by Scott and Smith [3], although there were different diagnoses in cited cases [2,4], or Moyamoya modification [6]. However, there was an association of many vascular abnormalities in this, as well as in the cases of Moyamoya phenomena from the Balkan peninsula [4,5] to Japan [6], and beyond.

References

1. Vasović L, Trandafilović M, Jovanović I, et al. Morphology of the cerebral arterial circle in the prenatal and postnatal period of Serbian population. Childs Nerv Syst 2013; 29:2249–2261.
2. Vranješević D, Jović NS, Milovanović D, Đukić A. Unilateral Moyamoya disease associated with acrofacial vitiligo in a 13-year-old patient—case report. Srp Arh Celok Lek 1994; 122:234–236. (In Serbian)
3. Scott RM, Smith ER. Moyamoya disease and Moyamoya syndrome. N Engl J Med 2009; 360:1226–1237.
4. Zaletel M, Surlan-Popović K, Pretnar-Oblak J, Žvan B. Moyamoya syndrome with arteriovenous fistula after head trauma. Acta Clin Croat 2011; 50:115–120.
5. Borota L, Bajić R, Marinković S, Maksimović R, Marković Z, Kovačević M. The main epidemiological, clinical and morphological features of Moyamoya disease in Yugoslavia. Clin Neurol Neurosurg 1997; 99:S49–S53.
6. Komiyma M, Nakajima H, Nishikawa M, et al. High incidence of persistent primitive arteries in Moyamoya and Quasi-Moyamoya diseases. Neurol Med Chir (Tokyo) 1999; 39:416–422.

BASIC AND ORAL HISTOLOGY AND EMBRYOLOGY
by Prof. Dr. Vesna Lačković, Prof. Dr. Ivan R. Nikolić and Prof. Dr. Vera Todorović,
edited and illustrated by Ivan R. Nikolić
– Critiques and Reviews –

REVIEW[1]
by Prof. Dr. Radivoj Krstic[2]

I am very pleased to give a brief opinion of the book *Basic and Oral Histology and Embryology* in the following lines.

This monumental book was made with enormous creative and didactic efforts combined with an excellent knowledge from our profession, all with the aim of aiding students in dealing more easily with the subject matter of histology and embryology. The didactic approach of the authors is systematic, ultramodern and rich, which is easily seen from the fact that all the structures that were dealt with were located, described, and illustrated in detail, so the students are able to get a very clear and up-to-date subject overview – from macroscopic anatomy, to molecular biology, both in terms of medical histology and embryology, as well as that of dentistry. In addition, parallel treatment of histology and embryology, together with numerous information boxes inside of the book, improves its quality.

All of the micrographs – either being light or electron micrographs – are of the best quality, whereas the drawings, tables and diagrams are clear and distinct. It is an especially good idea to indicate the origin of cells, tissues and organs by the choice of colour in a drawing.

The technical setup of the book is excellent: paper is of the best quality, which allows for the superb reproduction of details and colours.

The cover design with symbolic images from histology and embryology draws the reader's attention and, at the same time, gives an implication regarding the subject matter of the book – which makes it a complete success. Naturally, there is criticism for every book, my own and the one in question included, though, in this case, it is strictly cosmetical in nature and is of lesser importance.

Prof. Dr. Radivoj Krstić,
22nd June 2012

REVIEW

The manuscript titled *Basic and Oral Histology and Embryology*, whose authors are Vesna Lačković, Professor of Histology and Embryology at the Faculty of Medicine (the University of Belgrade), Ivan Nikolić, Professor of Histology and Embryology at the Faculty of Medicine (the University of Niš), who is also the editor of the book, and Vera Todorović, Professor of Histology and Embryology at the Faculty of Dental Medicine in Pančevo (the University Business Academy in Novi Sad), represents an exceptional book in the fields of histology and embryology, designed primarily for the students of the Faculty of Dental Medicine. It is a universal work, the content of which encompasses all of the teaching units of this subject's curriculum. The book discusses cytology, general histology, histological development of organs, as well as embryology, which can be found at the end of each chapter. There is a special attention given to histology and embryology of the oral cavity, which for the first time, in both our and foreign professional literature, constitutes an integral part

---

[1] The text is taken from an electronic letter sent to Prof. Dr. Ivan R. Nikolić on 22nd June 2012 by Prof. Dr. Radivoj Krstic.

[2] Prof. Dr. Radivoj Krstic is one of the currently most prominent histologists and illustrators, the Co-director of many years at the Institute of Histology and Embryology, Faculty of Medicine in Lausanne, Switzerland, whose five books were published by Springer, a global publishing company, and to whom this book is dedicated.

of a single textbook from histology and embryology for the students of the Faculty of Dental Medicine.

It is a book of 300 pages and of an exquisite technical setup (hard cover, glossy paper, full colour) in A4 format. The content is divided into 21 chapters and is written in a distinctive style of the writers, who have already proved themselves as the creators of some widely accepted textbooks, atlases, and practicums in the fields of histology and embryology. The text has three clearly distinct sections. The main text is intended for students of the General Dentistry studies and is characterized by its conciseness, with the emphasis on the necessary morphological, functional and embryological facts, which eases the understanding of a complex microscopic structure of cells, tissues and organs, especially of those that compose the oral cavity. Apart from the main text, there are also sections written in small print, which display additional information in the field of anatomy, physiology, or molecular biology. The yellow parts contain very concise embryology, while the blue ones indicate the information concerning clinical significance.

There is a special quality given to the manuscript by copious illustrations contained in over 500 colour drawings and schemes, light micrographs and electron micrographs, macroscopic representations, ultrasonic and X-ray shots. The cells in the drawings are painted in the colours of embryonic leaves (endoderm – yellow, mesoderm – red, ectoderm – blue), which facilitates the understanding of embryology. The photographs of the histological samples, during the preparation of which both routine and complex histochemical techniques of colouring were used, as well as the latest immunohistochemical techniques, are technically immaculate. Apart from the drawings and the photographs, the manuscript also contains tabular displays. At the end of the book, there is a bibliography and a glossary, which also improves the significance of the book. Since it displays the important and up-to-date facts from histology and embryology, as well as their connection to the clinical practice, this work will be very useful not only to dental students, but also to the students of other biomedical courses, both the undergraduates and the postgraduates.

Taking into account its universality, didacticism, illustrativeness and technical fitness, I suggest that the manuscript titled *Basic and Oral Histology and Embryology* be published as a textbook for dental students.

Academic Vladimir Bumbaširević,
Professor of Histology and Embryology
at the Faculty of Medicine in Belgrade,
Belgrade, 8th March 2012

REVIEW

General information

The title of the manuscript is *Basic and Oral Histology and Embryology*.

The editor and the illustrator is Prof. Dr. Ivan Nikolic, and the authors are Prof. Dr. Vesna Lačković, Prof. Dr. Ivan Nikolić and Prof. Dr. Vera Todorović. These are the authors with many years of experience who have

already published a significant number of monographs, textbooks for both undergraduates and postgraduates, atlases, practicums and handbooks. The publisher of this work is Data Status from Belgrade.

Technical information

It is a manuscript of 300 pages, technically very well equipped, hard-covered, with glossy paper and numerous photo documents in colour. The drawings and the micrographs are either presented individually or in the form of composite images. The manuscript contains 276 drawings, 440 micrographs, 43 electron micrographs, as well as many macroscopic images: direct sample slides, ultrasonic and X-ray photographs.

Content overview and the book organization

The content of the book is divided into 21 chapters: 1. Histology, basic histological methods and microscopy, 2. Cell, 3. Basic characteristics of tissues, organs and systems of organs, 4. General embryology, 5. Epithelial tissue, 6. Connective tissue, 7. Blood, bone marrow and haematopoiesis, 8. Muscle tissue, 9. Nervous tissue and nervous system, 10. Eye, the organ of sight, 11. Ear, the organ of hearing and balance, 12. Cardiovascular and lymphatic system, 13. Immune system and lymphoid organs, 14. Endocrine system, 15. Respiratory system, 16. Digestive system, oral cavity, 17. Digestive system, esophagus, stomach, small and large intestine, 18. Digestive system, liver, bile ducts, gallbladder and pancreas, 19. Urinary system, 20. Male and female reproductive systems, 21. Skin. The chapter *Oral Cavity* is the most elaborate. It was written in 77 pages and illustrated in 130 images. It deals with the teaching units that correspond to the curriculum for histology and embryology for the students of integrated dental studies: basic anatomic characteristics of head and its bones, oral cavity (general characteristics, division and content), salivary glands, oral mucosa, lips, cheeks, palate, gingiva, alveolar mucosa, tongue, lymphatic tissue of oral cavity, general characteristics of teeth and the surrounding tissue, enamel, pulpo-dentinal complex, dental cement, periodontium, alveolar extension and embryology of oral cavity, which is all followed by an emphasis on the clinical significance of certain structures.

There is a special attention given to a currently modern field that deals with dental stem cells. This section will also be useful to the dental students completing their doctoral studies. At the end of the book, there is a bibliography and a glossary, which facilitates the usage of the book.

Conclusion

Taking into account all of the stated facts, we can conclude that this is a universal, richly illustrated work in the field of basic and oral histology and embryology, prepared according to the regular curriculum of this subject, and therefore, I suggest that this work be published as a textbook for dental students.

Academic Vojislav Leković,
Professor at the Faculty of Dental Medicine,
the University of Belgrade,
Belgrade, 8th March 2012

REVIEW[3]
on the manuscript
Basic and Oral Histology and Embryology

Apart from the common information, regarding morphology of cells, tissues and organs, the manuscript, which appears in the form of a supplementary study material, follows the current trends of emphasizing the clinical significance, in order for the first-year students, who already study normal structures and functions of the organism, to have an insight into the importance of those same structures as well in cases when they are affected by pathological processes that show certain clinical manifestations, the knowledge of which is inspiring for further study. In this way the connection is established between preclinical, relatively complicated and arid disciplines, and clinical medicine, which represents the final aim of education of the majority of students. In this sense, the manuscript contains basic, informative and, in a popular manner displayed, nosological, etiological, pathological, pathophysiological and clinical facts concerning the most common diseases, which affect some tissues and organs (inflammations, tumors, immune system disorders and alike).

Conclusion

The manuscript *Basic and Oral Histology and Embryology*, edited by Ivan Nikolic, written by Vesna Lačković, Ivan Nikolić and Vera Todorović, on the account of its content, which fully integrates all of the segments of the subject Histology and Embryology for Dental Students, which is of an appropriate scope, richly illustrated, and which by its technical setting and a manner of displaying the content in its entirety does not fall behind similar works from the rest of the world literature, should be published as **a textbook for students of the integrated dental studies**, even though it can also be used by the students of other biomedical disciplines who have the subject Histology and Embryology as part of their curriculum.

Academician Vladisav Stefanović,
Professor of Internal Medicine
at the Faculty of Medicine in Niš

Translated from Serbian by
Jelena Mladenović,
Master Philologist in English Language and Literature

---

[3] An excerpt.

FACTA UNIVERSITATIS

Series
Medicine and Biology

Vol. 16, Nº 1, 2014

Contents